CONF-9507147--Abstr.

# Program and Extended Abstracts

# IUTAM Symposium on Hydrodynamic Diffusion of Suspended Particles

22-25 July 1995
YMCA of the Rockies
Estes Park, Colorado, U.S.A.

FG03-95ER14527

MASTER


Robert H. Davis
Editor

Department of Chemical Engineering
University of Colorado
Boulder, CO 80309-0424




University of Colorado at Boulder

# IUTAM Symposium on Hydrodynamic Diffusion of Suspended Particles

Hydrodynamic diffusion refers to the fluctuating motion of nonBrownian particles (or droplets or bubbles) which occurs in a dispersion due to multiparticle interactions. For example, in a concentrated sheared suspension, particles do not move along streamlines but instead exhibit fluctuating motions as they tumble around each other. This leads to a net migration of particles down gradients in particle concentration and in shear rate, due to the higher frequency of encounters of a test particle with other particles on the side of the test particle which has higher concentration or shear rate. As another example, suspended particles subject to sedimentation, centrifugation, or fluidization, do not generally move relative to the fluid with a constant velocity, but instead experience diffusion-like fluctuations in velocity due to interactions with neighboring particles and the resulting variation in the microstructure or configuration of the suspended particles. In flowing granular materials, the particles interact through direct collisions or contacts (rather than through the surrounding fluid); these collisions also cause the particles to undergo fluctuating motions characteristic of diffusion processes.

Although the existence and importance of hydrodynamic diffusion of particles have been embraced only in the past several years, the subject has already captured the attention of a growing number of researchers in several diverse fields (e.g., suspension mechanics, fluidization, materials processing, and granular flows). Nevertheless, there has not previously been a conference or symposium devoted to this subject. The purpose of this symposium is to bring active researchers and students together for the first time from the diverse fields in which hydrodynamic diffusion of particles is important. The expected achievements of this symposium are (i) the identification of hydrodynamic diffusion as a new paradigm which governs a wide variety of phenomena in suspension and granular flows, and (ii) cross-fertilization by key researchers in fields such as granular flows, composite materials processing, rheology, drop and bubble dispersions, and suspension transport.

**Acknowledgments**

The symposium is cosponsored by

*The International Union of Theoretical and Applied Mechanics*
*The National Science Foundation*
*The National Aeronautics and Space Administration*
*The Department of Energy - Office of Basic Energy Sciences*
*The Centre National de la Recherche Scientific*

Special thanks are extended to Professors Andreas Acrivos and George Batchelor for initiating interest in this symposium.

# Schedule and Program for the IUTAM Symposium on Hydrodynamic Diffusion of Suspended Particles, 22-25 July 1995, Estes Park, Colorado, USA

**Saturday 22 July 1995**

6:00 pm Dinner

**Session 1. Opening Session**

7:00 pm Opening Remarks by Session Chair: R. Davis

7:10 pm 1.1 *D. Koch, Cornell University, *What is so puzzling about hydrodynamic diffusion?*

8:00 pm Welcoming Reception

**Sunday 23 July 1995**

7:30 am Breakfast

**Session 2. Hydrodynamic Diffusion During Sedimentation and Fluidization**

8:30 am Opening Remarks by Session Chair: F. Feuillebois

8:35 am 2.1 *E. Guazzelli, ESPCI, *Experiments on sedimentation: Particle velocity fluctuations and hydrodynamic self-diffusion of sedimenting non-Brownian spheres*

9:10 am 2.2 F. Da Cunha, University of Brasilia, and E. Hinch, University of Cambridge, *Hydrodynamic dispersion in a sedimenting suspension of non-Brownian particles*

9:30 am 2.3 H. Brenner, MIT, L. Mondy, Sandia National Labs, and J. Abbott and A. Graham, Los Alamos National Lab, *Dispersion in concentrated suspensions*

9:50 am Break

10:20 am 2.4 H. Nicolai, Y. Peysson, and E. Guazzelli, ESPCI, *Settling of a heavy sphere in the midst of a suspension of lighter spheres*

10:40 am 2.5 J. Martin, N. Rakotomalala, and D. Salin, Université Pierre et Marie Curie, *Hydrodynamic dispersion of non-colloidal suspensions: Measurement from Einstein's argument*

11:00 am 2.6 B. Felderhof, Aachen, Germany, *Mean velocity in a suspension of droplets due to the thermocapillary effect*

11:20 am Discussion

11:45 am Lunch

**Session 3. Shear-induced Particle Migration and Diffusion**

1:00 pm Opening Remarks by Session Chair: D. Leighton

1:05 pm 3.1 *J. Brady, California Institute of Technology, *Shear-induced diffusion and particle migration*

1:40 pm 3.2 D. Leighton, University of Notre Dame, *Shear-induced migration in colloidal hard-sphere suspensions*

2:00 pm 3.3 F. Da Cunha, University of Brasília, and E. Hinch, University of Cambridge, *The effect of surface roughness in shearing suspension*

2:20 pm 3.4 L. Nitsche, University of Illinois, and J. Nitsche, SUNY at Buffalo, *Collision properties of non-simple bodies and their influence on hydrodynamic dispersion*

2:40 pm Discussion

3:00 pm Break

**Session 4. Applications of Hydrodynamic Diffusion in Suspension Flows**

3:30 pm Opening Remarks by Session Chair: R. Phillips

3:35 pm 4.1 *A. Acrivos, City College of CUNY, *Shear-induced diffusion and its effects on the rheology of concentrated suspensions*

4:10 pm 4.2 U. Schaflinger, Technical University, Vienna, *Motion of a sediment layer due to a laminar, stratified flow*

4:30 pm 4.3 I. Miskin, L. Elliott, and D. Ingham, University of Leeds, and P. Hammond, Schlumberger Cambridge Research Limited, *The shear induced diffusion of particles in a rectangular fracture channel*

4:50 pm 4.4 P. Nott, Indian Institute of Science, *A model for suspension flow accounting for shear-induced migration*

5:10 pm 4.5 A. Chow and R. Hamlin, Lockheed Palo Alto Research Lab, and C. Ylitalo, 3M Corporate Research Technology Development Lab, *Size segregation of concentrated, bidisperse and polydisperse suspensions during tube drawing*

5:30 pm Discussion

6:30 pm Barbecue Dinner

**Monday 24 July 1995**

7:30 am Breakfast

**Session 5. Particle Migration and Segregation in Granular Flows**

8:30 am Opening Remarks by Session Chair: J. Jenkins

8:35 am 5.1 *H. Buggisch, Universität Karlsruhe, Germany, *On mixing and demixing phenomena in granular shear flow*

9:10 am 5.2 M. Hunt, California Institute of Technology, *The effect of particle diffusion on heat transfer for flows of granular materials*

9:30 am 5.3 J. Jenkins, Cornell University, *Fick's law and species separation for a binary mixture of frictionless, nearly elastic spheres*

9:50 am Break

10:20 am 5.4 Y. Lan and A. Rosato, New Jersey Institute of Technology, *Particle transport in vibrated granular beds*

10:40 am 5.5 M. Nakagawa, Sandia National Laboratories, and S. Altobelli, A. Caprihan, and E. Fukushima, The Lovelace Institutes, *Unexpected behavior of particles in a horizontal rotating cylinder*

11:00 am Discussion

11:30 am Lunch

**Session 6. Computer Simulation Techniques for Suspensions and Dispersions**

2:00 pm Opening Remarks by Session Chair: J. Brady

2:05 pm 6.1 *A. Ladd, Cornell University, *Numerical simulations of hydrodynamic dispersion*

2:40 pm 6.2 A. Sangani, Syracuse University, and D. Koch, Cornell University, *Sedimentation at finite Stokes numbers*

3:00 pm 6.3 G. Ristow, Philipps-Universität, *Numerical predictions for elastohydrodynamic collisions*

3:20 pm Discussion

3:30 pm Break

**Session 7. Orientational and Configurational Dispersion**

4:00 pm Opening Remarks by Session Chair: E. Hinch

4:05 pm 7.1 *E. Shaqfeh, Stanford University, *Orientational and configurational diffusion in the slow flows of particles and polymers*

4:40 pm 7.2 R. Sundararajakumar and D. Koch, Cornell University, *The dynamics of semi-dilute and semi-concentrated fiber suspensions*

5:00 pm 7.3 O. Harlen, University of Leeds, and D. Koch, Cornell University, *Fibre suspensions in dilute polymer solutions*

5:20 pm 7.4 A. Szeri, University of California-Irvine, *Exploitation of Brownian motions for the optimal control of fiber orientation distributions*

5:40 pm Discussion

6:00 pm Dinner

**Poster Session and Reception**

7:00 pm Poster Setup

7:15 pm Initial Viewing

7:45 pm Two-minute Oral Presentations

8:30 pm Final Viewing

P.1 J. Blawzdziewicz, Polish Academy of Sciences, F. Feuillebois, ESPCI, and N. Lecoq, R. Anthore, and C. Petipas, URA, *Theoretical and experimental study of hydrodynamic interactions between several spheres*

P.2 V. Kumaran, Indian Institute of Science, *Diffusion and coalescence due to pair interactions in a suspension of bubbles in potential flow*

P.3 S. Zeng, T. Kerns, A. Zinchenko, and R. Davis, University of Colorado, *The nature of particle contacts in sedimentation*

P.4 M. Loewenberg, Yale University, *Deformation-induced drop dispersion*

P.5 G. Krishnan, MIT, and D. Leighton, University of Notre Dame, *Shear-induced structure in bidisperse suspensions*

P.6 Y. Wang, A. Acrivos, and R. Mauri, The City College of CUNY, *The longitudinal shear-induced gradient diffusivity of a monodisperse dilute suspension of spheres*

P.7 A. Averbakh, A. Shauly, A. Nir, and R. Semiat, Technion, Israel, *Application of laser-doppler anemometry in highly concentrated suspensions*

P.8 S. McCaffery, L. Elliott, and D. Ingham, University of Leeds, and A. Unwin, Schlumberger Cambridge Research Limited, *A Newtonian model for proppant transport in an inclined channel*

P.9 Y. Lan and A. Rosato, New Jersey Institute of Technology, *Self-diffusion in vibrated granular beds*

P.10 W. Kalthoff, S. Schwarzer, and H. Herrmann, ESPCI, and G. Ristow, Phillipps-Universität, *Application of a novel algorithm to hydrodynamic diffusion in sedimenting systems*

P.11 S. Altobelli and E. Fukushima, The Lovelace Institutes, and L. Mondy, Sandia National Lab, *Velocity and fluid fraction measurements in suspensions flowing through abrupt contractions and expansions*

P.12 R. Powell, J. Seymour, M. McCarthy, and K. McCarthy, University of California at Davis, *NMR imaging measurements of average and fluctuating velocity distributions in sphere suspension flow*

P.13 W. Wolthers, D. van den Ende, M. Duits, and J. Mellema, University of Twente, *The viscosity and sedimentation of aggregating colloidal dispersions in a Couette flow*

P.14 J. Brady, California Institute of Technology, and J. Morris, Koninklijke/Shell-Laboratorium, *Microstructure in a strongly-sheared suspension and its impact on rheology and self-diffusivity*

P.15 H.-K. Tsao and D. Koch, Cornell University, *Hydrodynamic diffusion in sheared, sedimenting suspensions at finite Reynolds numbers*

P.16 V. P. Korobeinikov, Russian Academy of Sciences and Russian National Committee on Theoretical and Applied Mechanics, *Unsteady flows of two-phase media in tubes due to local supply of mass and energy*

**Tuesday, 25 July 1995**

7:30 am Breakfast

**Session 8. Experimental Techniques for Suspensions and Dispersions**

8:30 am Opening Remarks by Session Chair: R. Powell

8:35 am 8.1 *D. Salin and J. Martin, Université Pierre et Marie Curie, *Experimental techniques for suspensions and dispersions*

9:10 am 8.2 A. Graham and J. Abbott, Los Alamos National Lab, E. Fukushima and S. Altobelli, The Lovelace Institutes, N. Phan-Thien, University of Sydney, L. Mondy, Sandia National Labs, and T. Stephens, Naval Air Warfare Center, *NMR imaging of particle migration in concentrated suspensions*

9:30 am 8.3 M. Lyon and L. Leal, University of California at Santa Barbara, *Experimental studies of the motion of concentrated suspensions in two-dimensional channel flow*

9:50 am Break

10:20 am 8.4 A. Shauly, A. Averbakh, R. Semiat, and A. Nir, Technion, Israel, *Shear-induced migration of particles in a flowing viscous concentrated suspension*

10:40 am 8.5 E. Fukushima, S. Altobelli, A. Caprihan, M. Nakagawa, and L. Wang, The Lovelace Institutes, *NMRI studies of granular flows in a rotating horizontal cylinder*

11:00 am Discussion

11:30 am Lunch

*denotes leadoff/invited speaker

# What is So Puzzling about Hydrodynamic Diffusion?

Donald L. Koch
School of Chemical Engineering
Cornell University
Ithaca, NY 14853

Small particles (with diameters less than about 1 μm) diffuse due to random impacts by the small molecules of the fluid in which they are suspended. Larger particles lack this Brownian motion, but often exhibit a diffusive motion which originates from their chaotic hydrodynamic interactions with other large particles in the suspension. The hypothesis of a diffusive motion that is independent of kT together with dimensional analysis leads to a number of simple and powerful results that explain greatly enhanced mixing in applications such as porous media, blood flows and sediment transport.

Why, then, is hydrodynamic diffusion considered puzzling? One reason is that deterministic equations for the motion of the fluid and particles lead to an apparently stochastic average behavior. In addition, Stokes flow reversibility implies that any diffusion occurring during the forward motion of a low Reynolds number suspension should (in principle) be undone by a reversal of the flow. We will briefly discuss these puzzles in the context of dispersion in porous media flows.

I believe, however, that the greatest obstacle to understanding hydrodynamic diffusion is the dearth of simple example calculations illustrating the phenomenon. Three important cases of hydrodynamic diffusion (which we might have hoped would be simple examples) are sedimentation and simple shear flow of dilute, monodisperse suspensions and dispersion due to flow through a dilute fixed bed of spheres. However, the sedimentation and fixed bed problems are complicated due to the dominance of many-body interactions occurring over length scales much larger than the particle diameter. The case of simple shear flow is not as simple as hoped because symmetry and Stokes flow reversibility imply that two-sphere interactions do not cause diffusion. Thus, one must consider interactions between three spheres or between two non-spherical particles.

The phenomenon of hydrodynamic diffusion is not limited to inertia-less suspensions of spheres. Two interesting new applications are orientational diffusion of non-spherical particles and diffusion due to hydrodynamic interactions in suspensions where inertia plays an important role. In the final section of the talk, we will discuss the hydrodynamic diffusion of particle orientation in a simple shear flow. The results will be applied to shear flow of a fiber suspension in a weakly viscoelastic fluid, where there is a competition between the tendency of the viscoelastic stress to align the fibers parallel to the vorticity axis of the simple shear flow and the randomizing tendency of orientational diffusion. A final complication to be noted for hydrodynamic diffusivities is that their values depend upon the microstructure of the suspension. The nonlinear coupling between diffusivity and microstructure in this fiber suspension leads to multiple steady states for the fiber orientation distribution.

# Experiments on sedimentation: Particle velocity fluctuations and hydrodynamic self-diffusion of sedimenting non-Brownian spheres

Elisabeth Guazzelli
Laboratoire de Physique et Mécanique des Milieux Hétérogènes,
URA 857 au CNRS, ESPCI,
10 rue Vauquelin, 75231 Paris CEDEX 05, France

Long range multibody hydrodynamic interactions play a key role in the motion of an individual sphere settling in the midst of a suspension of like non-Brownian spheres. Indeed, the sphere undergoes a random motion due to the fluid velocity disturbances caused by the surrounding spheres. This randomly fluctuating particle motion has a long time behavior characteristic of a diffusion process which is called hydrodynamic self-diffusion.

Ham and Homsy[1] were the first to investigate experimentally the diffusive nature of the motion of a test sphere in the midst of a dilute sedimenting suspension of like spheres. Large particle velocity fluctuations, ranging up to 46% of the mean, were observed and hydrodynamic self-diffusivities were measured for particle volume fraction ranging from 2.5% to 10%. Large velocity fluctuations were also found comparable to the mean in an experiment using a fluidized bed and a light scattering technique.[2]

Caflisch and Luke[3] and also Hinch[4] showed theoretically that for a dilute, random suspension the velocity variance grows in proportion to the characteristic length of the settling vessel. Koch and Shaqfeh[5] showed that the variance is finite if the pair probability exhibits a net deficit of one particle in the region surrounding any given particle and suggested that this screening might be produced by hydrodynamic effects. Numerical simulations which use the point-particle approximation or include the full hydrodynamic interactions between the particles have also investigated the problem of hydrodynamic diffusion in a sedimenting suspension (see for instance the work of Ladd[6], Koch[7], and Da Cunha[8] and references therein).

On a macroscopic scale, particle velocity fluctuations can lead to gradient-diffusion phenomena and thus are important for the understanding of mixing processes which inhibit separation. The spreading of the front between a sedi-

menting suspension and the clear fluid above it has been attributed to gradient-diffusion and gradient-diffusivities were estimated.[9, 10, 11, 12] Experiments on the steady state concentration profile of a fluidized bed as well as stationary propagating fronts give much larger values of gradient-diffusivities.[13] Again in the context of fluidized bed, Batchelor suggested that hydrodynamic gradient-diffusion has a stabilizing effect against the growth of concentration wave instabilities.[14] Stable region of fluidization were observed experimentally and gradient-diffusivities were estimated from Batchelor's stability criterion.[15]

This talk focuses on the hydrodynamic self-diffusivity of the particle random walk in an uniform suspension. It describes work with H. Nicolai, B. Herzhaft, E. J. Hinch and L. Oger on the sedimentation of non-Brownian spheres at low Reynolds number.[16] A few silvered glass spheres were tracked in a suspension of unmarked glass spheres, made optically transparent by matching the index of refraction of the suspending fluid to that of the glass spheres. Particle tracking was undertaken with a real time digital imaging system for particle volume fractions ranging from 0% to 40%. Mean velocity and velocity fluctuations in the direction of gravity and along the horizontal direction of the vessel were determined. The long time fluctuating particle motion was demonstrated to be diffusive in nature by examining the relaxation of the particle velocity auto-correlation functions as well as by studying the second-order moments of the particle displacements.

The fluctuations in settling speed were found to be large, ranging between 75% and 170% of the mean. The relative fluctuations increased at low concentrations to reach a maximum value of 170% at a particle volume fraction of 30% and then decrease at higher concentrations. The measured correlation times were found to be independent of the concentration. The self-diffusivities scaled as the product of the mean settling velocity and the particle radius below a particle volume fraction of 30%. Above a particle volume fraction of 30%, the self-diffusivities experienced a strong decrease. This work also showed a strong anisotropy of the diffusion process.

Further experiments with different vessel sizes were also undertaken while keeping the particle volume fraction constant at 5%.[17] Velocity fluctuations and self-diffusivities were found to be independent of the size of the vessel when the vessel width varied by a factor of four, in contradiction to the theories of Caflisch and Luke,[3] and of Hinch.[4] But a well-stirred experimental suspension may not be a suspension where the particles are randomly positioned as assumed by these theories. The screening mechanism of Koch and Shaqfeh is the only presently available theory that could lead to fluctuations and self-diffusivities that are independent of the vessel size.[5] However, the present experimental study is unable to prove that there is a deficit of one particle in the suspension surrounding any given particle as assumed by the screening theory. This still leaves open the problem of the ultimate structure of the sedimenting suspension which leads to finite values of the velocity fluctuations and self-diffusivities.

# Hydrodynamic Dispersion in a Sedimenting Suspension of Non-Brownian Particles

F.R. Da Cunha[1] & E.J. Hinch[2]


## Abstract

The particular problem which has been studied is the fluctuations in the sedimenting velocity of noncolloidal particles in a monodisperse suspension at low Reynolds number. We consider a suspension of point particles with excluded volume repulsion sedimenting in a rectangular box with periodic sides and impenetrable bottom and top. We have observed how the positions of the particles evolve in a finite container. We then discover that large fluctuations, which occur in sedimentation when inertia is very small, do not decay in time. We characterize the long time behaviour of the fluctuations by dispersion coefficients parallel and perpendicular to gravity. The strong anisotropy observed in the diffusion process is in good agreement with recent experiments.


## Introduction

The sedimentation problem addressed in this paper concerns fluctuations and dispersion as particle sediment. On a macroscopic scale, particle velocity fluctuations can lead to dispersion phenomenon that are important for understanding of mixing processes which inhibit separation.

We know the mean sedimentation velocity after Batchelor (1972). However, since the relative positions of the suspended spheres are continuously changing, the velocity of individual particles fluctuates during the sedimentation process. Recent experiments of Nicolai & Guazzelli (1994) disagree with the theoretical predictions of Caflish & Luke (1985) and Hinch (1988) which have suggested a dependence of the velocity fluctuations on the box size. Te important issue is to see whether the particles remain randomly and independently positioned as they fall. We will show some computer simulation of this, which reproduced the experimental correlation and anisotropy, but which had the size of the fluctuations increasing proportional to the size of the box.

## Governing Equation

Consider $N$ point-particles settling in a periodic box of dimensions $L \times L \times 2H$. Let $\mathbf{x}_i$ denote the position of the particle $i$. Suppose an external $\mathbf{f}_i$ is exerted on particle $i$ and let $\mathbf{u}_i$ be its translation velocity. In particular, we are interested in a new solution in which all components of the velocity field $(u, v, w)$ are periodic in $x$ and $y$ with period $L$, the horizontal components $u, v$ periodic in $z$ with period $H$, but the vertical component $w$ satisfying an impenetrable bottom and top condition of vanishing vertical velocity. Then we add a image system into the problem of solving Stokes flow in periodic box in order to obtain the complete solution of the new problem with impenetrable bottom and top and periodic sides. The element needed to compute the motion of the particles taking into account the hydrodynamic interaction between them is the following dimensionless equation

$$\mathbf{U}^i = \sum_{\alpha} \sum_{j}^{N} \mathcal{M}_{ij}^{ps}(\mathbf{R}_{\alpha,s}, \mathbf{R}_{\alpha,i}) \cdot \mathbf{F}_j + \frac{1}{V} \sum_{\mathbf{K}_\beta}{}' \sum_{j=1}^{N} \mathcal{M}_{ij}^{rs}(\mathbf{K}_\beta) \cdot \mathbf{F}_j \Theta,$$

with $\mathbf{F}_j = (0, 0, 1)$. Here the elements of the mobilities matrices $\mathcal{M}_{ij}^{ps}$ (physical space) and $\mathcal{M}_{ij}^{rs}$ (reciprocal space) and $\Theta$ are defined in Cunha (1994). This equation consist of two lattice sums. One in the real space over lattice vector $\mathbf{R}_\alpha$ and the other into the reciprocal space over reciprocal lattice vector $\mathbf{K}_\beta$. $\mathbf{R}_{\alpha,s}$ and $\mathbf{R}_{\alpha,i}$ are the relative position vectors associated with the source point and the image point respectively.

[1]University of Brasília, Department of Mechanical Engineering, Brasília-DF, Brazil.
[2]University of Cambridge, Department of Applied Mathematics and Theoretical Physics, Cambridge, UK.

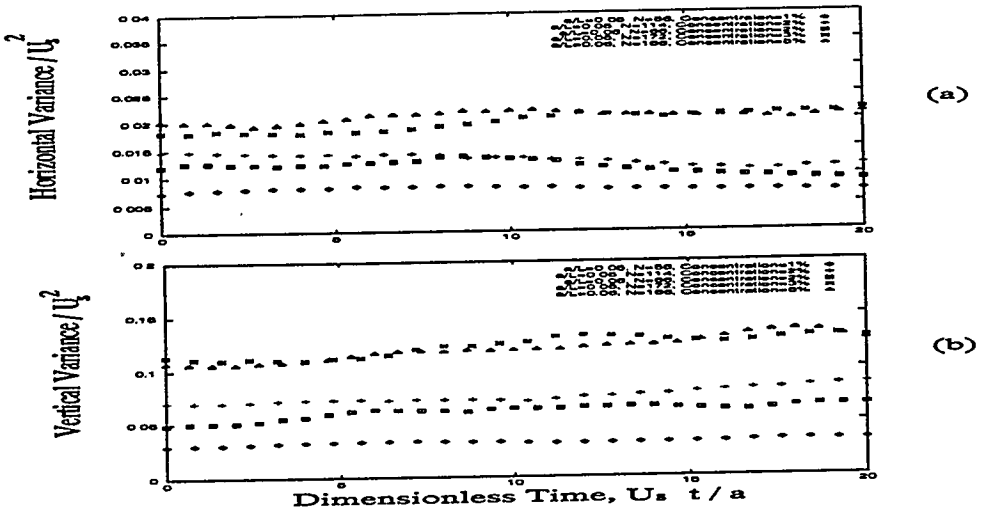


Figure 1: Results of the computer simulations for the time development of the dimensionless variances, both perpendicular (a) and parallel to gravity (b) for different conditions of the simulated system with the aspect ratio $H/L = 3$.

### Numerical results

The simulation all started with the particles located randomly and independently within the impenetrable box. The particle dispersion statistics was obtained over ten realisations (e.g. 10) which showed to produce meaningful statistics. The volume concentrations of the particles were in the range of dilute suspension ($\leq 5\%$) and different number of particles were simulated. Since $N_{min} = 25$ for the aspect ratios $a/L = 0.06$, $H/L = 3$ to a $N_{max} = 286$ for $a/L = 0.05$ and $H/L = 3$. Usually, $O(100)$ time steps yielding a dimensionless time of $O(0.04)$.

Figure 1 shows that the large velocity variances, both parallel ($\|$) and perpendicular ($\perp$) to the gravity direction, do not decay in time. The particles instead of to adopt configurations which would lead to finite variances in the sedimentation speed to remain nearly to the same initial structure and so with velocity fluctuations remaining proportional to $\phi L/a$, as the particles fall. The computer simulations predicted fluctuations growing with the size of the box, while the experiments (Nicolai & Guazzelli 1995) measured fluctuations that are independent of the size of box. One way for the theory and experiments to differ is for the positions of the particles not be independently random. As the experiments are reproductable and the stirring is different each time, one possibility is that the initial distribution evolves some form of fluctuations not like $\phi L/a$. The important question here is what is the difference between placing the particles initially at random in the computer simulations and stirring the suspension in laboratory.

Figures 2 compares numerical and experimental (Nicolai et al. 1994) time development of the normalized velocity fluctuation auto-correlation functions. The simulations and experiments both indicate that these functions decay in time as a single exponential toward zero, indicating that particle velocity becomes uncorrelated after long time. Finally we find that the amount of anisotropy in velocity fluctuations agrees well with results of numerical simulations by Ladd (1993) and with the recent theory of Koch (1994) both having found an $O(3)$. However the results of Ladd and Koch with respect to the ratio of diffusivities and correlation times were much different of the experiments and the present simulation. We have found $D_{\|}/D_{\perp} \sim O(10)$ throughout all computations and Nicolai et al. (1994) experiments an $O(5)$, while they suggested an $O(100)$. This large discrepancy can be justified by the fact that in Ladd's numerical simulations and Koch's theory both obtained a large anisotropy in correlations time $O(9)$ in contrast with the one that

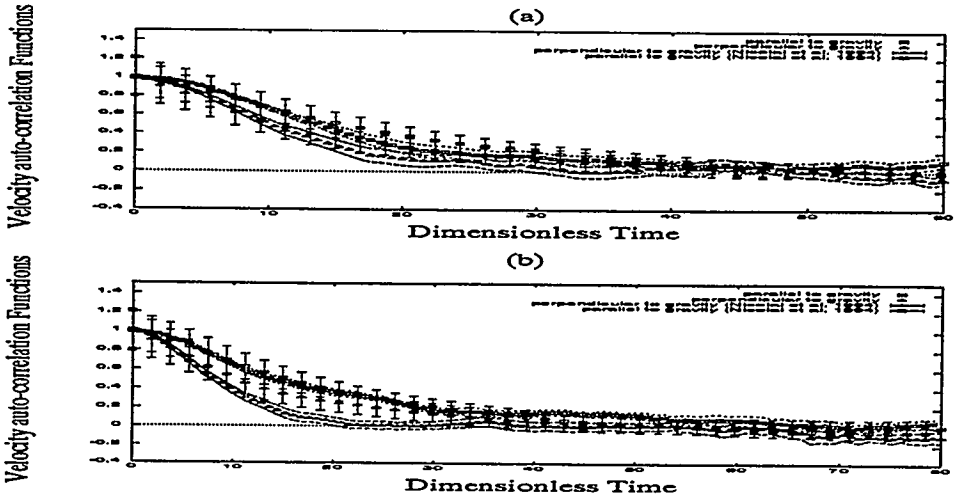


Figure 2: Normalized velocity fluctuation auto-correlation functions parallel and perpendicular to the gravity direction. (a) Computer simulations for $H/L = 3$, $a/L = 0.05$, $N = 114 \Rightarrow \phi = 2\%$ and (b) Computer simulations for $H/L = 3$, $a/L = 0.05$, $N = 172 \Rightarrow \phi = 3\%$. The error bars represent experimental data from Nicolai et al. (1994) with $\phi = 5\%$, $H/L = 4$, $H/w = 10$ and $w/a \approx 100$. The dashed lines indicates the uncertainly range of the present computer simulations.

has been found by us and Nicolai et al. (1994) measurements, i.e. $t_{\|}/t_{\perp} = O(2)$. At the same time Koch (1994) predicted that the time scale for the two self-diffusivities becomes much close when the influence of vertical boundary condition is removed. In this point we believe that the impenetrable box plays a vital role in simulating a sedimentation process. When a periodic bottom is considered the heavy part of the suspension falls indefinitely preserving the density excess. On the other hand if it imposed an impenetrable box, then there must be a convection current down on the heavy side, along the bottom, up the light side and cross the top. At a long time this convection decrease density fluctuations, and so reduces the correlation time, and increases horizontal fluctuations in velocity, producing the more realistic amount of anisotropy observed here.

## References

Batchelor (1972) Sedimentation in a dilute suspension of spheres. J. Fluid Mech. **240**, 651–657.

Caflish, R.E. & Luke, H.C. (1985). Variance in the sedimentation speed of suspension. Phys. Fluids **A28**(3), 759.

Cunha, F.R. (1994). Hydrodynamic dispersion in suspensions. PhD Thesis, DAMTP-University of Cambridge.

Hinch, E.J. (1988). Sedimentation of small particles. In Disorder and Mixing, Kluwer Academic Publishers, Boston, 153.

Koch, D.L. (1994). Hydrodynamic diffusion in a suspension of sedimenting point particles with periodic boundary conditions. suspensions of spheres. Phys. Fluids 6(9), 2894.

Ladd, A.J.C. (1993). Dynamical simulation of sedimenting spheres. Physics Fluids A(5), 299.

Nicolai, H. & Guazzelli, E. (1995). Effect of the vessel size on the hydrodynamic diffusion of sedimenting spheres. Phys. Fluids 7(1), 3.

# Dispersion in Concentrated Suspensions

**Howard Brenner**
*Massachusetts Institute of Technology, Cambridge, MA 02139*
**Lisa. A. Mondy**
*Sandia National Laboratories, Albuquerque, New Mexico 87185-0834*
**James R. Abbott** and **Alan. L. Graham**
*Los Alamos National Laboratory, ESA-EPE, Los Alamos, New Mexico 87545*

In order to probe homogeneous well-mixed suspensions with lightly intrusive probes that do not significantly disturb the microstructure, a series of falling ball experiments were performed under conditions such that the falling ball and the suspended particles were similar in size. Individual falling balls were allowed to settle through well-mixed suspensions of noncolloidal, neutrally buoyant spheres or rods of similar size in Newtonian liquids. In the center third of the containing cylinder, three-dimensional trajectories of the falling ball and instantaneous pressure drops across the falling ball were measured experimentally. The objective was to determine the effect of the discrete nature of the suspension on the dispersion of the momentum and pressure drop due to the falling ball.

In these experiments, the discrete nature of the suspension is readily apparent. A large ball will fall relatively smoothly through a suspension of smaller particles. The passage of a smaller ball of similar size or smaller than the suspended particles displays much larger variations. Periods of slow motion, as the falling ball settles almost directly on a suspended spheres or packed collection of spheres, alternate with periods of rapid motion as the ball moves between suspended particles.

The primary experimental parameters investigated were the size of the falling ball and the volume fraction, size, and geometry (spheres vs. rods) of the suspended particles. The experimentally measured trajectories were used to determine the variances in position of the settling sphere about the average trajectory along the centerline of the cylinder. Whereas a statistical analysis reveals that averages of 10-20 drops are required to produce reproducible average velocities to within a few percentage points of one another, several hundred ball drops would sometimes be required to obtain reproducible second moments within 20% of each other. We find that unlike the horizontal variances, the vertical variances were affected by short-time deterministic behavior relating to the instantaneous local configuration arrangement of the suspended particles.

For sufficiently long intervals between successive observations, the trajectories of the balls were observed to disperse about their mean settling paths in a random manner. This points to the existence of a Gaussian hydrodynamic dispersivity that characterizes the linear temporal growth of the variances in position of a falling ball.

Suspensions of 0.650 and 3.18 mm spheres with solids concentrations $\phi$ from 0.15 to 0.50 display a non-isotropic dispersivity, with the vertical dispersivity being 10-20 times larger than the horizontal dispersivity. The vertical dispersivity $\hat{D}_v$ (made dimensionless with the diameter of the suspended spheres and the mean settling velocity) was observed to decrease with increasing falling ball size at $\phi$ of 0.15 and 0.30. While the best fit shows that $\hat{D}_v$ increases with increasing ball size at $\phi$ of 0.50, an error analysis shows that a constant value for $\hat{D}_v$ is within 95% confidence limits based on the error limits shown in Fig. 1. For falling balls equal in size to the suspended spheres, $\hat{D}_v$ increased linearly with increasing volume fraction $\phi$ of solids (Abbott, 1993).

Other experiments were performed in suspensions of neutrally buoyant rods of aspect ratio of 20. Dispersivities observed in suspensions of rods and rendered dimensionless with the rod length,

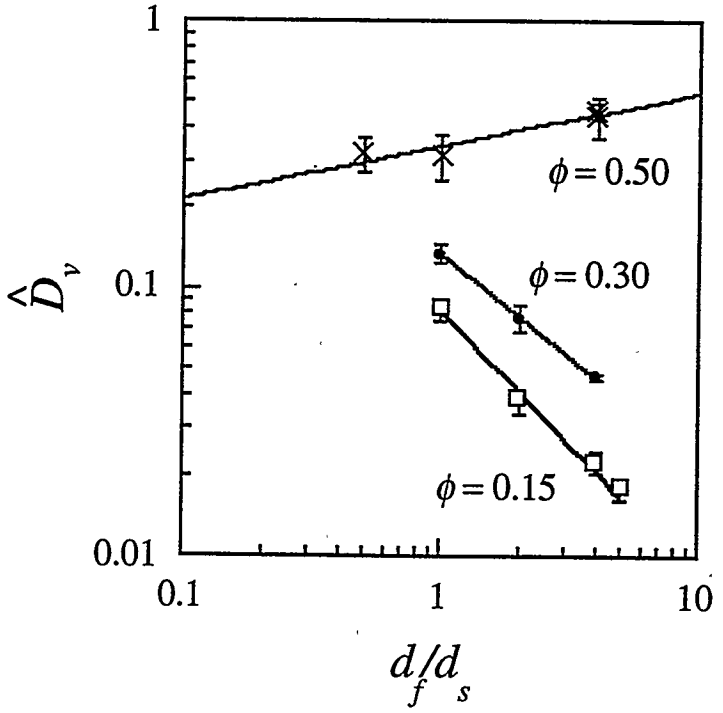


Figure 1: The vertical dimensionless dispersivity is shown as functions of the relative particle size for various concentrations.

showed no statistically significant dependence upon the falling ball diameter. In addition, these dispersivities were observed to increase approximately linearly when plotted against the specific viscosity of the suspension of rods.

For a sphere settling along the axis of a circular tube of radius $R_0$ filled with a pure viscous liquid, the pressure drop $\Delta P$ is related to the drag D on the sphere by

$$C \equiv \frac{\Delta PA}{D} = 2\left(1 - \left(\frac{b}{R_0}\right)^2 - \frac{2}{3}\left(\frac{a}{R_0}\right)^2\right) \tag{1}$$

where A is the cross sectional area of the cylinder, b is the distance from the sphere center to the cylinder axis, and a is the radius of the falling ball (Pliskin and Brenner 1963, Feldman and Brenner 1968). In pure Newtonian fluids at low to moderate Reynolds numbers, the value of C is determined to by the local velocity to the average velocity in a pressure driven flow. This results in a value of 2 for a small sphere settling at the center of a large cylinder. Equation 1 assumes that a no-slip condition exists at the cylinder wall. If perfect slip occurred at the cylinder walls, the value of C becomes 1.

In these experiments, the pressure drop associated with a ball settling in suspensions of spheres (a=3.17 mm) at $\phi$=0.30 and $\phi$=0.50 were examined. The settling spheres ranged in size from one-half to two times the size of the suspended spheres. Once again the discrete nature of the suspension was apparent with large fluctuations in the instantaneous $\Delta P$ observed. The average values of C* (C corrected for the size of the settling sphere) obtained from these experiments are shown in Fig. 2 along with the 95% confidence limits of the 10 ball drops used to obtain each data point. As in Newtonian fluids, C* was found be fairly independent of the relative size of the falling ball to the suspended particles. However, the values of C are consistently less than 2, and in the case of the largest falling balls statistically distinguishable from 2.

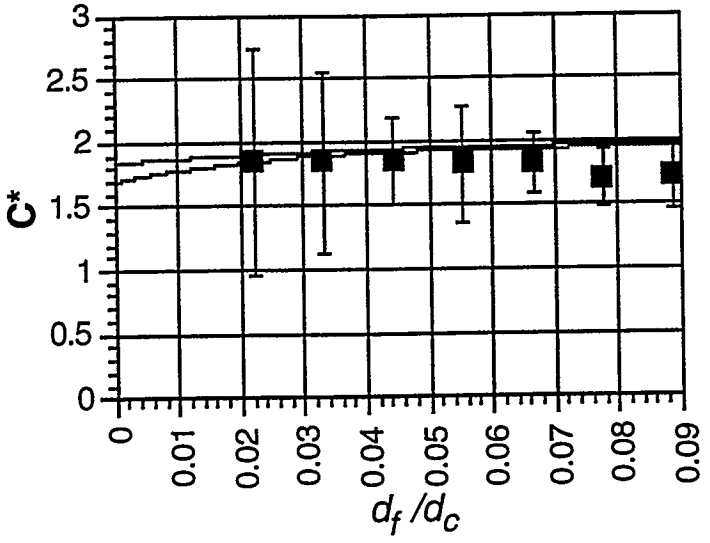


Figure 2: The relative pressure drop corrected for the size of the settling sphere as given by the second correction term in Eqn. 1 with error bars shown as a function of the diameter of the settling sphere to the diameter of the cylinder. The two lines represent the fitted corrections based on the dimensionless horizontal dispersivities, assuming a minimum and maximum value for the dimensionless dispersivities as a function of settling sphere size.

This deviation from the theoretically predicted values is possibly attributable to either of two factors. First, as described above, the falling ball's trajectory deviates from the centerline axis of the cylinder due to the interactions with the suspended particles. As shown in Eq. 1, these deviations of the trajectories would reduce the observed pressure drop. Using the dimensionless horizontal dispersivities (Abbott, 1993), the corrections to Eq. 1 that account for the average off-center position of the falling ball were obtained as shown in Fig. 2.

Although arguably the corrections fit all the data within the 95% confidence limits, the averages for the larger balls consistently lie below the predicted values. An alternate or perhaps additional correction may be attributable to the no-slip boundary condition on the containing cylinder wall that was used to derive Eq. 1. The presence of slip would be further reduce C below the value of 2. The determination of the appropriateness of the no-slip boundary condition in concentrated suspensions is the subject of ongoing investigations in our laboratories.

References

1. Abbott, J. R. 1993 Dispersive Processes in Concentrated Suspensions. PhD Thesis. Massachusetts Institute of Technology.

2. Feldman, G. A. and H. Brenner 1968 Experiments on the Pressure Drop Created by a Sphere Settling in a Viscous Liquid. Part 2. Reynolds Numbers for 0.2 to 21,000 *J. Fluid Mech* . **32** , 705-720.

3. Pliskin, I. and H. Brenner 1963 Experiments on the Pressure Drop Created by a Sphere Settling in a Viscous Liquid *J. Fluid Mech* . **17** , 89-96.

# Settling of a heavy sphere in the midst of a suspension of lighter spheres

Hélène Nicolai, Yannick Peysson and Elisabeth Guazzelli
Laboratoire de Physique et Mécanique des Milieux Hétérogènes,
URA 857 au CNRS, ESPCI,
10 rue Vauquelin, 75231 Paris CEDEX 05, France

In a sedimenting suspension of identical spheres, the continual change in the configuration of neighboring spheres and the resulting hydrodynamic interactions cause variations in the motion of a test sphere. After a large enough numbers of interactions, the test sphere executes a random walk through the suspension which has been described as a hydrodynamic self-diffusion process. Ham and Homsy[1] were the first to measure the coefficient of self-diffusion in a sedimenting suspension of non-Brownian spheres. These results were confirmed and extended by Nicolai and Guazzelli[2] and by Nicolai et al.[3].

A further problem on hydrodynamic diffusion is to examine the effect of polydispersity on the hydrodynamic diffusion process. The investigation of the motion of a single sphere of different settling velocity falling through an otherwise monodisperse suspension, which is an interesting problem in itself, is the first step toward the understanding of a fully polydisperse suspension.

In order to understand this first problem, different marked test spheres of different sizes and densities were tracked in a monodisperse suspension made optically transparent by matching the index of refraction of the suspending fluid to that of the glass spheres.[2, 3] The ratio, $R_s$, between the Stokes' velocity of the test particle and that of an isolated sphere of the suspension was varied from 1 to 13 while the particle volume fraction of the suspension was kept constant at 20.0%. The Reynolds number and Stokes number of the test particles were always smaller than $10^{-2}$. Statistical analyses of the particle local velocities yield the mean settling velocity, the vertical and horizontal velocity fluctuations and the particle velocity auto-correlation functions.

The mean settling velocity of the test particle was found to scale with the Stokes' velocity of the test particle, just as if the test particle settled in a fluid of effective viscosity. Conversely, the vertical and horizontal velocity fluctuations scaled with the Stokes' velocity of an isolated sphere of the suspension. Vertical fluctuations were found to be approximately twice as large as horizontal fluctu-

ations. The vertical and horizontal fluctuations of the test sphere were found to be of the same order of magnitude as the vertical and horizontal, respectively, fluctuations of the spheres of the suspension[3]. Indeed, the test sphere acted as a tracer which probed the velocity fluctuations of the fluid. However, a small increase of the vertical velocity fluctuations was observed as $R_s$ was increased. Moreover, the settling speed was found to experience a slight but continuous decrease along the vertical direction of the vessel for the fastest particles.

To analyze the long-time behavior of the test particle fluctuating motion, the relaxation of the autocorrelation functions of the horizontal and vertical velocity fluctuations was examined. For small values of $R_s$, both horizontal and vertical correlation functions decreased as a single exponential toward zero and had a similar relaxation. This behavior is similar to that found by Nicolai at al.[3] for the autocorrelation functions of the velocity fluctuations of the spheres of the suspension. As $R_s$ was increased ($R_s \geq 5$), the horizontal and vertical correlation functions exhibited a very different relaxation behavior. The horizontal function decayed more rapidly. It became negative and went through a minimum before approaching zero from below. Conversely, the vertical function decreased very slowly and still very smoothly. The vertical correlation time was found to increase with $R_s$ while the horizontal correlation time to decrease. The long time motion of the test sphere was shown to be diffusive in nature and the anisotropy of the diffusion process was found to increase with $R_s$.

An important finding of this study is the behavioral change in the motion of the test particle for $R_s \geq 5$. A plausible explanation would be that the test particle modifies the structure of the suspension. The test particle would then settle in a zigzag course and then build up a structure around it.

# References


[1] J. M. Ham and G. M. Homsy, "Hindered settling and hydrodynamic dispersion in quiescent sedimenting suspension," Int. J. Multiphase Flow **14**, 533 (1988).

[2] H. Nicolai and E. Guazzelli, "Effect of the vessel size on the hydrodynamic diffusion of sedimenting spheres," Phys. Fluids **7**, 3 (1995).

[3] H. Nicolai, B. Herzhaft, E. J. Hinch, L. Oger, and E. Guazzelli, "Particle velocity fluctuations and hydrodynamic self-diffusion of sedimenting non-Brownian spheres," Phys. Fluids **7**, 12 (1995).

**I.U.T.A.M. Symposium on-Hydrodynamic Diffusion of Suspended Particles**
Estes Park, Colorado, 22-25 july 1995

# HYDRODYNAMIC DISPERSION of NON-COLLOIDAL SUSPENSIONS: MEASUREMENT from EINSTEIN'S ARGUMENT

**J.Martin, N.Rakotomalala and D.Salin**
Laboratoire Fluides, Automatique et Systémes Thermiques *
Batiment n°502 Campus Universitaire 91405 Orsay Cedex France

Hydrodynamic dispersion[1-4] is responsible for the spreading of the sedimentation front in a non-colloidal monodisperse suspension. Hindered settling has an opposed effect and leads to the self-sharpening of the front. Following Einstein's argument[5] for the diffusion coefficient of colloidal dispersions, we postulate[6] that the steady-state concentration profile in a suspension of non-colloidal monodisperse particles reflects the dynamic equilibrium resulting from a balance between gravity-driven convection and hydrodynamic dispersion. Using an acoustic technique the steady state concentration profile of a counterflow stabilized suspension, a fluidized bed, as well as stationary propagating sedimentation fronts inside the bed were determined. From these profiles we can derive the concentration dependence of the hydrodynamic dispersion coefficient.

For a suspension statistically homogeneous in each horizontal direction, the volume fraction, C(x,t), is a function of the vertical direction x (downwards oriented) and time t. The mean velocity of the suspension is $V=CV_p+(1-C)V_f$, where $V_p$ ,and $V_f$ are the particle and fluid velocities respectively (all velocities are algebraic quantities). In the absence of inertia and concentration gradients, the momentum equation gives[7] $V_p-V=U(C)$, which expresses the balance between viscous and buoyancy forces. To account for the hydrodynamic dispersion, we postulate that the steady-state concentration profile in a suspension of non-colloidal monodisperse particles reflects the dynamic equilibrium resulting from a balance between gravity-driven convection and hydrodynamic dispersion. Therefore we express the particle flux $J=CV_p$ as the sum of a convective and a diffusive flux, to get

$$CV_p = C\,(\,U(C) + V\,) - D(C)\,\nabla C \qquad (1)$$

Substitution in the equation for the conservation of particles yields the convection-diffusion equation leading to a steady state in the laboratory frame of reference ($\partial C/\partial t = 0$, $V= -q$, where q is the volume fraction injection velocity):

$$C\,[U(C)-q] = D(C)\,\partial C/\partial x \qquad (2)$$

Eq.2 expresses the fact that the net convective flux due to an external force (gravity) through a plane moving at the suspension velocity is counterbalanced by the diffusion flux. This is Einstein's basic argument used to derive the diffusion coefficient of a colloidal suspension[5]. This is the same stationary shape profile which should be observed at the top of a sedimenting suspension[8] if polydispersity effects are negligible.

Experiments were performed in a column 60 cm high of a circular cross section (4cm) .We determine the concentration profile by measuring variations in the sound speed in several cross sections along the bed, as the sound speed in suspensions is related to the volume fraction of particles[6] (accuracy in concentration measurements, 0.1%, the spatial resolution to 1 mm). The liquid used is a water-glycerol mixture ($\eta=2.10^{-3}$ SI). The spherical glass beads have diameter $2a = 68.5\ \mu m$, with 95 % particles in the range 63-74μm. In the experiments, the particle Reynolds number is less

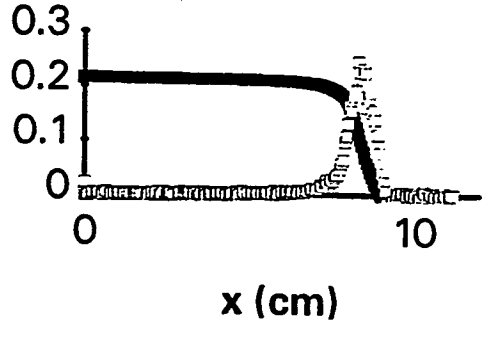

than 0.1 and Brownian motion is negligible. Fig.1 shows a typical concentration profile (■) C(x) and its gradient (□) $\partial C/\partial x$, for a flow rate corresponding to an average concentration of $C_0$~22 %. The profile consists of two parts, a top front of extent L, where the concentration increases from 0 to nearly $C_0$ and a long tail where the concentration is nearly constant to $C_0$. Using different flow rates q, we can determine the relation $U(C)=V_0(1-C)^p$ with p~5.0±0.2. Subsequently using the measured values of C and $\partial C/\partial x$, we can deduce the hydrodynamic coefficient D(C) from (2). Note that the smaller the flow rate, the sharper the front, making the measurements more difficult ( front width $L\sim D(C)/C_0$). For $C_0$=10%, L is of the order of 2 cm. Thus, larger concentrations require the design of a different experimental procedure that yield larger front widths.

We take advantage of both sedimenting suspension and fluidized bed features: the bed provides a steady homogeneous suspension in its bulk; reducing abruptly the flow rate from $q_1=U(C_1)$ to $q_2=U(C_2)$, a relative sedimentation is expected to occur, from $C_1$ to $C_2$, ($C_1<C_2$) with a front propagating from bottom to top. As the settling velocity (U(C)) is a decreasing function of concentration, smaller concentrations fall faster than larger ones, leading to a sharp (self-sharpening[14]) shock front. Because self-sharpening and hydrodynamic dispersion have opposing effects, this leads to a stabilised dispersed profile which propagates at a constant velocity $V_S$ without changing its shape [10,15]. We can obtain travelling wave of the form C(X), $X=x-V_St$, where C(X) is the solution of $C[U(C)-q-V_S] = D(C)\partial C/\partial X+A$. Fig.2 shows the concentration variation as a function of time, versus the variable X, at two different positions in the bed for an abrupt decrease of the flow rate from $q_1$ to $q_2$ corresponding to $C_1$ ~15 % and $C_2$ ~33 %. It is seen that the shape of the profiles is identical at the two different locations indicating a travelling front, the velocity of which was determined to be constant. This is the first observation of a stationary propagating front in a sedimenting suspension. We can then measure the diffusion coefficient.

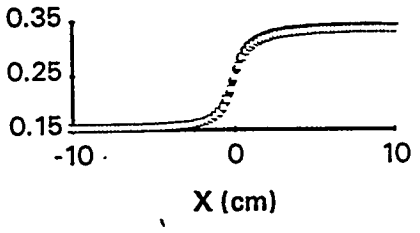


Our data[6] clearly show that D(C)/aU(C) increases roughly linearly with the volume fraction up to 15% and is almost constant in the range 15-30 %; it vanishes when approaching the packing concentration (~60%). The scattering of each data set leads to an overall accuracy of 10% on D, but we have not used any kind of data reduction. Note that the D determination is controlled by the knowledge of not only the flux F(C), but its derivatives (Fig.1). Thus for small concentration jumps around initial concentration larger than 35 %, the D determination is not very precise but the trend is there. We point out that the low concentration values of D are almost thrice as large as those previously determined from sedimentation front broadening[2,3,8]. And although in our experiments the Reynolds number (0.1) is larger than their ($10^{-3}$), the normalized dispersion coefficient remains the same when it was decreased, indicating that viscous forces are dominating. The values found are twenty times larger than those reported[2] based on the velocity fluctuations of a single particle or of the whole suspension[4]. This supports the contention that the latter measurements only capture the self-diffusion part of hydrodynamic dispersion.

* Associated with the Centre National de la Scientifique.

1: R. H. Davis and K. H. Birdsell, AIChE. J. **34**,123 (1988). R. H. Davis and M. A. Hassen, J. Fluid. Mech. **196**, 107 (1988).
2: J. Ham and G. M. Homsy, Int. J. Multiphase. Flow **14**, 533 (1988).
3: S. Lee, Y. Jang, C. Choi and T. Lee, Phys. Fluids **A 4**, 2601 (1992) .
4: J.Z. Xue, E. Herbolzheimer, M.A. Rutgers, W.B. Russel and P.M Chaikin, Phys. Rev. Lett. **69**, 1715 (1992) and references therein.
5: A. Einstein, Ann. d. Phys. **19**, 371 (1906)
6: J.Martin, N.Rakotomalala and D.Salin, Phys Rev Lett. **74**, 1347 (1995) and references therein.
7: G.K. Batchelor, J.Fluid Mech. **52**, 245 (1972); ibid, **193**, 75 (1988).
8: J.Martin, N.Rakotomalala and D.Salin, Phys Fluids Lett. **6**, 3215 (1994).

# Mean velocity in a suspension of droplets due to the thermocapillary effect

B.U. Felderhof
Institut für Theoretische Physik A
RWTH Aachen
Aachen, Germany

We study a suspension of droplets in an ambient fluid subject to gravity and a uniform temperature gradient. The surface tension of the droplets is taken to be so large that the droplets remain spherical. Due to the temperature dependence of the surface tension a droplet in a spatially varying temperature field experiences a force driving it in the direction of higher temperature. Since the thermal conductivity of droplets and ambient fluid differ, the temperature field is a complicated function of position. As a consequence, the microscopic description of the system encompasses the fluid flow field, the pressure field, the droplet positions and velocities, as well as the temperature field.

We show that the macroscopic description of such a suspension can be derived in the framework of a general scheme involving a multiple scattering expansion. The scheme leads to macroscopic average equations, as well as expressions for the transport coefficients occurring in these equations. We consider in particular the thermocapillary coefficient that relates the difference of mean droplet velocity and mean fluid velocity to the mean local temperature gradient. The expression for this coefficient is shown to be free of long range divergences, so that it is determined by the local microstructure of the suspension.

We calculate the thermocapillary coefficient as a function of droplet volume fraction in a mean field approximation, with correction terms due to pair correlations. The correction terms require the complete solution of the pair droplet problem in a uniform temperature gradient. This is obtained conveniently in terms of a series expansion in inverse powers of the distance between droplet centers. An arbitrary number of terms in this expansion can be evaluated by a concise matrix formulation.

# Shear-induced diffusion and particle migration

John F. Brady*

*Division of Chemistry and Chemical Engineering*
*California Institute of Technology*
*Pasadena, CA 91125*

Diffusion occurs in a wide variety of settings ranging from Brownian motion of submicron-sized particles to particle dispersion in high-Reynolds-number granular flows. Kinematically, the self-diffusivity can be related to the particle velocity-fluctuation autocorrelation function, showing quite generally that the diffusivity scales as the magnitude of the velocity fluctuations squared, $(v')^2$, times the correlation time for velocity fluctuations, $\tau$. Knowledge of the physical mechanisms generating velocity fluctuations and governing the correlation time can lead to simple scaling estimates for the self-diffusivity. In simple shear flow of nonBrownian particles at low Reynolds number $(v')^2 \sim O[(\dot{\gamma}a)^2]$, and $\tau \sim \dot{\gamma}^{-1}$, yielding the shear-induced self-diffusivity $D \sim O(\dot{\gamma}a^2)$, where $\dot{\gamma}$ is the magnitude of the shear rate and $a$ the particle size. The above scaling is borne out by experiment and numerical simulation, despite questions of flow symmetry and reversibility at low Reynolds numbers. It is shown that the effect of weak Brownian motion is singular and results in a shear-induced self-diffusivity that is independent of Brownian motion as the Peclet number, $Pe = \dot{\gamma}a^2/2D$, becomes large. Indeed, there is a continuous variation in the self-diffusivity with $Pe$ from the Brownian to the hydrodynamically dominated regime. The results from experiment and simulation will be discussed and compared.

Self diffusion describes the motion of an individually tagged particle and is to be distinguished from diffusion of all the particles down a concentration gradient, known as the collective or gradient or mutual diffusivity. The collective diffusivity is given by the product of the particles' mobility and the driving force, which in Brownian systems is the osmotic compressibility,

*This work was done in collaboration with T.N. Phung, P.R. Nott, and J.F. Morris.

$\partial\Pi/\partial\phi$, where $\phi$ is the volume fraction. This concept can be generalized to shearing flows where the osmotic pressure is now a function of concentration and shear rate or Peclet number, $\Pi(\phi, Pe)$.

Finally, there is particle migration, which is taken here to mean particle flux that is *not* the result of concentration gradients as this has already been included in the collective diffusivity. Migration refers to flux in a compositionally homogeneous suspension due to, for example, variations in shear rate or shear stress and need not necessarily be a "diffusive" motion. In a thermodynamic system variations in the thermal temperature give rise to particle flux down gradients in temperature – the Soret effect. Similar phenomena can occur in suspensions. The velocity fluctuations may be viewed as a measure of the "temperature", and since the velocity fluctuations are proportional to the shear rate, variations in shear rate will give rise to a flux analogous to the Soret effect. Alternately, noting the role played by the osmotic pressure in driving particle flux, a simple argument based on stress and Cauchy's equation of motion can predict migration: In a steady unidirectional flow, for example flow in a tube or channel, the variation in stress normal to the direction of motion must be constant. By dimensional analysis for low-Reynolds-number suspensions all stresses scale as $\eta\dot{\gamma}\mathcal{F}(\phi)$, where $\eta$ is the viscosity of the suspending fluid and $\mathcal{F}(\phi)$ is a nondimensional and monotonically increasing function of volume fraction.[†] If the shear rate varies, the volume fraction must vary so as to keep the stress constant. Where the shear rate is large the concentration will be low, and vice versa. In channel or tube flow this predicts migration of particles to the center. This concept is not limited to monodisperse spherical suspensions, nor to motion at low Reynolds number, and can predict migration in a variety of situations.[‡]

[†]We have assumed the ratio of the particle size to the length scale for variation normal to the direction of motion is small.

[‡]In geometrically more complex flows normal stresses and normal stress differences must be considered.

# Shear-Induced Migration in Colloidal Hard-Sphere Suspensions

D. T. Leighton, Jr.

*Department of Chemical Engineering*
*University of Notre Dame*
*Notre Dame, IN 46556*

Shear-induced migration in non-colloidal suspensions has been demonstrated to cause particles to migrate across streamlines due to gradients in concentration and in shear stress or shear rate (Leighton and Acrivos, 1986, 1987; Chapman 1990; Chapman and Leighton, 1991; Abbot, et al., 1991). While the experimental evidence for such migration is compelling, theoretical models describing the migration processes have been limited to either numerical simulations in simple flow fields (Nott and Brady, 1994) or to semi-empirical calculations. In this paper we describe theoretically the migration behavior in a closely related system: a dilute solution of highly charged colloidal spheres in which the effective hard sphere radius is much greater than the actual particle radius. For such a suspension the particles interact with the fluid through the Stokes flow equations independent of their electrical charge, and with each other electrostatically uninfluenced by their hydrodynamic disturbance velocities. This enables us to calculate the trajectory followed by the two interacting spheres exactly in this limit even for complex flow geometries, and to use these trajectories to determine the shear-induced migration behavior.

To see how such migration takes place, consider two spheres of radius a separated by a distance 2r interacting in a simple shear flow. The particles will be driven together by the shear flow with a hydrodynamic force which scales as:

$$F_h = 6\pi \dot{\gamma} \mu a^2 \frac{r}{a}$$

times some function of the angle of interaction where $\dot{\gamma}$ is the shear rate, $\mu$ is the fluid viscosity, a is the particle radius, and 2r is the separation distance between the particles. If the spheres are charged, this force will be resisted by an electrostatic force which scales as:

$$F_e = \pi \varepsilon \varepsilon_0 \left(\frac{kT}{ze}\right)^2 \Psi_A^2 \frac{1 + 2\kappa a \frac{r}{a}}{\left(\frac{r}{a}\right)^2} \exp\left(-2\kappa a \left(\frac{r}{a} - 1\right)\right)$$

where we have followed the notation of Russel, *et al.*, (1989). The ratio of these two forces is given by:

$$\frac{F_e}{F_h} = 2\pi \frac{D_0}{\dot{\gamma} a^2} \frac{n_b a^3}{(\kappa a)^2} \Psi_A^2 \frac{1 + 2\kappa a \frac{r}{a}}{\left(\frac{r}{a}\right)^3} \exp\left(-2\kappa a \left(\frac{r}{a} - 1\right)\right)$$

which depends on the Peclet number $(D_0/\dot{\gamma}a^2)^{-1}$ , the dimensionless ion concentration $n_b a^3$, the dimensionless surface potential $\Psi_A$, and the ratio of the Debye length to the sphere radius $\kappa a$. For the choice of physical parameters $2a = 0.5\mu m$, $n_b = 1.44 \times 10^{-6}$ M, $\dot{\gamma} = 10\ s^{-1}$, $\varepsilon = 80$, and $\mu = 0.01$p, we obtain the dimensionless values $\kappa a = 1$, $D_0/\dot{\gamma}a^2 = 1.4$, $n_b a^3 = 13.6$ and $\Psi_A = 4$ (saturation potential). This leads to the ratio of forces:

$$\frac{F_e}{F_h} = \lambda \frac{1 + 2\,\kappa a\, r^*}{(r^*)^3} \exp(-2\,\kappa a\,(r^* - 1))$$

where $\lambda = 1.9 \times 10^3$ and $r^* = r/a$ is the dimensionless separation.

To see how this leads to migration, consider the simple shear flow given by $u_i = \dot{\gamma}\, x_2\, \delta_{i1}$. We define the coordinate system $x_1 = r\cos(\theta)$, $x_2 = r\sin(\theta)\cos(\phi)$, and $x_3 = r\sin(\theta)\sin(\phi)$. In this coordinate system, the angle $\phi$ is unchanged during the particle interaction, and the radial position of the particles relative to the origin may be found from the expression:

$$\frac{d\,r^*}{d\,\theta} = -\,r^* \cot(\theta) + \frac{\lambda}{\sin^2(\theta)\cot(\phi)} \frac{1 + 2\,\kappa a\, r^*}{(r^*)^2} \exp(-2\,\kappa a\,(r^* - 1))$$

in which, subject to *a posteriori* justification, we have assumed the hydrodynamic interaction between the particles to be negligible and have ignored the effects of Brownian motion. This equation is integrated for the above value of $\lambda$ in figure 1. As may be seen, the trajectories for any initial separation are closely approximated from an effective hard-sphere trajectory with dimensionless radius $b/a = 4.7$. Because the minimum separation between two particles is thus greater than 8 radii, the assumption that hydrodynamic interactions are negligible is justified. Further, since the ratio $D_0/\dot{\gamma}b^2 = 0.063 << 1$ we are justified in ignoring Brownian effects. Finally, the equilibrium charge distribution assumed in obtaining the electrostatic force balance is reasonable since $D_i/\dot{\gamma}b^2 = 145 >> 1$ where $D_i$ is the ion diffusivity.

Based on this analysis it is reasonable to approximate the interaction of two charged particles for this particular range of physical parameters as effective hard spheres of radius b, which do not interact hydrodynamically and for which Brownian motion is negligible. With this simplification it is possible to calculate the rate with which particles are displaced across streamlines due to two particle interactions in complex flow geometries. We have examined a number of geometries:

*Self-Diffusion in simple shear:* Because particles are displaced from their original streamline during each interaction, they will execute a non-Brownian

Figure 1. Particle Trajectories With Electrostatic Repulsion

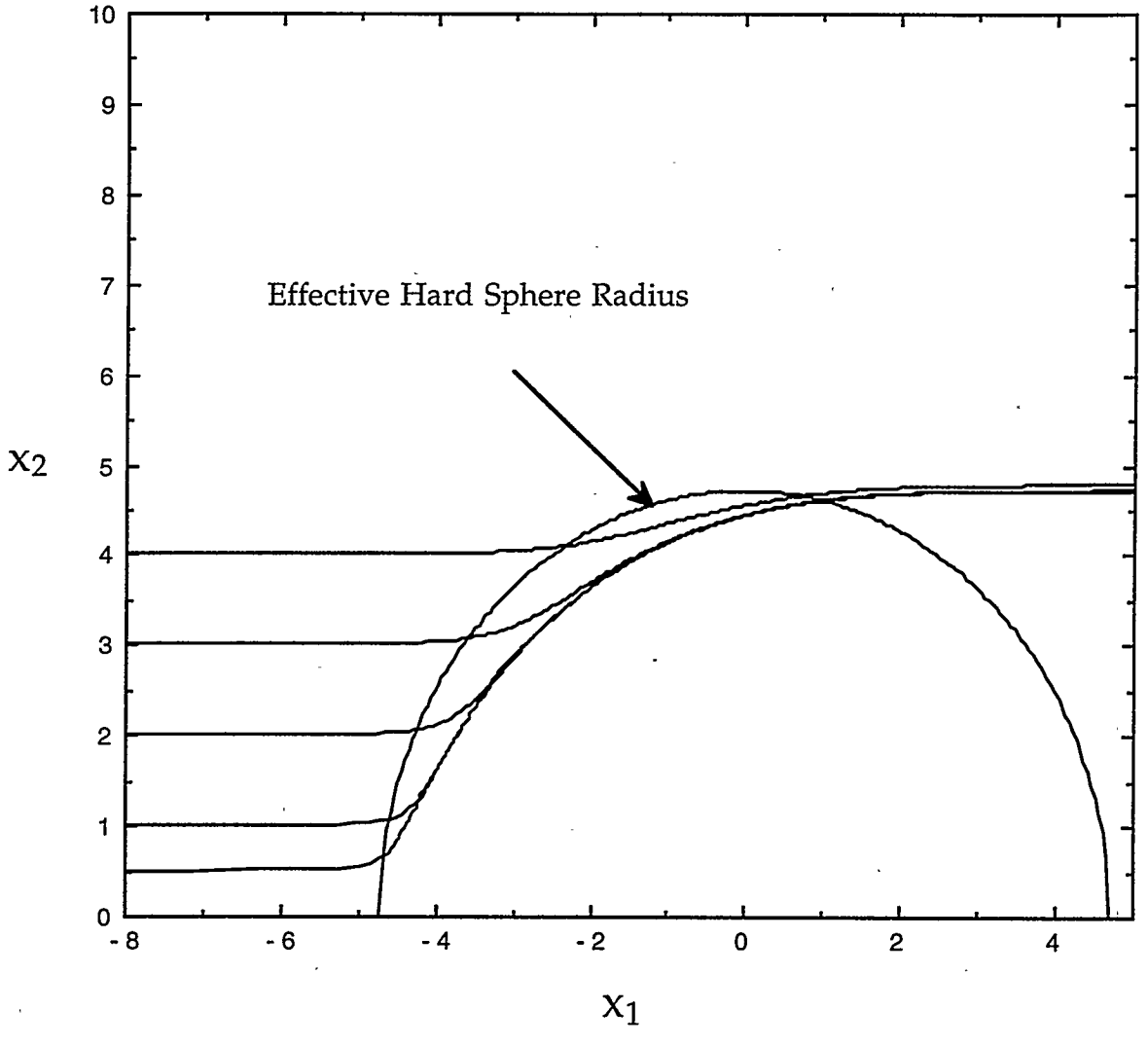

random walk in a shear flow. By determining the displacement during each interaction and the rate with which such interactions occur, it is possible to calculate the long-time random walk self-diffusion coefficients. These are:

$$D_{\parallel}^{sd} = \frac{4}{15\pi}\dot{\gamma} b^2 \left(\frac{4\pi}{3} b^3 n\right)$$

and

$$D_{\perp}^{sd} = \frac{2}{15\pi}\dot{\gamma} b^2 \left(\frac{4\pi}{3} b^3 n\right)$$

where $D_{\parallel}^{sd}$, the diffusivity in the plane of shear, is twice the diffusivity normal to the plane of shear $D_{\perp}^{sd}$.

*Drift due to gradients in concentration:* In addition to a random walk, particles also experience a deterministic drift from regions of high concentration to low as a consequence of experiencing more particle interactions particles approaching from regions of higher concentration. Again by looking at the rate of particle interactions, the drift can be directly calculated:

$$u_2^d = \frac{8}{5\pi}\dot{\gamma} b^2 \left(\frac{4\pi}{3} b^3 \frac{\partial n}{\partial x_2}\right)$$

and

$$u_3^d = \frac{4}{5\pi}\dot{\gamma} b^2 \left(\frac{4\pi}{3} b^3 \frac{\partial n}{\partial x_3}\right)$$

where again the drift due to gradients in the number density of particles n is twice as great in the plane of shear as normal to the plane. Note that the flux due to this drift is six times greater than that arising from the random walk diffusivities alone.

*Drift in unidirectional quadratic shear flows:* In addition to migration due to gradients in concentration, particles may also migrate due to gradients in shear rate. This occurs because more particles approach a test particle from regions of higher shear rate. We impose a unidirectional quadratic shear flow of the form:

$$u_i = \delta_{i1}\left[u|_{\tilde{y}} + \frac{\partial u}{\partial x_j}\Big|_{\tilde{y}}(x_j - y_j) + \frac{\partial^2 u}{\partial x_j \partial x_k}\Big|_{\tilde{y}}(x_j - y_j)(x_k - y_k)\right]$$

We define the dyadic:

$$A_{jk} = \frac{\partial^2 u}{\partial x_j \partial x_k}$$

which is a constant with only three independent non-zero elements. In the limit that $||A|| b << \dot{\gamma}$ we may calculate the drift due to each element independently. Thus:

$$u_2^d = -\left(\frac{4}{5\pi}\frac{\partial^2 u}{\partial x_2^2} + \frac{2}{5\pi}\frac{\partial^2 u}{\partial x_3^2}\right) b^2 \left(\frac{4\pi}{3} b^3 n\right)$$

and

$$u_3^d = -\frac{4}{5\pi}\frac{\partial^2 u}{\partial x_2 \partial x_3} b^2 \left(\frac{4\pi}{3} b^3 n\right)$$

Note that these expressions imply that migration due to gradients in shear rate will be different in plane-Poiseuille flow than in tube-Poiseuille flow.

*Drift in curved flow fields:* In addition to any gradients in shear rate, particles interacting along curved streamlines will experience a radially outward displacement during each interaction due to a radial component to the repulsive force. For cone and plate flow, the streamlines are curved but there are no gradients in shear rate. Provided that $b/R << 1$ where R is the radial position, the drift velocity in this geometry is given by:

$$u_r^d = \frac{16}{15\pi}\frac{\dot{\gamma}}{R} b^2 \left(\frac{4\pi}{3} b^3 n\right)$$

while for parallel-plate flow the drift is given by:

$$u_r^d = \frac{4}{15\pi}\frac{\dot{\gamma}}{R} b^2 \left(\frac{4\pi}{3} b^3 n\right)$$

The drift in parallel-plate flow may be interpreted as the combination of drift due to gradients in shear normal to the plane of shear, and drift due to curvature where the latter term is the same as in cone and plate flow:

$$u_r^d = \left(\frac{16}{15\pi}\frac{\dot{\gamma}}{R} - \frac{12}{15\pi}\frac{d\dot{\gamma}}{dR}\right) b^2 \left(\frac{4\pi}{3} b^3 n\right)$$

It is interesting to note that the two effects nearly cancel out. This is consistent with recent experimental observations in concentrated non-colloidal suspensions in parallel-plate flow.

# The effect of Surface Roughness in Shearing Suspension

F.R. Da Cunha[1] & E.J. Hinch[2]

## Abstract

In the absence of Brownian motion, inertia and inter-particle forces, two smooth spheres collide in a simple shear flow in a reversible way returning to their initial streamlines. Because the minimum separation during the collision can be less than $10^{-4}$ of the radius, quite a small surface roughness can have a significant irreversible effect on the collision. We calculate the change between the initial and final streamlines caused by roughness. Repeated random collisions in a dilute suspension lead to a diffusion of the particles across the streamlines. We calculate the shear-induced diffusivity for both self-diffusion and down-gradient diffusion.

## Introduction

Shear-induced dispersion is important in mixing particles across streamlines of pipe and channel flows (Leighton & Acrivos 1987). Earlier Acrivos, Batchelor, Hinch, Koch & Mauri (1992) calculated the dispersion along, rather than across, the streamlines, which involved a far field interaction between two pairs of spheres. In this paper we explore the effect of surface roughness on the collisions between two spheres. We will suppose that the asperities exert a normal force between the surfaces of two spheres which resists their becoming closer than the asperities but which does not exert any resistance as they separate.

In a dilute suspension we need only consider in detail the interaction between two spheres. Let the centres of the two spheres be $\mathbf{X}(t)$ and $\mathbf{Y}(t)$. The relative motion $\mathbf{x}(t) = \mathbf{X}(t) - \mathbf{Y}(t)$ is described by Batchelor & Green (1972). Non-dimensionalising lengths with the radius of the spheres $a$ and times with the inverse shear-rate $1/\gamma$, they give

$$\dot{x} = y + ex - \frac{2}{B}y, \quad \dot{y} = ey - \frac{2}{B}x, \quad \dot{z} = ez,$$

where $e = xy(B-A)/r^2$ *and* $r^2 = x^2 + y^2 + z^2$. Expressions for the mobility functions $A(r)$ and $B(r)$ and models of roughness can be found in a recent paper by Cunha & Hinch (1995).

## Numerical results

The governing equations for the trajectories of the pair of particles were integrated numerically using a 4th order Runge-Kutta scheme. The time-step can

[1]University of Brasília, Department of Mechanical Engineering, Brasília-DF, Brazil.
[2]University of Cambridge, Department of Applied Mathematics and Theoretical Physics, Cambridge, UK.

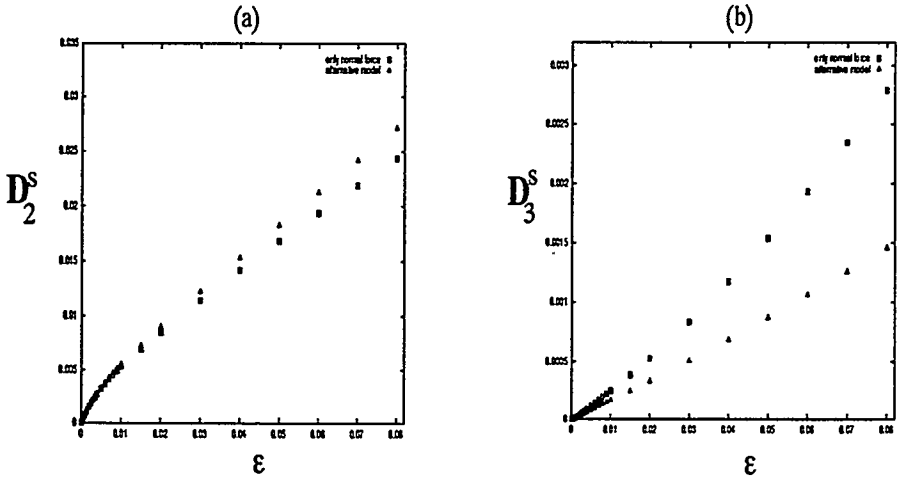


Figure 1: The self-diffusivities as a function of the surface roughness; (a) for diffusion in the direction of the gradient of velocity, and (b) for diffusion in the direction of the vorticity.

be larger in the far-field $r > 2.5$, where we took $\delta t = 0.005$. In the intermediate region $2.01 < r < 2.5$ we reduced the time-step to $\delta t = 0.01$. In the lubrication region $2 < r < 2.01$, the time-step was reduced further to $\delta t = 0.001$ to ensure that the radial separation changed little in one step. The errors in the numerical integration were then less than $10^{-3}$.

In this paper the random walk is across the streamlines and is due to collisions with other particles in the shear flow. We will calculate the diffusivities for displacements in the $y$-direction and in the $z$-direction.

We first consider a dilute suspension with a uniform concentration. Since we are assuming that each of these collisions is uncorrelated, we have dimensionless self-diffusivities

$$D_i^s = a^2\gamma\phi\frac{3}{8\pi}\int_{-\infty}^{\infty}\int_{-\infty}^{\infty}(\Delta X_i)^2|y_2^{-\infty}|\,dy_2^{-\infty}dy_3^{-\infty} \qquad (i=2,3).$$

The above integral was evaluated numerically over the grid of $y_2^{-\infty}y_3^{-\infty}$ points using a trapezoidal rule. The spacing of 0.05 between points produced an error less than 0.1%. Now in recent experiments Leighton (private communication) has found self-diffusivities of $2.7\times10^{-4}a^2\gamma$ at a concentration of $\phi = 0.01$ and $5.6\times10^{-4}a^2\gamma$ at $\phi = 0.025$. From the vertical scales of figure 1, we note that for a surface roughness of $\epsilon = 0.02$ our $D_2^s = 0.008a^2\gamma\phi$ gives $8\times10^{-5}a^2\gamma$ at $\phi = 0.01$ and $2\times10^{-4}a^2\gamma$ at $\phi = 0.025$. Thus while interactions

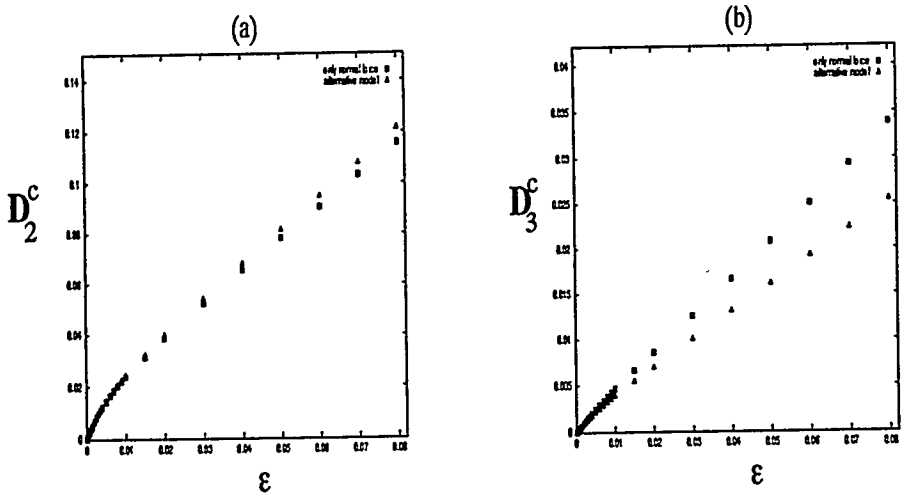


Figure 2: Down-gradient diffusivities. See caption to figure 1 for details.

between more than two spheres must be important at these concentrations, it seems that surface roughness also not be neglected.

We finally consider a suspension which has a small gradient in the concentration in a direction across the streamlines, separately in the direction of the velocity gradient and in the direction of the vorticity, i.e. $n(\mathbf{x}) = n_o + x_i \frac{\partial n}{\partial x_i}$ $(i = 2, 3)$. This yields a net flux of particles across the streamlines which is proportional to the concentration gradient, the coefficient of proportionality being a diffusivity $D_i^c$ (see Cunha & Hinch 1995 for details). Figure 2 shows down-gradient diffusivities larger than self diffusivities by a factor of 5 for the direction of the velocity gradient and by a factor of 10 for the direction of the vorticity.

## References

Acrivos, A., Batchelor, G.K., Hinch, E.J., Koch, D.L. & Mauri, R. (1992) Longitudinal shear-induced diffusion of spheres in a dilute suspension. J. Fluid Mech. **240**, 651–657.

Batchelor, G.K. & Green, J.T. (1972) The hydrodynamic interaction of two small freely-moving spheres in a linear flow field. J. Fluid Mech. **56**, 375–400.

Cunha, F.R. & Hinch, E.J. (1995) Shear-induced dispersion in a dilute suspension of rough spheres. submitted to J. Fluid Mech.

Leighton, D.T. & Acrivos, A. (1987) Measurement of shear-induced self-diffusion in concentrated suspensions of spheres. J. Fluid Mech. **177**, 109–131.

Leighton, D.T. (1993) private communication.

# Collision Properties of Non-Simple Bodies and their Influence on Hydrodynamic Dispersion

Ludwig C. Nitsche* and Johannes M. Nitsche†

*Department of Chemical Engineering
University of Illinois at Chicago
810 South Clinton Street
Chicago, Illinois 60607

†Department of Chemical Engineering
Clifford C. Furnas Hall
State University of New York at Buffalo
Buffalo, New York 14260

The phenomenon of shear-induced diffusion,[1–7] central to the theory and practical applications of viscous suspension mechanics, depends critically on the outcome of interparticle hydrodynamic interactions and collisions on the microscopic scale. Perfectly smooth spherical particles suffer net longitudinal displacements, but no net lateral displacements, as a result of binary encounters.[8] Irreversibility, produced for example by surface roughness,[9] can produce net lateral movements. This talk summarizes an investigation of the collision mechanics of several model particles incorporating structural elements additional to the basic two-smooth-sphere problem.

(i) Binary trajectories are calculated for spherical entities combining a hard hydrodynamic core with a slightly-displaced steric shell, representing a simple, radially symmetric representation of the effects of surface roughness.[9] This structure eliminates the lubrication singularity (as would a thin porous layer at the surface[10]) and allows interparticle contact to occur, thereby bringing non-hydrodynamic forces and irreversibility into play. For suitable initial configurations, particle interaction occurs as a three-step process involving approach with pre-collision hydrodynamic interaction, contact and collective rotation as a doublet until a tensile stress is experienced, and separation with post-collision hydrodynamic interaction. Lateral and longitudinal displacements are determined as functions of the initial relative position for various values of the steric shell thickness. Additional calculations address the influence of (non-hydrodynamic) colloidal forces. Approximate expressions for the Stokes resistance coefficients of spheres interacting near a plane wall are used to study how hydrodynamic wall effects influence the collision process.

(ii) Slender body theory[11,12] is used to characterize the hydrodynamic interaction of thin cylindrical particles. These calculations, based on detailed solution of the pertinent coupled integral equations for the axial linear force densities, lead to an assessment of the quantitative accuracy of the lowest-order slender body approximation used in recent analyses of hydrodynamic dispersion.[13,14]

(iii) To complement analyses of rigid nonspherical particles[13–15], deformable, porous bodies are here modeled as three-dimensional, girder-like assemblies of beads and (nonlinear) springs — representing a discrete version of volumetrically distributed hydrodynamic resistance. Lateral and longitudinal displacements for binary encounters are computed, and the results are generalized for the presence of a plane wall. The potential energy of deformation is tracked along each particle trajectory.

Averages over initial positions and (where applicable) conformations are used to estimate the contributions of interparticle contact and configurational effects to the shear-induced self-diffusion coefficient in the dilute limit.


[1]E.C. Eckstein, D.G. Bailey and A.H. Shapiro, Self-diffusion of particles in shear flow of a suspension. *J. Fluid Mech.* **79**, 191 (1977).

[2]D. Leighton and A. Acrivos, Viscous resuspension. *Chem. Eng. Sci.* **41**, 1377–1384 (1986).

[3]D. Leighton and A. Acrivos, Measurement of shear-induced self-diffusion in concentrated suspensions of spheres. *J. Fluid Mech.* **177**, 109–131 (1987).

[4]D. Leighton and A. Acrivos, The shear-induced migration of particles in concentrated suspensions. *J. Fluid Mech.* **181**, 415–439 (1987).

[5]D.L. Koch, On hydrodynamic diffusion in sheared suspensions. *Phys. Fluids A* **1**, 1742–1745 (1989).

[6]A.L. Graham, S.A. Altobelli, E. Fukushima, L.A. Mondy and T.S. Stephens, Note: NMR imaging of shear-induced diffusion and structure in concentrated suspensions undergoing Couette flow. *J. Rheol.* **35**, 191–201 (1991).

[7]J.R. Abbott, N. Tetlow, A.L. Graham, S.A. Altobelli, E. Fukushima, L.A. Mondy and T.S. Stephens, Experimental observations of particle migration in concentrated suspensions: Couette flow. *J. Rheol.* **35**, 773–795 (1991).

[8]A. Acrivos, G.K. Batchelor, E.J. Hinch, D.L. Koch and R. Mauri, Longitudinal shear-induced diffusion of spheres in a dilute suspension. *J. Fluid Mech.* **240**, 654–657 (1992).

[9]J.R. Smart and D.T. Leighton, Measurement of the hydrodynamic surface roughness of noncolloidal spheres. *Phys. Fluids A* **1**, 52–60 (1989).

[10]Y. Solomentsev, A. Kotov and V. Starov, Hydrodynamical interaction of two particles covered with a porous layer. *Int. J. Multiphase Flow* **18**, 739–750 (1992).

[11]G.K. Batchelor, Slender-body theory for particles of arbitrary cross-section in Stokes flow. *J. Fluid Mech.* **44**, 419–440 (1970).

[12]W.B. Russel, E.J. Hinch, L.G. Leal and G. Tieffenbruck, Rods falling near a vertical wall. *J. Fluid Mech.* **83**, 273–287 (1977).

[13]M. Rahnama, D.L. Koch, Y. Iso and C. Cohen, Hydrodynamic, translational diffusion in fiber suspensions subject to simple shear flow. *Phys. Fluids A* **5**, 849–862 (1993).

[14] M. Rahnama, D.L. Koch and E.S.G. Shaqfeh, The effect of hydrodynamic interactions on the orientation distribution in a fiber suspension subject to simple shear flow. *Phys. Fluids* **7**, 487–506 (1995)

[15]S. Kim, Singularity solutions for ellipsoids in low-Reynolds-number flows, with applications to calculation of hydrodynamic interactions in suspensions of ellipsoids. *Int. J. Multiphase Flow* **12**, 469 (1986).

# Motion of a sediment layer due to a laminar, stratified flow

by U. Schaflinger
Institute of Fluid Mechanics and Heat Transfer, Technical University,
Vienna, Austria

Advanced oil prospecting has become an important field in science and engineering. Several techniques have been developed in the last few years to increase the output of oil fields (Unwin & Hammond, 1994). In one specific method, a two-phase mixture of small solid particles, which are either sand, porcelain or even crushed walnut shells, and a highly viscous Newtonian fluid is pumped via the drill hole into the cracks of the surrounding rocks. The high pressure widens the fractures in which particles separate under gravity from the flowing carrier fluid and the sediment eventually moves as a resuspended layer due to viscous effects (Leighton & Acrivos, 1986). After the shut down of the flow, the sediment of particles is supposed to keep the cracks open, thereby increasing its void fraction and a subsequent reversed flow of oil is possible. The whole process can be considered as a typical practical example of viscous resuspension in a two-dimensional channel (Schaflinger et al., 1990) since all Reynolds numbers associated with this flow are small. In order to control the process, it is very important to estimate the entrance region until all particles have separated from the carrier fluid and to determine the distance the sediment layer has traveled within the cracks (Schaflinger, 1993).

Resuspension is a process by which an initially settled layer of heavy particles in contact with a clear fluid it is set into motion by a laminar shear flow. When a clear fluid flows above an initially settled bed of heavy, non-Brownian particles, at least part of the sediment layer will resuspend, even at low Reynolds numbers. The physics of viscous resuspension has been recently extensively investigated (Acrivos, 1993). Several uni-directional flows such as a plane Couette flow, a plane film flow, and a 2-D Hagen-Poiseuille channel flow were investigated based on a theoretical model developed by Leighton & Acrivos (1986).

For simplification, we suppose the cracks to be two dimensional channels and average the previously obtained base-state results (Schaflinger et al., 1990) for the flow and the volume concentration of particles. Then, the entrance of an originally well mixed suspension flowing into a two-dimensional channel and the subsequent propagation of the emerging sediment layer can be investigated by applying the theory of kinematic waves (Witham, 1974). Schaflinger et al. (1995) have shown that at the entrance region particle separation due to gravity is usually the dominating effect. This is because, when a well-mixed but dilute suspension of heavy particles enters the channel, the flux is negligible at first due to shear-induced diffusion and becomes important only at a later state, i.e. when the flow has already segregated into a pure liquid and a concentrated suspension. Thus, we assume local equilibrium in the spatially growing sediment layer between the flux due to gravity and hydrodynamic diffusion. In such a case, the entrance length is equal to the distance until the resuspended sediment layer has reached its maximum height, i.e. when all particles have separated from the original suspension (fig. 1).

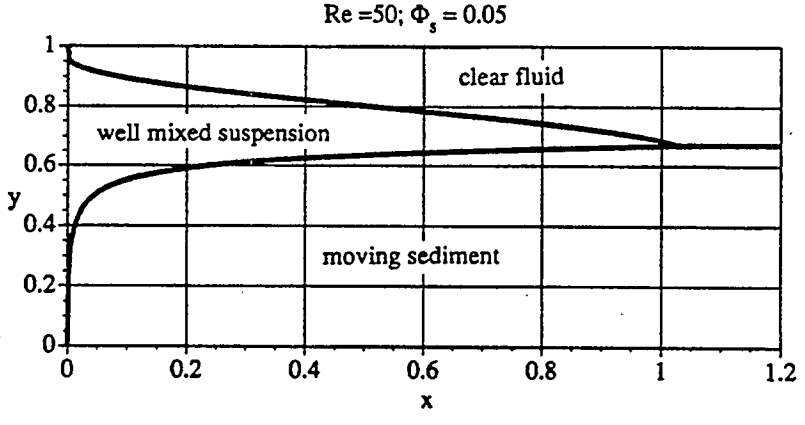


Figure 1. Entrance of a well mixed suspension with particle volume concentration $\Phi_S$ into a two-dimensional channel.

Eventually, we attain numerically a flux diagram for both the kinematic wave velocity and the kinematic shock velocity and we show that a sudden onset and a sudden end of a sediment layer move as a combination of kinematic shocks and kinematic waves. Both velocities are much smaller than the average velocity of the clear liquid.

Therefore we are able to estimate the time until a certain amount of particles has traveled into a given length of fracture.

Experimental observations of the motion of a sudden end of a sediment layer in a two-dimensional channel flow correspond well with the theory if the flow-rate of clear liquid is small, which is usually the case in oil prospecting. If the flow-rate is increased, however, we observe strong instabilities and eventually wave breaking at the interface between the resuspended sediment and the clear liquid (Zhang et al., 1992; Schaflinger, 1994). In this case, the speed of the dynamic waves is much faster than the velocity of kinematic waves or kinematic shocks. Thus, the observed propagation of a sudden end of sediment is significantly larger than predictions based on a theory of kinematic waves.

## Literature


ACRIVOS, A. 1993 The rheology of concentrated suspensions of non-colloidal particles. In *Particulate Two-Phase Flow*. ed. ROCO, M., Butterworth-Heinemann, Boston.

LEIGHTON, D. & ACRIVOS, A. (1986) Viscous resuspension. *Chem. Engng. Sci.* **41**, 1377-1384.

SCHAFLINGER, U., ACRIVOS, A. & ZHANG, K. 1990 Viscous resuspension of a sediment within a laminar and stratified flow. *Int. J. Multiphase Flow* **16**, 567-578.

SCHAFLINGER, U. 1993 Transport of a sediment layer due to a laminar, stratified flow. *Fluid Dynamics Research* **12**, 95-105.

SCHAFLINGER, U. 1994 Interfacial instabilities in a stratified of two superposed flow. *Fluid Dynamics Research* **13**, 299-316.

SCHAFLINGER, U., ACRIVOS, A. & STIBI, H. 1995 An experimental study of viscous resuspension in a pressure-driven plane channel flow. *Int. J. Multiphase Flow*, (in press).

UNWIN, A.T. & HAMMOND, P.S. 1994 A simple phenomenological model for shear driven particle migration in concentrated viscoelastic suspension. IUTAM Symposium on Liquid-Particle Interactions in Suspension Flow, Grenoble, France.

WITHAM, G.B. 1974 *Linear and Nonlinear Waves.* (Wiley, New York).

ZHANG, K., ACRIVOS, A. & SCHAFLINGER, U. 1992 Stability in a two-dimensional Hagen-Poiseuille resuspension flow. *Int. J. Multiphase Flow* **18**, 51-63.

# THE SHEAR INDUCED-DIFFUSION OF PARTICLES IN A RECTANGULAR FRACTURE CHANNEL

I. MISKIN, L. ELLIOTT, D.B. INGHAM, P.S. HAMMOND*
Department of Applied Mathematical Studies, University of Leeds, Leeds LS2 9JT, England
*Schlumberger Cambridge Research Limited, P.O. Box 153, Cambridge, CB3 0HG, England

## ABSTRACT

It has been observed that in laminar shear flows particles within suspension migrate in the direction of decreasing shear. This phenomena, termed 'shear-induced diffusion' arises from the hydrodynamic interactions between neighbouring particles. In this paper a simple model for the flow of a particulate suspension within a rectangular channel is studied with the effects of shear-induced difusion included. An equation is formulated for the particle concentration which is solved initially for a fully developed steady one-dimensional gravity driven flow down an inclined channel. The problem is then developed by adding a pressure driven flow perpendicularly across the gravity driven flow. The concentration, momentum and conservation of mass equations have been solved numerically under a wide variety of operating conditions and initial feed concentrations, and typical concentration and velocity profiles at various angles of inclination of the channel and strengths of cross flow are presented.

## INTRODUCTION

The phenomena of viscous resuspension is of practical importance in many industrial operations. One of the most common processes in industry involves the separation between a particulate phase and the continuous fluid which constitute a particular slurry. Often this is achieved using gravity settling, which is a relatively slow process when particles are small and the fluid is viscous. Thus, the effect of viscous resuspension could significantly reduce the performance of these settling devices. However, if properly exploited, viscous resuspension can have a positive influence on some industrial operations, such as the process by which proppant particles are placed within a hydraulic fracture in the hydrocarbon industry. When a fracture is created, a fluid containing proppant particles is pumped into it. Ideally, the proppant particles should settle evenly along the entire length of the fracture so that when pumping ceases the fracture is wedged open by the sedimented particles. By taking advantage of viscous resuspension effects it is possible to entrain particles from a settled bed back into the bulk shear flow which will enable them to be convected deep into the fracture channel and thus avoid the possibility of closure.

The purpose of this paper is to examine theoretically viscous resuspension, using a similar model to that employed by Leighton & Acrivos (1986) and Schaflinger et al. (1990), initially for a fully developed steady one-dimensional gravity-driven flow down an inclined channel and then to extend the problem by adding a perpendicular pressure-driven flow across the inclined plane. This latter situation is a reasonable model for proppant flows in inclined fractures provided that the angle of inclination, $\alpha$, is assumed to be sufficient for entrainment to occur without particles being contained in a stagnant packed bed along the lower surface of the fracture.

# THE CONCENTRATION EQUATION

Consider the flow of a suspension, consisting of uniform spherical particles, down an inclined channel of height $2B$ which is at an angle $\alpha$ to the horizontal when there is a constant pressure gradient applied across the channel, i.e. in the $x^*$-direction, see figure 1. The volume of flux of clear fluid per unit depth flowing in the $x^*$ and $y^*$-directions are $\lambda Q$ and Q, respectively, where Q is an adjustable parameter. In this paper we take the region of interest sufficiently far from the inlet regions and down the incline that all the components of the velocity are functions of $z^*$ alone and therefore the $z^*$-component of velocity is zero. The velocity components are $U^*$ and $V^*$ in the $x$ and $y^*$-directions, respectively.

As the suspension flows some particles within it will begin to sediment, due to the effect of gravity, while others will resuspend because of the diffusion caused by the shear flow. If steady state is achieved, i.e. the sedimentation flux balances the shear-induced diffusive flux of particles, the flow basically consists of two distinct regions, namely a region of clear fluid above a region of suspension which has a variable concentration, see figure 2. We consider the suspension to consist of rigid spherical negatively buoyant particles, which are of uniform size and density and which do not aggregate, settling at very small Reynolds numbers from a suspension comprised of an incompressible Newtonian fluid. The particle flux due to sedimentation in the $z^*$-direction is given by

$$N_g = -\phi f(\phi)\left[\frac{2}{9}a^2 g\frac{(\rho_2-\rho_1)}{\mu_1}\right]\cos\alpha \tag{1}$$

for a rectangular channel inclined at an angle $\alpha$ to the horizontal, see figure 1, where $\phi$ is the local particle concentration, $g$ is the acceleration due to gravity, $a$ is the particle radius, $\mu$ is the viscosity, $\rho$ is the density, $\left[\frac{2}{9}a^2 g\frac{(\rho_2-\rho_1)}{\mu_1}\right]$ is the dimensional Stokes settling velocity, the subscripts 1 and 2 refer to the clear fluid and the particle properties, respectively, and $f(\phi)$ is called the hindered settling function. In this work the hindered settling function was chosen to be the same as that used by Leighton & Acrivos (1986), Schaflinger et al. (1990) and Zhang & Acrivos (1994), namely,

$$f(\phi) = \frac{1-\phi}{\mu_r} \tag{2}$$

where $\mu_r$ is the relative viscosity between the suspension and the clear fluid and is given by Leighton & Acrivos (1987) as

$$\mu_r = \frac{\mu_m}{\mu_1} = \left[1+\frac{1.5\phi}{1-\frac{\phi}{\phi_o}}\right]^2 \tag{3}$$

where $\phi_o$ is the volume fraction of particles in the state of close packing and typically takes the value 0.58, see Leighton & Acrivos (1986), and the subscript $m$ denotes the suspension properties. The flux due to shear-induced resuspension is given by

$$N_s = -K_c a^2\left(\phi^2\frac{d\dot{\gamma}^*}{dz^*}+\phi\dot{\gamma}^*\frac{d\phi}{dz^*}\right)-K_\mu\phi^2\dot{\gamma}^*\left(\frac{a^2}{\mu_r}\right)\frac{d\mu_r}{d\phi}\frac{d\phi}{dz^*} \tag{4}$$

see Phillips et al. (1992), where $K_c$ and $K_\mu$ are constants of proportionality which have to be determined experimentally and $\dot{\gamma}^*(z^*)$ is the dimensional absolute shear rate. In our calculations, $K_c$ and $K_\mu$ are taken to be 0.43 and 0.65, respectively, i.e. the values suggested by Phillips et al. (1992). For a steady state to exist we require

$$N_g + N_s = 0 \tag{5}$$

The quantities used in the non-dimensionalisation process for the length and shear stress are $2B$ and $2B\rho_1 g\sin\alpha$, respectively. By substituting expressions (1) and (4) into equation (5), non-dimensionalising and re-arranging we obtain

$$\frac{d\phi}{dz} = -\frac{\frac{2}{9}\epsilon(1-\phi)\cot\alpha + K_c\phi\frac{d}{dz}\left[\left\{\tau_m^{x\,2}+\tau_m^{y\,2}\right\}^{\frac{1}{2}}\right]}{\left\{\tau_m^{x\,2}+\tau_m^{y\,2}\right\}^{\frac{1}{2}}\left[\frac{(K_\mu-K_c)}{\mu_r}\frac{d\mu_r}{d\phi}\phi+K_c\right]} \tag{6}$$

where $\kappa$ is the modified Shields number which gives a measure of the ratio between viscous and buoyancy forces and is given by

$$\kappa = \frac{9}{16}\frac{\mu_1 Q}{B^3 g(\rho_2-\rho_1)} \tag{7}$$

and the dimensionless shear stress within the suspension layer, $\tau_m$, is given by

$$\dot{\gamma}_m = \frac{\tau_m}{\mu_r} = \frac{1}{\mu_r}\left[\tau_m^{x\,2}+\tau_m^{y\,2}\right]^{\frac{1}{2}} \tag{8}$$

where the superscripts $x$ and $y$ denote quantities in the $x^*$ and $y^*$-directions, respectively.

## RESULTS

For the case with no cross flow, it is shown that as the angle of inclination increases a constant concentration profile is reached within the resuspension layer and the velocity has its maximum value at the particle-clear fluid interface. Thus, the resuspension is restricted due to the existence of a plane on which the shear stress vanishes and hence it is not possible to obtain solutions at larger angles of inclination.

When $\lambda \neq 0$, i.e. there is a cross flow present, increasing the flow rate sufficiently in the $y^*$-direction at a fixed angle of inclination produces a value for the concentration within a thin layer close to the centre of the channel that approaches the limit of maximum packing, namely, $\phi = 0.58$. When the channel is inclined at larger angles to the horizontal, the ratio of the volume of clear fluid flowing in the $x^*$-direction to that in the $y^*$-direction at which this maximum packing condition is reached is found to decrease. When the initial feed concentration, $\phi_s$ increases, the number of particle-particle interactions increases and the value of $\kappa$, a measure of the flow rate in the $y^*$-direction, at which the maximum packing condition is reached decreases.

Finally, it is important to point out that the analysis has been based upon the generalization of the experimental result stating that the shear-induced diffusion coefficient is proportional to the absolute shear rate. Since this result has only been verified for simple uni-directional flows it requires further experimental investigation.

## REFERENCES


1. Leighton D. & Acrivos A. 1986 Viscous Resuspension. *Chem. Engng Sci.* 41, 1377-1384.
2. Leighton D. & Acrivos A. 1987 The shear-induced migration of particles in concentrated suspensions. *J. Fluid Mech.* 181, 415-439.
3. Phillips R.J., Armstrong, R.C., Brown, R.A., Graham, A.L. & Abbott, J.R. 1992 A constitutive equation for concentrated suspensions that accounts for shear-induced particle migration. *Phys. Fluids A* 4, 30-40.
4. Schaflinger U., Acrivos A. & Zhang K. 1990 Viscous resuspension of a sediment within a laminar and stratified flow. *Int. J. Multiphase Flow* 16, 567-578.

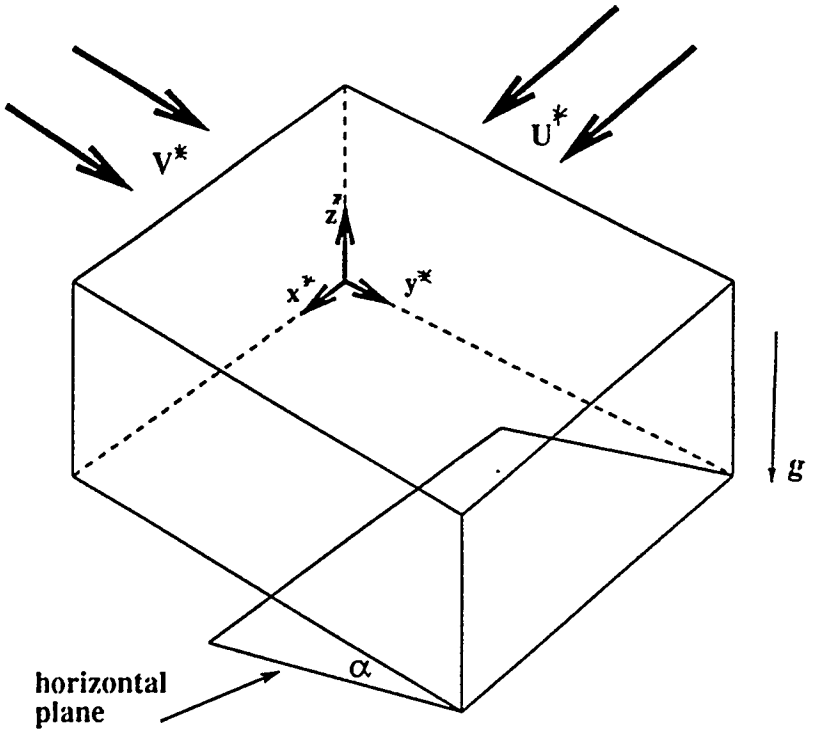


Figure 1. The schematic diagram and coordinate system.

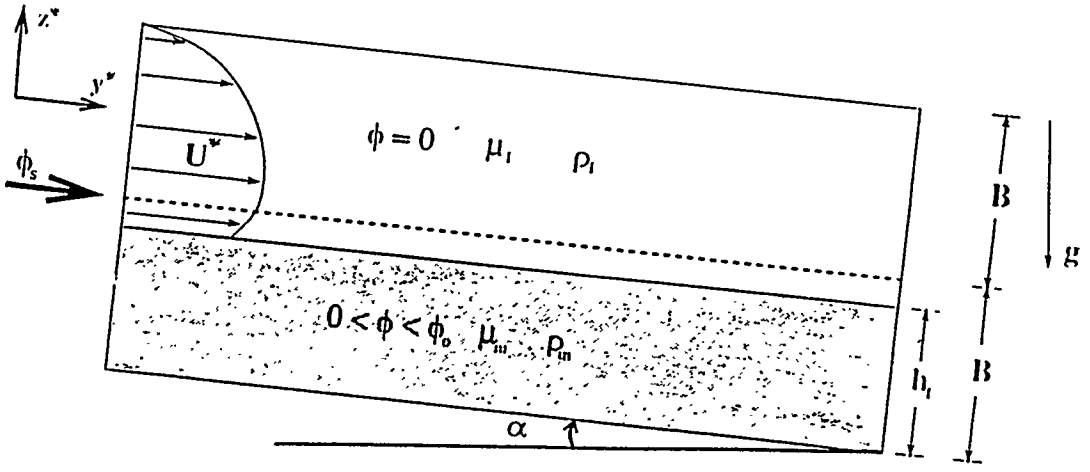


Figure 2. The cross section of the channel in the y-z plane.

# A model for suspension flow accounting for shear-induced migration

Prabhu R. Nott
Department of Chemical Engineering
Indian Institute of Science
Bangalore 560012, INDIA

The compelling experimental evidence of many recent studies (Leighton & Acrivos, 1987; Sinton & Chow, 1991; Koh *et al*, 1994) on the shear-induced migration of particles in suspensions when subjected to inhomogeneous flows (i.e., flows with a gradient in the shear rate) has generated interest in formulating models that can predict particle segregation in these situations. The earliest such effort was by Leighton & Acrivos (1987), who proposed the so-called "diffusion model" in which the migration of particles was due to diffusive fluxes driven by gradients in the interaction frequency, concentration, effective suspension viscosity and even shear stress. The particle concentration field is then derived by solving the diffusion equation in conjunction with the momentum equation for the suspension.

Their model was appealing due to its simplicity and the qualitative agreement of its predictions with some experimental data (e.g., Couette flow). However, their predictions for flow in channels or tubes departed qualitatively from experimental observations. Moreover, their model predicts migration in some curvilinear flows where no migration has been detected.

More recently, Nott & Brady (1994) proposed a model for suspension flow, dubbed the "suspension balance model", which implicitly takes account of inhomogeneities in particle concentration arising due to inhomogeneities in the imposed flow. Unlike the model of Leighton & Acrivos, there is no diffusion of particles in this description. Cross-stream migration of particles arises simply from the requirement that the macroscopic "particle pressure" balances the inertial and body forces in the particle phase momentum equation. The particle temperature, which is the mean square fluctuational velocity of particles, is a fundamental quantity in this model and is determined by solving a balance equation for the fluctuational energy. Thus, balances for mass, momentum and fluctuational energy for the particle phase determine the concentration, velocity and the particle temperature fields. This description rests on the analogy with that of compressible Newtonian fluids and of granular materials.

In this presentation, we focus on the suspension balance model of Nott & Brady and compare its predictions with that of the diffusion model and with the simulations of Nott & Brady. We also use data from the simulations to test the hypotheses of this model. While we confine ourselves in this presentation to the creeping flow regime, it is our intention to relax this assumption in future studies.

## Steady, fully developed channel flow

We consider here the steady, fully developed flow in a semi-infinite rectangular channel of width $H$. Flow is in the $x$- direction and all gradients are in the $y$-direction. We further stipulate that the densities of the fluid and the particles are

equal. The governing equations in dimensionless form are:

$$\frac{d}{dy}\left(p(\phi)\sqrt{T}\right) = 0 \tag{1}$$

$$\frac{d}{dy}\left(\eta_p(\phi)\frac{du}{dy}\right) - \frac{dp}{dx} - \epsilon^{-2} f_d(\phi)(u - u_s) = 0 \tag{2}$$

$$\eta_p(\phi)\left(\frac{du}{dy}\right)^2 - \alpha(\phi)T + \epsilon^2 \frac{d}{dy}\left(\kappa(\phi)\frac{dT}{dy}\right) = 0 \tag{3}$$

where $\phi$, $u$ and $T$ are the concentration, average velocity and temperature fields, respectively, of the particle phase and $u_s$ is the bulk velocity of the entire suspension. The parameter $\epsilon = a/H$ is usually very small, $a$ being the radius of the suspended particles. Equations (1), (2) and (3) are balances for the $y$- and $x$- momenta and fluctuational energy of the particle phase, respectively. The reader is referred to Nott & Brady (1994) for an elaboration of the above equations and the forms chosen for the phenomenological functions of $\phi$, viz. $p$, $\eta_p$, $f_d$, $\alpha$ and $\kappa$.

The similarity between this description and the treatment of compressible fluids and granular materials is apparent: the concentration (or density) distribution arises not from a diffusion equation, but simply from the $y$- momentum balance, which holds that in the absence of a body force the gradient of "particle pressure" in the $y$-direction vanishes. The particle pressure is a function of the concentration and the particle temperature and the latter is nominally determined from (3), the balance for fluctuational energy.

An important conclusion from (2) is that the phase slip (i.e., the difference $u - u_s$) is $O(\epsilon^2)$; therefore, it is sufficient to determine the average suspension velocity from the momentum equation for the entire suspension from

$$\frac{d}{dy}\left(\eta_s(\phi)\frac{du_s}{dy}\right) - \frac{dp}{dx} = 0 \tag{4}$$

Another conclusion one can make is from (3), that the boundary condition for $T$ will only affect the boundary layer at the wall (at the center, symmetry is assumed).

Figure (1) compares the predictions of the model with boundary conditions $T = 0$ and $dT/dy = 0$ at the wall with the predictions of the diffusion model (Koh *et al*, 1994) and the simulations of Nott & Brady. For our calculations, symmetry of $u$ and $T$ is imposed at the center, no slip at the walls and the integral constraint

$$\int_0^1 \phi \, dy = \phi_A$$

specifies the average concentration of particles in the channel. It is quite apparent that the choice of boundary condition for $T$ does not affect the solution in the channel interior, though it strongly determines the nature of solution in the boundary layer at the wall. While the simulations suggest that the particle temperature vanishes at the walls, a more detailed study on this aspect is necessary. Perhaps an energy boundary condition of the type used in the modeling of granular flows (Hui *et al*, 1984) is appropriate. While the diffusion model predicts a cusp-like concentration profile with $\phi = \phi_m$ at the center, the present model predicts a profile that agrees qualitatively with the simulation data.

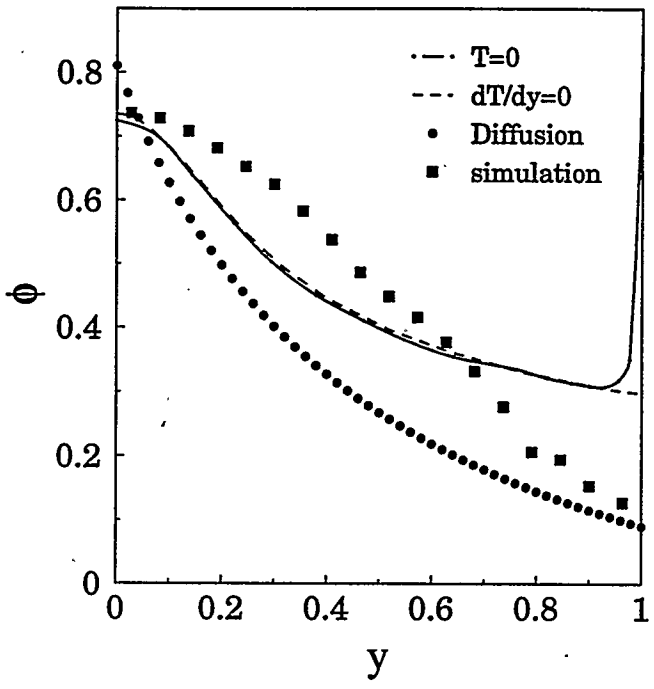


Figure 1: *Comparison of predictions of the suspension balance model, the diffusion model and Stokesian Dynamics simulation for steady, fully developed flow in a rectangular channel for* $H/a = 18$ *and* $\phi_A = 0.45$.

## Unsteady, fully developed channel flow

We now consider the unsteady segregation of particles in a channel which is initially filled with a homogeneous suspension. We assume that the flow is always fully developed (i.e., no variation along the $x$- direction). While this condition cannot be realized in a laboratory experiment, it is satisfied in dynamic simulations where periodic boundary conditions are employed.

The equation of continuity now determines the developing concentration field,

$$\frac{\partial \phi}{\partial t} + \frac{\partial}{\partial y}(v\phi) = 0, \tag{5}$$

and the balance for $y$- momentum assumes the form

$$\epsilon^2 \frac{\partial}{\partial y}\left(\frac{4}{3}\eta_p \frac{\partial v}{\partial y}\right) - \frac{\partial}{\partial y}\left(p(\phi)\sqrt{T}\right) - f_d(\phi)v = 0 \tag{6}$$

where $v$ is the velocity in the $y$- direction. The fluctuational energy balance acquires two more terms,

$$-\epsilon^2 p(\phi)\sqrt{T}\frac{\partial v}{\partial y} + \frac{4}{3}\epsilon^4 \eta_p(\phi)\left(\frac{\partial v}{\partial y}\right)^2 + \eta_p(\phi)\left(\frac{\partial u}{\partial y}\right)^2 - \alpha(\phi)T + \epsilon^2 \frac{\partial}{\partial y}\left(\kappa(\phi)\frac{\partial T}{\partial y}\right) = 0, \tag{7}$$

while the $x$- momentum balance remains unchanged from (4).

While rendering the above equations in non-dimensional form, the scale one arrives at for $v$ is $\epsilon^2 u_0$, where $u_0$ is the scale for $u$. The time scale (for achieving steady state) is then $\tau = H/v = \epsilon^2 H/u_0$, which is exactly the conclusion that Nott & Brady arrived at on assuming a diffusive migration of particles.

For a specified concentration profile, $\phi(y)$, equations (6)and (7) must be solved for the $T$ and $v$ fields. The latter is substituted in (5) and time integrated to derive $\phi(y)$ at the next time step starting from the initial condition

$$\phi(y) = \phi_A \quad \text{at } t = 0.$$

The development of the concentration profile with time for $H/a = 18$ and $\phi_A = 0.45$ is shown in figure (2); the system appears to be close to steady state after a dimensionless time of 1.

## Test of the particle pressure hypothesis

An important hypothesis of this model is that the particle pressure determines the concentration field. For creeping flow, the constitutive form of the particle pressure must be, from dimensional grounds,

$$\Pi = \frac{\eta}{a} p(\phi)\sqrt{T} \tag{8}$$

where $\eta$ above is the viscosity of the fluid. In channel flow, this pressure must be constant across the channel in the absence of body forces. In dimensionless form, $p(\phi)\sqrt{T} = p_0$, where $p_0$ is a constant and a function only of $\epsilon$ and $\phi_A$. The implies that

$$\ln\left(p(\phi)\right) = \ln\left(\frac{1}{\sqrt{T}}\right) + \ln p_0 \tag{9}$$

and therefore that plots of $\ln\left(\frac{1}{\sqrt{T}}\right)$ versus $\phi$, for different values of $\epsilon$ and $\phi_A$, will be a family of curves parallel to each other, but with different intercepts. This hypothesis was tested on the simulations of Nott & Brady (1994) and is shown in figure (3). The data are for simulations four different values of $\epsilon$, but with a constant $\phi_A$ of 0.4. It appears from this plot that the curves for different values of $\epsilon$ are not parallel to each other, rather the slope seems to increase with decreasing $\epsilon$. However, it must be noted that the simulations were performed for channels with "bumpy" walls, i.e. the channel walls were composed of stationary particles. This could lead to a contribution to the particle temperature that is independent of interactions between suspended particles but depends only on particle-wall interactions. If this were the case, the "wall-effect" would decay as $\epsilon$ decreases, which appears to be the case in figure (3).

The issues raised in this presentation point to the necessity for more experimental evidence, particularly on the mean fluctuational velocity of particles. This would be of help, not only in substantiating the models, but also in understanding the origins of shear-induced diffusion and migration and the nature of particle interactions in concentrated suspensions.

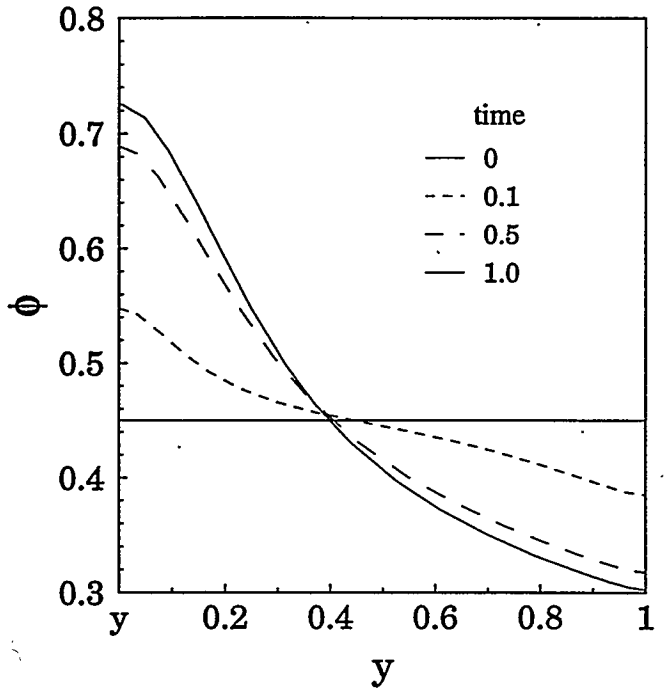


Figure 2: *Predictions of the model for unsteady, fully developed flow in a rectangular channel for* $H/a = 18$ *and* $\phi_A = 0.45$.

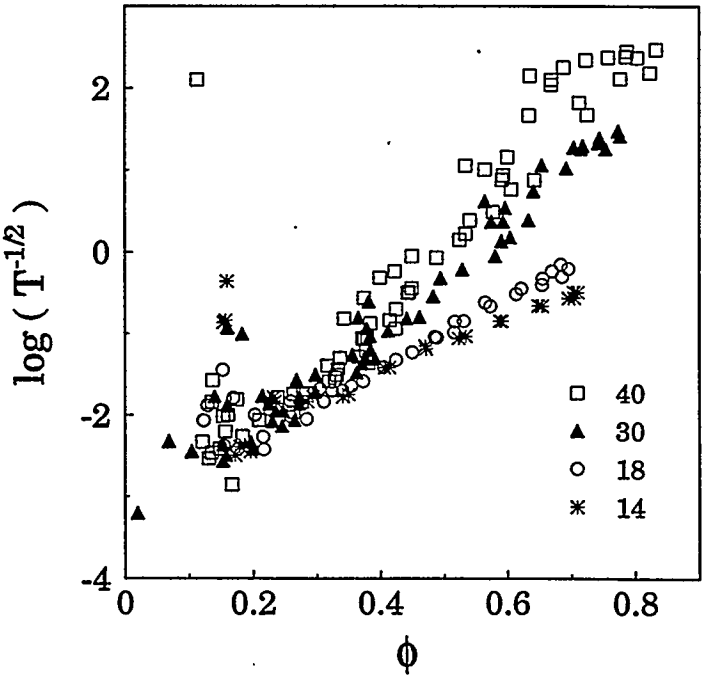


Figure 3: *Verification of the particle pressure hypothesis on the simulations of Nott & Brady.*

## References

Koh, C. J., Hookham, P. & Leal, L. G. 1994 An experimental investigation of concentrated suspension flows in a rectangular channel. *J. Fluid Mech.* **266**, 1.

Hui, K., Haff, P.K., Ungar, J. E. & Jackson, R. 1984 Boundary conditions for high-shear grain flows. *J. Fluid Mech.* **145**, 223.

Leighton, D. & Acrivos, A. 1987 The shear-induced migration of particles in concentrated suspensions. *J. Fluid Mech.* **181**, 415.

Nott, P. R. & Brady, J. F. 1994 Pressure-driven flow of suspensions: simulation and theory. *J. Fluid Mech.* **275**, 157.

Sinton, S. W. & Chow, A. W. 1991 NMR flow imaging of fluids and solid suspensions in Poiseuille flow. *J. Rheol.* **35**, 735.

# SIZE SEGREGATION OF CONCENTRATED, BIDISPERSE AND POLYDISPERSE SUSPENSIONS DURING TUBE DRAWING

Andrea W. Chow, Richard D. Hamlin
Lockheed Missiles and Space Co., 0/93-50, B/204
3251 Hanover Street, Palo Alto, CA 94304

and

Caroline M. Ylitalo
3M Corporate Research
St. Paul, MN 55144

June 22, 1995

Prepared for:
IUTAM Symposium on Hydrodynamic Diffusion of Suspended Particles
22-25 July, 1995
Estes Park, Colorado

# SIZE SEGREGATION OF CONCENTRATED BIDISPERSE AND POLYDISPERSE SUSPENSIONS DURING TUBE DRAWING

*Andrea W. Chow, Richard D. Hamlin*, Lockheed Missiles and Space Co., 0/93-50, B/204, 3251 Hanover Street, Palo Alto, CA 94304, and
*Caroline M. Ylitalo*, 3M Corporate Research, St. Paul, MN 55144

## I. INTRODUCTION

In a non-homogeneous flow field, shear-induced particle migration causes concentration non-uniformity in concentrated solid suspensions. For suspensions consists of more than one narrow size distribution of particles, shear-induced migration can also lead to size segregation due to the size dependence of the migration rate. [1] This paper reports some experimental observations on the shear-induced size segregation phenomena of concentrated bidisperse and polydisperse suspensions when suspensions were drawn up a tube. Our experiments are extensions of those by Chapman [2] who has examined the accumulation of particles behind an advancing meniscus of monodisperse suspensions to study the shear-induced migration phenomenon.

## II. EXPERIMENTAL

*Materials*

The bidisperse suspensions consist of two sizes of glass spheres (Class 5A precision grade Microbeads, Cataphote Inc., Jackson, Mississippi) with diameters 105 - 125 μm and 44 - 53 μm. The two sizes have volume-average median diameters of 118 and 48 μm, and number-average median diameters of 117 and 46 μm, respectively. The specific gravity of the glass spheres is reported to be 2.42. Suspensions with solids volume fraction ($\phi$) of 0.30, 0.40, and 0.50 were examined. Volumetric ratios of large to small spheres were 1:1 for the 0.30 and 0.40 volume fraction suspensions, and 1:1, 3:1, and 1:3 for the 0.50 suspensions. The polydisperse suspensions consist of poly(methyl methacrylate), PMMA, spheres (Lucite 47G, DuPont, Wilmington, Delaware) with sizes ranging from 25 μm to 250 μm. The volume-averaged and the number-averaged median diameters are 128 μm and 56 μm, respectively. The specific gravity of the PMMA spheres is 1.186.

The suspending fluid for the glass spheres was prepared from equal weights of Ucon oil (75-H-90,000, Union Carbide, Danbury, Connecticut), water, and ethylene glycol. It has a viscosity of 3.9 Poise and a density of 1.085 g/cm$^3$ at 25°C. The fluid used for the PMMA spheres consists of 0.1 weight fraction of Ucon oil, 0.45 water, and 0.45 ethylene glycol, with a viscosity of 0.25 Poise and a density of 1.070 g/cm$^3$ at 25°C. A few drops of Triton X-100 (Rohm and Haas, Philadelphia, Pennsylvania), a surfactant, were added to the suspending liquids to improve wetting of the particles and hence assist dispersion of the solids.

*Tube Drawing Experiments*

Semi-transparent Teflon tubes ranging in the inside diameter (ID) between 1.58 mm and 6.26 mm were used. In the tube drawing experiments, a well-mixed suspension was first drawn up the circular Teflon tube with the top end connected to a vacuum line. After the suspension traveled a desired distance, the vacuum was broken and the tube was

quickly rotated to a horizontal position. It was placed on a flat, horizontal surface to allow the particles to settle under the influence of gravity. After about 2 to 30 min, the packed meniscus region could be clearly distinguished at the point where the particles filled the entire cross section of the tube without settling away from the upper wall as shown schematically in Figure 1.

For size analysis, several small sections were cut at different regions along the tube (see Figure 1). The length of the cut sections varied between 1 cm for the largest tubes (6.26 mm in diameter) to 2 cm for the smallest tubes (1.58 mm in diameter), and the number of sections cut from each tube was between 8 and 11 depending on the total length of the tube occupied by the suspension. Those tube sections were weighed, and the contents of each were emptied into a small vial. The net weight of the suspension occupying each section was determined by the difference between the total weight of the filled tube section minus the weight of the cleaned tube section. With the known liquid and solid densities and the suspension weight and volume, the particle concentration profile along the tubes can be determined.

The size distribution in each cut section was analyzed using a Coulter Multisizer. A small amount of the suspension sample (about 1 $cm^3$) was dispersed in a large amount of electrolyte so that the final particle concentration in the electrolyte solution was approximately 1 ppm. The electrolyte was prepared by mixing Isotone II electrolyte solution with 0.25 volume fraction of glycerol to increase the viscosity which suppresses the sonic peak artifacts in the measurements. The dilute suspension was then placed in a stirred reservoir from which the suspension could be drawn at a controlled rate through an orifice of known size. The orifice is equipped with electrodes that measure the change in the electric resistance across the gap. When a particle passed through the orifice, the change in the electric resistance was recorded and translated into particle size (with the assumption that the particles are spherical in shape). After a statistically significant number of particles had been counted, the number- or volume-averaged median particle diameter can be computed.

## III. RESULTS

Figure 2 illustrates the results of particle size analysis along the tube in which a $\phi$=0.30 bidisperse suspension with equal volumes of large to small glass spheres was drawn. The number above each histogram corresponds to the location along the tube illustrated in Figure 1. The histograms are presented in numbers of particles versus log diameter, with the left and right peaks representing the 48 μm and 118 μm glass beads, respectively. Sample 1 was taken from the well-mixed bulk suspension, thereby illustrating the size distribution right at the entrance to the tube. Sample 8 was taken from the tip of the packed meniscus region. The plot in the bottom summarizes the size distribution data by showing the peak area ratio of large to small particles at each location versus the normalized distance along the tube, with the origin at the entrance of the tube. Each data point represents an average of 4 size analysis runs using the Coulter Multisizer. The data in Figure 2 clearly demonstrate that large particles indeed migrate faster toward the meniscus region, resulting in a net enrichment of large particles in the meniscus region and a depletion of in the middle region. This phenomenon is a manifestation of the fact that the shear-induced diffusivity (D) is a strong function of the particle radius (a), $D \sim a^2$ for monodisperse suspensions [3], although the exact diffusivity scaling for bidisperse suspensions is not yet established.

The effects of size segregation in bidisperse suspensions as a function of total particle volume fraction and size distribution were examined. Figure 3 compares the size ratio along the tube for the 0.30 and a 0.50 volume fraction bidisperse suspensions with equal volumes of large and small spheres. We found that size segregation is more

pronounced in the less concentrated suspension. The ratio in the meniscus region is over three times its value in the bulk for the 0.30 bidisperse suspension compared to less than twice the bulk value for the 0.50 volume fraction suspensions. This trend may be due to less available free space in the suspensions with higher solids concentration, thereby impeding the preferential migration of the large particles through the denser particles matrix.

When the volume fraction of solid is fixed at 0.50 but the volume ratio of large to small particles is allowed to vary from 1:3 to 3:1, we observed that size fractionation is more pronounced in the sample containing more large particles as shown in Figure 4. In this figure, the abscissa is the measured peak ratios of the large to small particles normalized by the ratio in the bulk sample. This normalization is necessary to facilitate a direct comparison of the three samples. We believe that the difference in the enrichment factor is at least partly due to the difference in the maximum packing fraction ($\phi_{max}$) of these suspensions.

Size segregation have also been observed in polydisperse suspensions. Figure 5 illustrates the changes of the number-averaged mean particle diameter (normalized by the bulk suspension value) as a function of the normalized length for a 0.30 volume fraction PMMA suspension. The mean particle size along the tube decreases after the entrance region to some minimum in the plateau area, then increases at the transition region to reach a maximum value in the packed meniscus. As in the bidisperse suspensions, the meniscus region is enriched in large particles in the expense of the middle region.

## IV. CONCLUSIONS

When suspensions are drawn up a tube, the particles migrate inward away from the high shear region near the wall toward the center. As more particles move into the faster moving streamlines in the center, there is a net particle flux moving toward the advancing meniscus region, resulting in a steady growth in the length of the densely-packed meniscus region. For suspensions containing a range of particle sizes, the larger ones migrate faster than the smaller ones, yielding an enrichment of large particles in the meniscus region as illustrated in our results. This enrichment effect is more pronounced at lower normalized solid volume fraction ($\phi/\phi_{max}$).

## ACKNOWLEDGMENT

This research is funded by the Lockheed Independent Research program. We would like to thank Mr. Kevin Crispin for his assistance in using the Coulter Multisizer and Professor David Leighton for many helpful discussions.

## REFERENCES

1. A. L. Graham, S. A. Altobelli, Eiichi Fukushima, L. A. Mondy, and T. S. Stephens, "Note: NMR imaging of shear-induced diffusion and structure in concentrated suspensions undergoing Couette flow," J. Rheol., 35, 191 (1991).
2. B. Chapman, PhD. Dissertation, University of Notre Dame, 1990.
3. D. Leighton and A. Acrivos, "The shear-induced migration of Particles in concentrated suspensions," J. Fluid Mech, 181, 415 (1987)

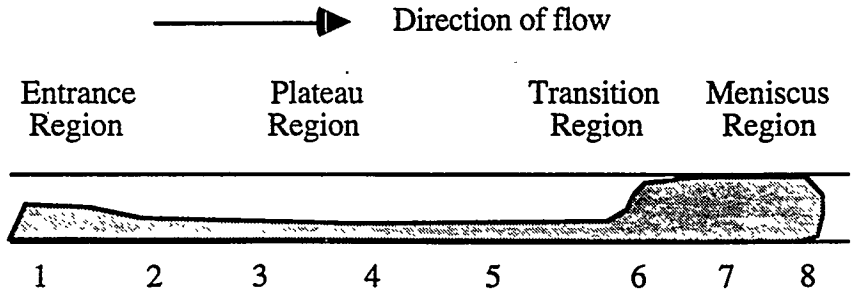


Fig. 1. Schematic diagram showing the solid phase profile in the tube drawing experiment after sedimentation of the particles and the location of the cut section for size analysis.

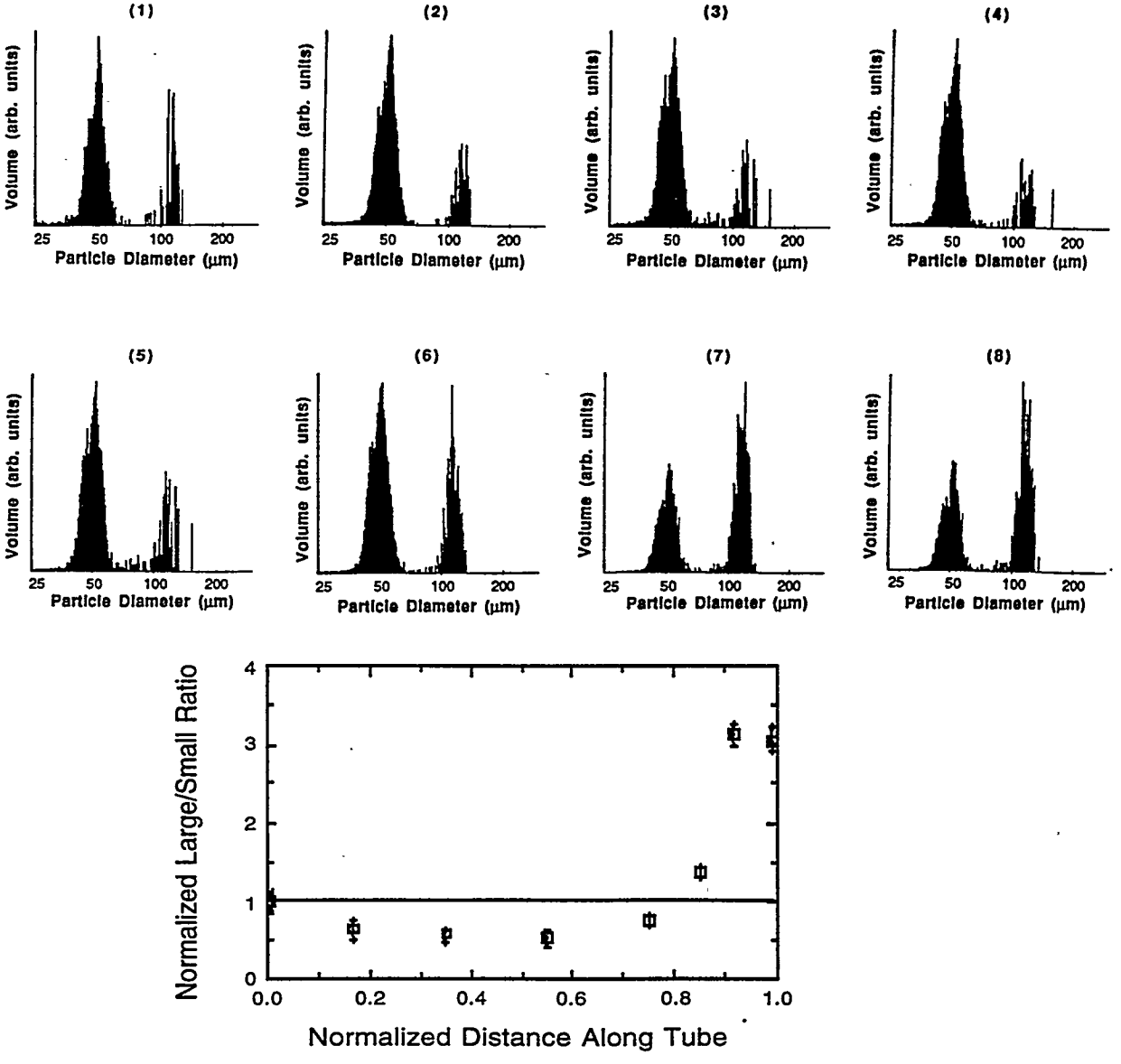


Fig. 2. Size distribution of $\phi$=0.30 bidisperse glass sphere suspension along the tube.

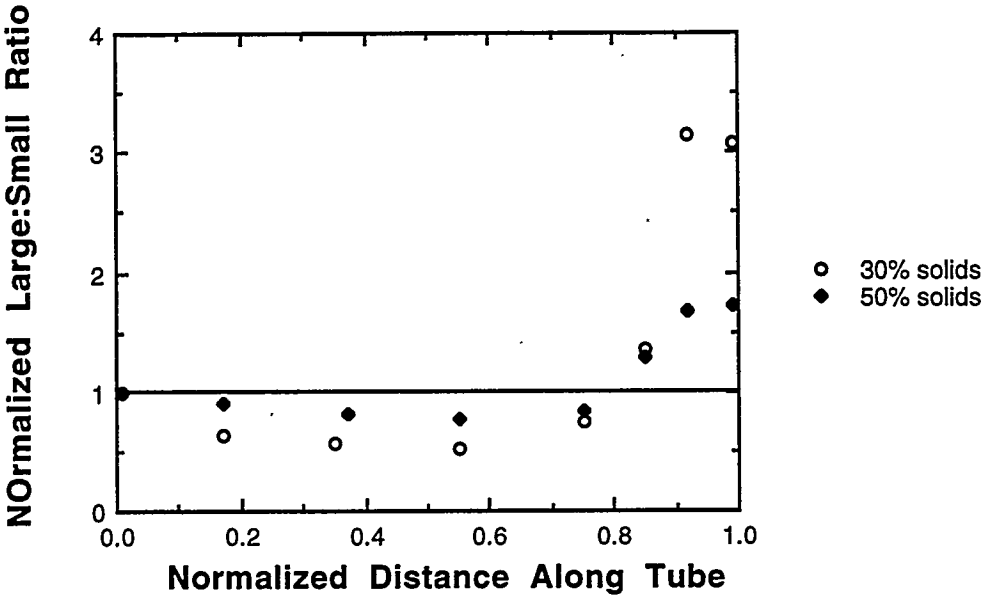


Fig. 3. Size ratio along the tube for the 0.30 and 0.50 volume fraction bidisperse suspensions with equal volumes of large and small spheres.

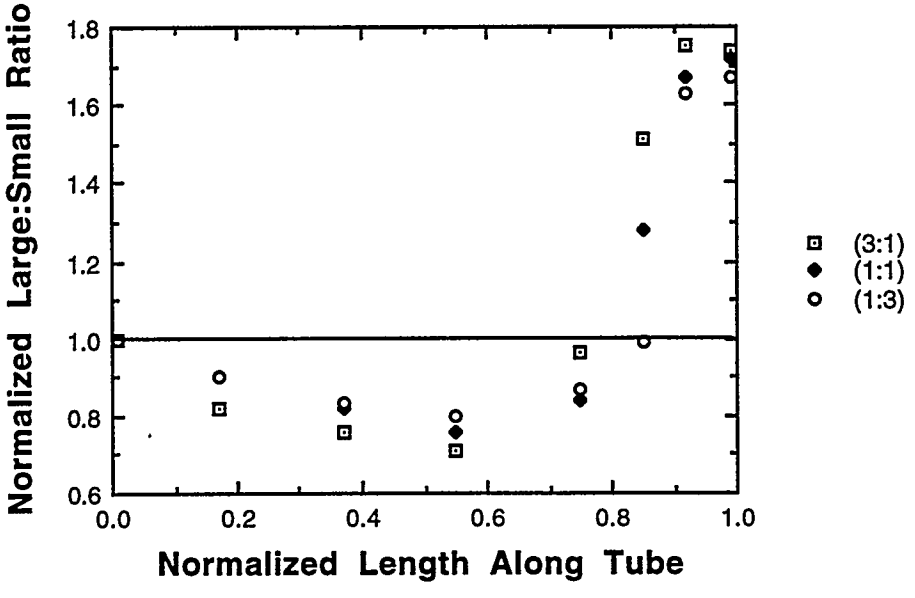


Fig. 4. Size ratio along the tube for the 0.50 volume fraction bidisperse suspensions with large to small sphere ratio of 1:3, 1:1, and 3:1.

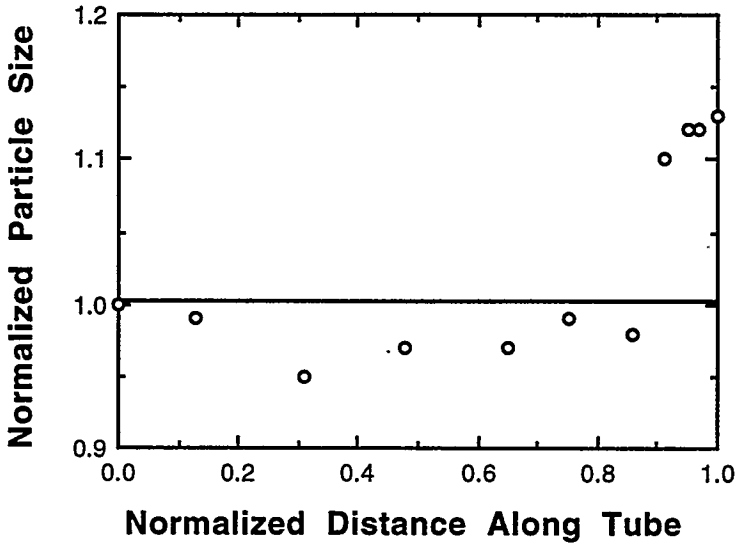


Fig. 5. Averaged particle size along the tube for the 0.50 volume fraction polydisperse suspension.

# On Mixing and Demixing Phenomena in Granular Shear Flow

H. Buggisch, Karlsruhe, Germany

In shear flow the individual grains of a bulk material move relative to each other. If the mean particle-particle distance is small and the shear rate is high this leads to particle collisions, resulting in a random motion of the grains, which loose their permanent contact. Hence fast flowing granular materials behave in many respects like gases[3,4,5,7].

In slow shear flow of closely packed granular materials the grains remain in more or less permanent contact. Nevertheless fluctuating motions can be observed as well, caused in this case by fluctuations of quasi-static contact forces, particles being "squeezed" into "holes" between the neighbouring particles.

The random motions of particles superimposed to the mean shear deformation both in rapid and slow flow result in particle diffusion and may result also in particle segregation [1,2,4,6,7]. This will be the topic of the talk. In the first part of this contribution the author will give an overwiew over some work published in the literature on modelling mixing and gravity segregation in fast shear flow.

In the second part he will present some work of his own research group on mixing and demixing phenomena in slow shear flow.

The basic idea, underlying the modeling of mixing by shearing, done by the author and his coworkers [2,6] was, that in closely packed granular systems the particles move in more or less organized manner in "columns" (like the cars on a highway) until they meet a gap in the neighbouring columns into which they can jump. The frequency of jumps should be proportional to the shear rate (i.e. the relative speed of neighbouring columns) and inversely porportional to the mean gap distance. The packing structure of the granular medium is assumed to depend upon the particle size distribution, but to be independant from the magnitude of the shear rate $\kappa$ inside the shear zone (where $\kappa \neq 0$). A similar model has been proposed by Bridgwater [1] which differs from our model, however, by predicting a proportionality of the diffusion intensity to the volumetric particle density whereas we predict a proportionality to the number density.

Experiments have been done using a Couette-apparatus and a Ring-shear-device. The model bulk used in the Couette-experiments consisted of cylindrical rods marked by colour, the rods being closely packed into the gap between the walls with their axes parallel to the axis of the Couette-apparatus. In the ring shear experiments, glass spheres were used as model granulate.

In these experiments the predictions of the theoretical model could be confirmed, whereby the mean gap distance was used as a fitting parameter [2]. In recent experiments the effect of the particle size distribution upon the mean gap distance was studied [6]. The result was, that in almost monodisperse systems the gap distance becomes extremely large, because the grains organize themselves in crystal-like large clusters.

During experiments with mixtures segregation of particles of different size was found. In the Couette-apparatus this phenomenon could not be explained by volume forces. Hence the author and his coworkers have proposed a phenomenological model, postulating a flux of small particles relative to the large ones driven by the gradient of the shar rate [2]. Predictions of this theory have been confirmed by comparison with the observed segregation effects. In the ring shear experiments an additional downward flux of small particles could be identified, which is due to the influence of gravity. This also has been modelled, and the results have been compared with the observations.

**Literature**


[1] Bridgwater, J., Foo, W.S. and Stephans, D.J.
"Particle Mixing and Segregation in Failure Zones - Theory and Experiment", Powder Technology, 41, (1985)

[2] Buggisch, H. and Löffelmann, G.
"Theoretical and experimental investigation into local granulate mixing mechanisms", Chem. Eng. Proc., 26, (1989)

[3] Campbell, C.S.,
"Rapid Granular Flows", J. Fluid Mech., 203, (1990)

[4] Hsiau, S.S. and Hunt, M.L.,
"Kinetic Theory Analysis of Flow-Induced Particle Diffusion and Thermal Conduction in Granular Material Flows", HTD-Vol. 204, General Papers in Heat Transfer, ASME, (1992)

[5] Jenkins, J.T. and Savage, S.B.,
"A Theory for the Rapid Flow of Identical Smooth, Nearly Elastic Spherical Particles", J. Fluid Mech., 130, (1986)

[6] Peciar, M., Buggisch, H. and Renner, M.,
"Experimental investigation into the influence of particle size distribution upon the local mixing mechanisms in a flowing bulk material", Chem. Eng. Proc., 33 (1993)

[7] Savage, S.B. and Lun, D. K. K.,
"Particle size segregation in inclined chute flow of dry cohesionless granular solids", J. Fluid Mech., 189, (1988)

# The Effect of Particle Diffusion on Heat Transfer for Flows of Granular Materials

M.L. Hunt

Division of Engineering and Applied Science
Mail Code 104-44
California Institute of Technology
Pasadena, CA 91125

Heat transfer in flows of granular materials may be due to several factors: gaseous convection, particle convection, particle-to-particle conduction, heat generation due to shearing of the material, and thermal radiation. For different mixing processes and heat-exchange geometries, the relative contributions of these mechanisms to the overall heat transfer may be significantly different. However, few studies have examined heat transfer in granular flows to assess the dominant mechanisms (Hunt, 1990). Some results can be inferred from fluidized bed literature, especially regarding the contribution from thermal radiation and from particle-to-particle conduction. However, the results from fluidized bed studies regarding gaseous and particle convection are not readily applicable to granular flows since the relative motion of the fluid and solid phases differ considerably in these two flows. In fluidized beds the particles are suspended and may be convected by the gas. In granular flows the fluid phase has a negligible effect on the movement of the particles; instead the motion of the particles is due to gravitational acceleration (flow down a chute) or by a motion of the bounding walls (flow in a solids mixer), and to the particle-to-particle and particle-wall collisions. Hence for some granular flows, the contribution of the fluid convection might be secondary to that of the particle convection.

The focus of the current work is on the contribution of particle convection to heat transfer in granular flows. The work examines the relation between the mixing or diffusion of the granular material and the enhancement of the effective thermal conductivity. Recently, the work by Hsiau and Hunt (1993) and by Savage and Dai (1993) developed an expression for the self-diffusion coefficient for a granular material flow using dense gas kinetic theories. The diffusion coefficient, $D$, is shown to increase with the particle diameter, $d$, the square-root of the granular temperature, $\gamma^{1/2}$, and decrease with increasing solid fraction $\nu$ through the radial distribution function $g_0(\nu)$, which accounts for the increase in particle collision rate due to the finite size of the particles. By a similar analysis, Hsiau and Hunt (1993) found a corresponding relation for the effective thermal conductivity by analyzing the heat flux that resulted from the particle motion across a thermodynamic temperature gradient. The analysis assumes that the particles are at a uniform temperatures (small Biot number approximation), and that the surrounding fluid is conductive but stationary. The result of the analysis showed that like the self-diffusion coefficient, the effective thermal conductivity increased with granular temperature and

decreased with increasing solid fraction. The expression for the thermal conductivity is as follows:

$$k_{eff} = \rho_p c_p d\gamma^{1/2} \Big/ \left(9\pi^{1/2}\nu g_0(\nu)\right)$$

where the density and specific heat, $\rho c$, are properties of the particles. This result is consistent with the limit of small Biot-Fourier number, $BiFo=\Delta t/\sigma$, in which the time between particle collisions, $\Delta t$, is much smaller than the thermal time constant of the particle, $\sigma$. For very large Biot-Fourier numbers, the effective thermal conductivity is proportional to the granular temperature,

$$k_{eff} = \rho_p c_p \nu\sigma\gamma \, .$$

The current work focuses on evaluating the effective thermal conductivity using a two-dimensional hard-sphere molecular dynamics simulation. Computer simulations have been used routinely in granular flow studies to investigate the mechanics of the flow, and recently in examining the variation of the self-diffusion coefficient (Dai, 1993). The computer simulation technique has not been used previously for heat transfer studies.

The first studies have examined the variation in the effective thermal conductivity for a range of *BiFo* and for a range of solid fractions, $\nu$. Consistent with the kinetic theory analysis, the particles are assumed to have a constant temperature. The particles exchange heat with the surrounding fluid through a heat transfer coefficient. The granular flow has no mean motion; however, the particles are free to move within the bed because of their non-zero granular temperature. The particles collide elastically and no thermal energy is exchanged during a collision. A high-temperature and a low-temperature thermal reservoir are placed at either end of the bed. The simulation is then used to evaluate the heat flux between the reservoirs, and this result is used to determine the effective thermal conductivity. The limiting cases at high and low *BiFo* are consistent with the kinetic theory analysis. Although the current configuration does not correspond to a physically realistic configuration the simulation can be modified to examine flows with an overall motion, such as the experimental studies by Wang and Campbell (1992).

References:

Dai, R., 1993, Granular Flow Studies through Kinetic Theory and Numerical Simulation Approaches, PhD thesis, McGill University, Montreal, Canada.

Savage, S.B. and Dai, R., 1993, Studies of Granular Shear Flows. Wall Slip Velocities, Layering, and Self-Diffusion, **Mechanics of Materials, 16**, 225-238.

Hsiau, S.S. and Hunt, M.L., 1993, Kinetic Theory Analysis of Flow-Induced Particle Diffusion and Thermal Conduction in Granular Material Flows, **Journal of Heat Transfer, 115**, 541-548.

Hunt, M.L., 1990, Comparison of Convective Heat Transfer in Packed Beds and Granular Flows, Annual Review of Heat Transfer, III, ed. C.L. Tien, Hemisphere Publishing Co., New York, Ch. 6, 163-193.

Wang, D.G. and Campbell, C.S., 1992, Reynolds Analogy for a Shearing Granular Material, **Journal of Fluid Mechanics, 244**, pp. 427-546.

# Fick's Law and Species Separation for a Binary Mixture of Frictionless, Nearly Elastic Spheres

**James T. Jenkins**
**Department of Theoretical and Applied Mechanics**
**Cornell University**
**Ithaca, New York 14853-1503**

We consider the kinetic theory for a binary mixture of smooth, inelastic spherical grains that interact through binary collisions.

We first review how a relation between the relative velocity of the two species and the spatial gradient of their number densities, the spatial gradient of the mixture fluctuation kinetic energy, and the difference in the external force on each type of sphere is obtained from the species momentum balances as an approximation.

Next, we consider two simple problems involving separation of the two types of spheres associated with differences in their size, mass, and coefficients of restitution. In the first, separation is driven by gravity in a uniform field of mixture fluctuation energy. Here, we focus on a steady homogeneous shearing flow in which one species is dilute and, given the sizes, masses, and coefficients of restitution, determine whether the dilute constituent sinks or floats. In the second, separation is driven in the absence of gravity by the spatial gradient of the mixture fluctuation energy. Without making any simplifying assumption regarding the concentrations, and given the sizes, masses, and coefficients of restitution, we determine when separation of the species will occur and predict its direction in relation to that of the gradient of fluctuation energy.

It is important to point out that while these two separation problems are typical of those phrased in terms of the kinetic theory for binary mixtures of inelastic particles, other separation mechanisms in dry systems of particles are possible. Typically, these do not involve so simple an interparticle interaction as instantaneous binary collisions and, as a consequence, are not so easy to describe.

# PARTICLE TRANSPORT IN VIBRATED GRANULAR BEDS

Yidan Lan and Anthony D. Rosato
Particle Technology Laboratory
Mechanical Engineering Department
New Jersey Institute of Technology
Newark, NJ 07102

The use of particulates is widespread in a host of industries (i.e., chemical, agricultural, pharmaceuticals, ceramics, mineral processing, and advanced materials) concerned with handling and processing of granular materials. Despite the worldwide use and applications of bulk solids, the design of efficient and reliable systems remains highly problematic. This is essentially due to the fact that although the flow of particulates appears deceptively similar to fluids, there is no general understanding or model of even the most seemingly simple flows capable of describing behavior over the spectrum of possible flow regimes (energetic, intermediate and quasistatic). Often bulk granular materials are subject to vibrations in handling processes, such as in hoppers and chutes, to promote and enhance flow. Vibrated beds exhibit a rich variety of interesting phenomena, (eg., fluidization [1,9,15], convection [4,5,6,8,10,12,17], arching [11,19], surface waves [11] and size segregation [2, 13].

In this paper, we present steady state three-dimensional discrete element simulations of convective transport in a granular bed which is energized by a flat floor sinusoidally oscillating in the vertical direction at amplitude $a$ and frequency $\omega$. The computational cell is a rectangular parallelopiped having flat side walls, an open top and lateral periodic boundaries. Particles are modeled as inelastic, frictional spheres of diameter $d$ and the contact laws used are those developed by Walton and Braun [18]. The normal force between two such contacting spheres, governed by linear loading and unloading springs of stiffnesses $K_1$ and $K_2$, respectively, produces a constant effective normal restitution coefficient $e = \sqrt{K_1/K_2}$. The tangential force model, patterned after Mindlin's theory, contains a tangential contact stiffness $K_T$ (involving a Coulomb friction coefficient $\mu$ and an initial tangential stiffness $K_o$) which decreases with tangential displacement. Full sliding of the contact occurs at the friction limit where $K_T$ is reduced to zero.

In the simulations, plastic spheres of diameter $d = 0.1m$ are used having a density $\rho = 1200\ kg/m^3$, and a loading stiffness $K_1 = 2.8 \times 10^6$ is chosen. We note that sensitivity tests showed that the use of this value produced a maximum overlap between contacting spheres of less than one percent of the diameter. This in accordance with the behavior of uniformly sheared granular materials, governed by a pressure which varies as the square of the shear rate and validated by kinetic theory models [7].

The first series of simulations are done in a cell of width $W = 6d$ at a floor shaking acceleration $\Gamma = a\omega^2 = 10g$. The normal restitution coefficient $e = 0.9$ and $\mu = 0.8$ for the side walls and flow particles. A convective flow occurs in which particles rise upwards in the center of the bed and move down near the side walls. This has also been observed in experiments of Savage [16], Evesque and Rajchenbach [3], and in two-dimensional simulations of Gallas et al. [6] and Taguchi [17]. We note that particle rotation was neglected in the latter simulations in contrast to our studies where transfer of tangential momentum at the contact point causes spheres to spin. Results also show clearly that low displacement amplitudes ($a < 0.25d$) produce very little convection in the cell

A change in the friction properties of the walls and flow spheres affects the sense of the convection field. In this study, $f = 7$ Hz, $a = 0.5d$, $\Gamma = 10g$, $W = 6d$. When smooth spheres and frictional walls are used (i.e., $\mu = 0$, $\mu_w = 0.8$), a downward flow appears in the center of the cell and upward along the walls, in contrast to the pattern observed in the case above where $\mu = \mu_w = 0.8$.

If the computational cell is made wider, i.e., $W = 20d$, long-term velocity field averages show a symmetric convection pattern of two vortex-like structures (Fig. 1). It would seem that the velocity field history

over a cycle should have the same type of symmetry as revealed in the long-term average. However, an animation, from which several snaps are presented in Fig. 2, revealed that sections of the bed collide with the floor at different instants giving rise to the long-term field of Fig. 1. When a much wider cell is used ($W = 100\ d$), the long-term average velocity field in the center of the bed does not show any pattern while two convection cells of approximately 8 particle diameters wide appear at the side walls. (Fig. 3). Again, an inspection of the instantaneous velocity field shows a behavior similar to that observed in the *20d* cell. A projection of the rescaled sphere configuration in the shaking plane at phase point $\phi = 3\pi/2$ (Fig. 4) shows regions at the bottom which are devoid of particles, indicative of the formation and breakup of arches within the bed over a time scale different from the shaking period. These simulated results support several of the experimental observations which appear in the literature [19].

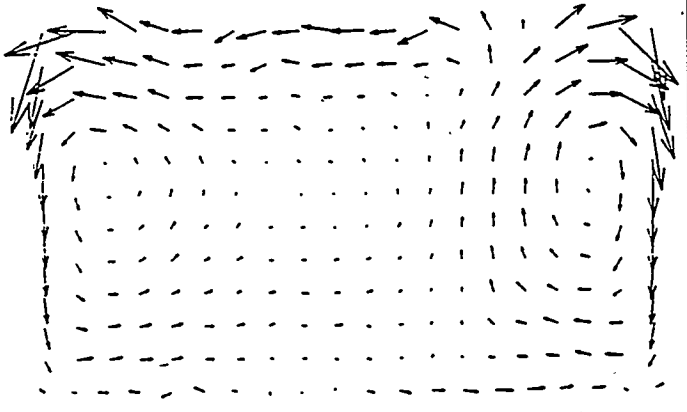

**Fig. 1:** Long-term average velocity field ($W/d = 20d$, $\Gamma=10g$, $a = 0.5d$, $e = 0.9$).

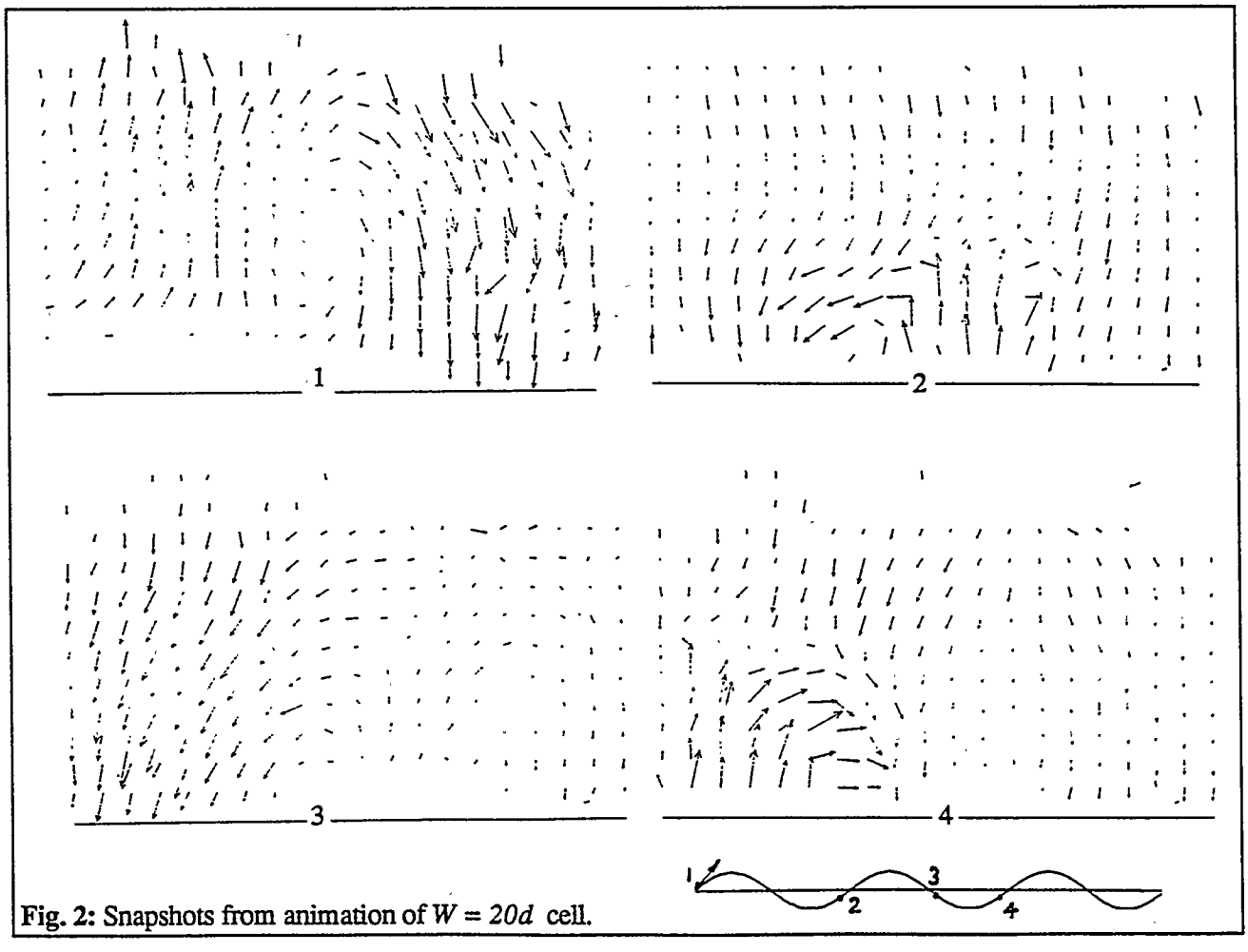


**Fig. 2:** Snapshots from animation of $W = 20d$ cell.

Preliminary computations of the normal components of the pressure tensor have been done showing that the major contribution is the collisional part. This tensor has a large gradient in the shaking direction with a lack of symmetry in the lateral directions. Further studies are in progress to obtain a complete picture of the phenomena.

Fig. 3: Long-term average velocity field ($W/d = 100d$, $a = 0.5d$, $\Gamma = 10g$, $f = 7$Hz).

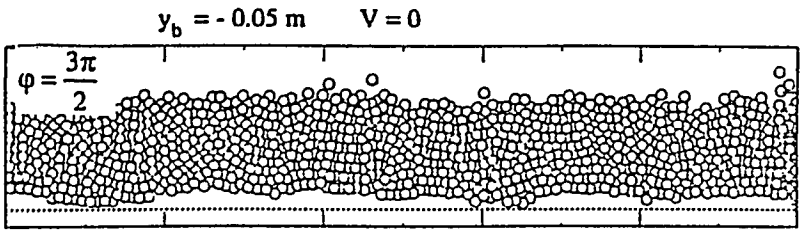


Fig. 4: Projection of rescaled sphere configuration onto shaking plane at phase point $\phi = 3\pi/2$

## References


1. E. Clement, J. Rajchenbach, *Europhys. Lett.* **16**, 133 (1991).
2. J. Duran, T. Mazozi, E. Clement, J. Rajchenbach, *Phys. Rev. E* **50**, 5138 (1994).
3. P. Evesque and J. Rajchenbach, *Phys. Rev. Lett.* **62**, 44 (1989).
4. M. Faraday, *Philos. Trans. R. Soc. London* **52**, 299 (1831).
5. S. Fauve, S. Douady, and C. Laroche, **50**, 187 (1989).
6. J. A.C. Gallas, H.J. Hermmann, and S. Sokolowski, *Phys. Rev. Lett.* **69**, 1371 (1992).
7. J. T. Jenkins and M. W. Richman, *Arch. Rat. Mech. Anal.* **87**, 355 (1985).
8. J. B. Knight, H. M. Jaeger, and S. R. Nagel, *Phys. Rev. Lett.* **70**, 3728 (1993).
9. Y. Lan and A. D. Rosato, *Phys. of Fluids* , in press, (1995).
10. S. Luding, E Clement, A. Blumen, J. Rajchenbach, and J. Duran, *Phys. Rev. E* **50**, R1762 (1994).
11. F. Melo, P. Umbanhowar, and H. L. Swinney, *Phys. Rev. Lett.* **72**, 172 (1994).
12. J. Rajchenbach, *Europhys. Lett.* **16**, 149 (1991).
13. A. D. Rosato, K. J. Strandburg, F. Prinz, and R. H. Swendsen, *Phys. Rev. Lett.* **58**, 1038 (1987).
14. A. D. Rosato, R. N. Dave, A. La Rosa, and E. Mosch, *Proceedings of the AIChE 1st Intl. Particle Technology Forum* (AIChE, American Institute of Chemical Engineers, New York, 1994), pp. 325-330.
15. M. W. Richman and R. E. Martin, *Proceedings of the 9th Conference on Engineering Mechanics*, ed. by L. D. Lutes and J. N. Niezwecki (ASCE, New York, 1992), pp. 900-903.
16. S. B. Savage, *J. Fluid Mech.* **194**, 457 (1988).
17. Y.-H. Taguchi, *Phys. Rev. Lett.* **69**, 1367 (1992).
18. O. R. Walton and R. L. Braun, *Acta Mech.* **63**, 73 (1986).
19. C. R. Wassgren, C.E. Brennen, and M. L. Hunt, under review, *J. Appl. Mech.* (1995).

## Unexpected Behavior of Particles in a Horizontal Rotating Cylinder

Masami Nakagawa*, Stephen A. Altobelli, Arvind Caprihan and Eiichi Fukushima
The Lovelace Institutes, 2425 Ridgecrest Dr. SE, Albuquerque, New Mexico 87108
*New Address: Sandia National Laboratories, Organization 6212, Mail Stop 0709,
P.O. Box 5800, Albuquerque, New Mexico 87185-0709

Recently, segregation phenomena of particles have gained much attention from different disciplines of science and engineering. Studies of sand dune ripples, planetary rings and segregation in fluidized beds are some of the examples. Here we focus our attention on radial and axial segregation in a horizontal rotating cylinder. These phenomena have been perceived as two independent segregation processes, however, based on our recent non-invasive MRI (Magnetic Resonance Imaging) measurements, we consider them as a series of evolving events. This paper reports an experimental observation of a possible missing link for transition mechanisms between radial segregation, which has been extensively investigated as a two-dimensional phenomenon, and full three-dimensional axial segregation.

In late 1930's, Oyama (Oyama, 1939) reported results of his axial segregation experiment and ever since reports on axial segregation have appeared sporadically (Weidenbaum, 1958; Donald and Roseman, 1962; Bridgwater et al., 1969; Rogers and Clements, 1971; Das Guputa et al., 1991; Kukdrna et al., 1992; Fauve et al., 1993; for example). Nakagawa (Nakagawa, 1994) reported temporal changes of the number of bands and random nature of the initial band formation of sand particles with continuous size distribution. He also pointed out that the number of axial bands decreases with time and the final configuration consisted three bands. In that experiment, sand particles were used but due to their NMR insensitivity, it was not possible to obtain any information about internal structures. More recently, Nakagawa repeated a similar experiment using two different sizes of pharmaceutical pills. These particles are hard, uniform in size and shape, and contain vitamin oil which gives excellent MRI signals. Based on MRI of internal structures of each segregating constituent in a rotating cylinder, it was possible, for the first time, to conjecture that three-dimensional nature of radial segregation affects the formation of the initial axial bands and dynamics of band merging.

In the binary mixture experiment, the cylinder with length to diameter ratio of 7 was half-filled with 50-50 volume mixture of pharmaceutical particles of 1 and 4 mm diameters. Particles were initially well mixed. After 200 rotations, the internal structure of the mixture was non-invasively imaged by the NMR imaging technique. An unevenly shaped core of small particles was found to extend throughout the cylinder. This demonstrates the three dimensional formation of radial segregation. After 3000 rotations, another NMR image was taken which revealed three axially separated bands of small and large particles, a band of small particles in the middle and two bands of large particles adjacent to it. Figure 1 shows NMR images of both segregation at different slices along the axis of the cylinder.

In this experiment, we observed that radial segregation occurred first and was succeeded by axial segregation. Although radial and axial segregations are usually treated separately, they are related events occurring on different time scales, in this case. There are many observations of axial segregation attributed to differences in dynamic angle of repose (Savage,1993; Hill and Kakalios,1994; Zik, et al., 1994), however, the present example suggest that there is a more complex three-dimensional mechanism which alters a radially segregated state into an axial one. A more detailed study of this evolution mechanism is expected to give more insights into mechanism(s) of band merging.

**References**

•J. Bridgwater, N.W. Sharpe and D.C. Stocker, Trans. Inst. Chem. Engrs. **47**, 114 (1969) •M.B. Donald and B. Roseman, Br. Chem. Engng. **7**, 749 (1962) •S. Fauve, C. Laroche, and S. Douady, Physics of Granular Media, 277 (Nova Science Publishers, Commack, NY, 1993) •S. Das Gupta, D.V. Khakhar, and S.K. Bhatia, Chem. Eng. Sci. **46**, 1513 (1991) •K. M. Hill and J. Kakalios, Phys. Rev. E. **49**, 3610 (1994) •M. Nakagawa, Chem. Engng. Sci. **49**, 2540 (1994) •Y. Oyama, Bull. Inst. Phys. Chem. Res. Japan Rep. 5, **18**, 600 (1939) •A.R. Rogers and J.A. Clements, Powder Tech. **5**, 167 (1971) •S.D. Savage, Disorder and Granular Media, 255 (North-Holland, Amsterdam, 1993) •S.S. Weidenbaum, Advances in Chem. Engng. **12**, 211 (1958) •O. Zik, D. Levine, S.G. Lipson, S. Shtrikman, and J. Stvans, Phys. Rev. Lett.. **73**, 644 (1994).

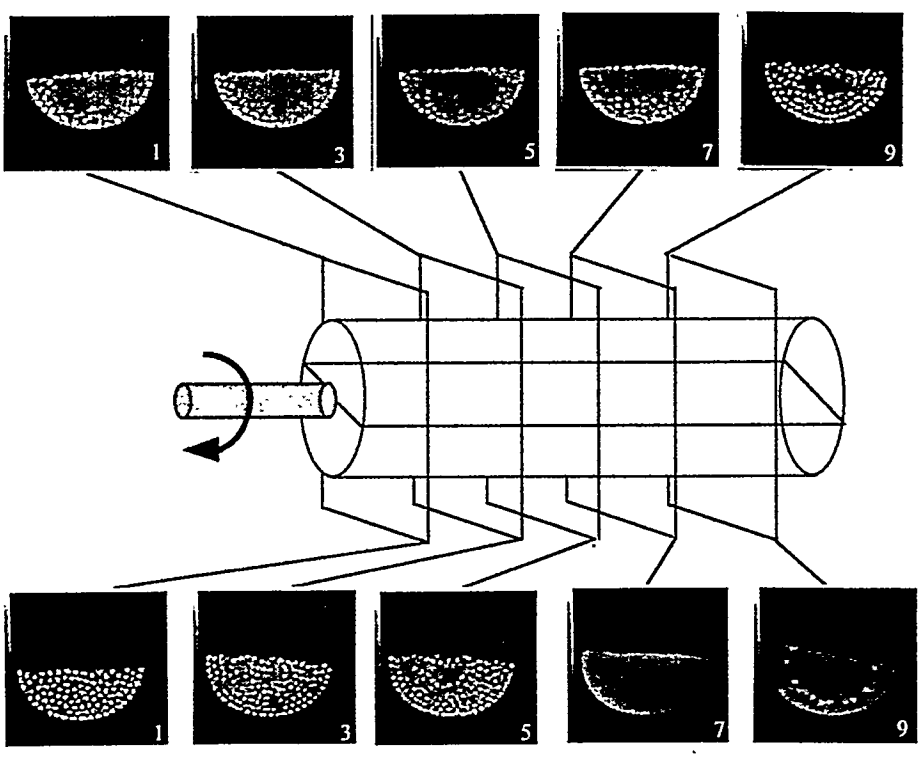


Figure 1. NMR Images of Radial and Axial Segregation.

Both large and small particles contain the same vitamin oil, however, NMR signals can distinguish them because they have different volume fraction of liquid core. Large particles appear as white dots and small particles appear as gray in the images. The small particles are too small to be distinguished individually for this imaging procedure because of the average over the slice thickness of 8mm. Image 9 of axial segregation shows large particles in the thin band immediately adjacent to the end cap.

# Numerical simulations of hydrodynamic dispersion

A. J. C. Ladd

*Department of Theoretical and Applied Mechanics,*
*Cornell University*
*Ithaca, New York 14853.**

June 29, 1995

**Abstract**

Hydrodynamic dispersion and stability are often sensitive to subtle changes in the underlying suspension microstucture, which are difficult to observe experimentally. Numerical simulation can be used to examine these microstructural changes directly, as well as to predict their effect on fluctuations in particle velocity. In this talk I will summarize the results of previous simulations, and discuss their limitations. I will also describe some more recent results and indicate directions for future research.

*Permanent address:
*Lawrence Livermore National Laboratory,*
*Livermore, California 94550.*

# Sedimentation at finite Stokes numbers

A. S. Sangani
Department of Chemical Engineering and Materials Science
Syracuse University, Syracuse, NY 13244

D. L. Koch
School of Chemical Engineering
Cornell University, Ithaca, NY 14853

## Abstract

We consider sedimentation of monodispersed spherical particles of radius $a$ through a gas under conditions of vanishingly small Reynolds number $Re = \rho a U_0/\mu$ and finite Stokes number $St = (2\rho_p/9\rho)Re$. Here, $\rho$ and $\mu$ are, respectively, the density and viscosity of the gas, $\rho_p$ is the density of the particles, and $U_0 = (2\rho_p/9\mu)a^2 g$ is the Stokes sedimentation speed of the particles, $g$ being the magnitude of the gravitational acceleration. The conditions of small Reynolds number and finite Stokes number are approximately satisfied by particles with radius of 100 $\mu m$. For such particles, the inertia of the particles must be accounted for in predicting the sedimentation velocity, velocity variance and hydrodynamic diffusivity tensors, and the stability criterion for the uniform state of sedimenting suspensions. In this talk, we shall present theories for determing above quantities as a function of $St$ and the volume fraction $\phi$ of particles, and compare their predictions with the results obtained by Stokesian simulations.

When inertia is important, the particles can overcome lubrication forces without substantial loss in their kinetic energies, and as a result come into physical contact with each other. In Stokesian simulations therefore we allow for the fact that the continuum lubrication appoximations will breakdown when a pair of particles approach each other within a distance comparable to the mean free path of the gas molecules, thus allowing collisions to occur between particles.

The simulations indicate that the particle velocity variance decreases with increasing $\phi$ and increasing $St$. Also the anisotropy of velocity variance is

found to decrese with the increasing $St$. These results are in agreement with an extension of the theory of Koch(1990) to take account of effects of finite particle volume fraction. In this theory the energy contained in the particle velocity flucutuations results from the correlation in the force exerted on the particles by the fluid velocity fluctuations. The anisotropy of the velocity variance at small Stokes numbers results from the anisotropy of the fluid velocity fluctuations, while the particle velocity variance becomes more isotropic at high Stokes numbers due to interparticle collisions.

Our numerical simulations show that the particle velocity variance is independent of box size while the hydrodynamic diffusivity incresases with the size of the box used in the simulations. This result can be explained qualitatively as follows. On a relatively small length scale, the particle velocity is unaffected by hydrodynamic interactions and the interactions are similar to those in fixed beds (Koch 1990). This leads to Brinkman screening of the velocity disturbance which in turn yields a finite, variance that is independent of system size. On a relatively large length scale, however, the particles relax to the fluid velocity and thus the large length scale motion, which controls the hydrodynamic diffusivity, is determined by a set of averaged equations in which the presence of particles contributes to the Reynolds stress. As shown by Koch (1992), this leads to a system-size-dependent diffusivity.

Koch D. L. 1990 Kinetic theory for a monodisperse gas-solid suspension. *Phys. Fluids A* **2**, 1711.

Koch D. L. 1992 Anomalous diffusion of momentum in a dilute gas-solid suspension. *Phys. Fluids A* **4**, 1337.

# Numerical Predictions for Elastohydrodynamic Collisions

Gerald H. Ristow

6.3

Fachbereich Physik, Philipps-Universität, Renthof 6, 35032 Marburg, Germany

Granular media like grains, pills, beads, etc. are the base materials for most industrial products or production processes. Despite their wide use no complete physical model has yet been established to describe the different experimental findings like e.g. clogging, spontaneous heap formations, power law distributions for wall stresses and density waves (for a review see e.g. [1]).

For dry granular media, numerical predictions of two-dimensional systems using molecular dynamics and other techniques have proven to give even quantitative results in a moderate amout of computer time [2]. Even elliptical particles or arbitrary polygons can be treated efficiently and simulations in three spatial dimensions were done as well.

But not all situations can be well approximated by dry granular materials. The effect of the surrounding air or fluid becomes important in certain cases. To deal with such a situation, the algorithm has to be changed completely since the time resolved evaluation of the primitive variables of the fluid (velocity and pressure) takes far more computer time than the calculation of the interactions between grains. In addition, the interactions between fluid and particles have to be considered as well.

Since a full three-dimensional system with more than a few tens or hundred particles on a fine spatial grid cannot predict long or even medium time behavior for moving fluids, my approach was inspired by the theory of elastohydrodynamic collisions [3, 4] and with dry granular media in mind. For granular materials, the most important physical input is the energy loss during particle-particle or particle-wall collisions. If the surrounding fluid has a low viscosity, e.g. air, the particles will still rebound but the restitution coefficient does depend on the fluid viscosity, the radii of the colliding particles and other material properties.

The forces acting on the particles in the fluid take into account repulsive and dissipative forces in the normal direction and shear forces in the tangential direction during collisions. The forces of the fluid on the particles are calculated by a full evaluation of the stress tensor for an incompressible fluid over the particle's surface. The time dependent motion of the fluid is calculated using an iterative procedure on a MAC grid [5]. The boundary conditions for the numerical treatment of the Navier-Stokes equations include the particles' surfaces as moving boundaries having the velocity of the corresponding solid particle.

To test the validity of the numerical algorithm, the forces on a fixed box in a two-dimensional channel filled with water were calculated. The numerical results for the vertical force $F_s$ measured in cgs units for different values of the maximal fluid velocity ($\sim$ Re) are indicated by circles in the figure below. The dotted line shows the analytic prediction for the Stokes regime (Re $<$ 1) which states a linear dependence on Re. For Re $>$ 1, the algorithm clearly resolves the deviations from the Stokes regime and the grids used were sufficiently large for the grid effects to be negligible.

Using only a few spheres or cubes on a fine three-dimensional grid, I intend to obtain numerically the dependence of the restitution coefficient on the material and fluid properties. This will be compared to theoretical [3] and experimental [4] results available.

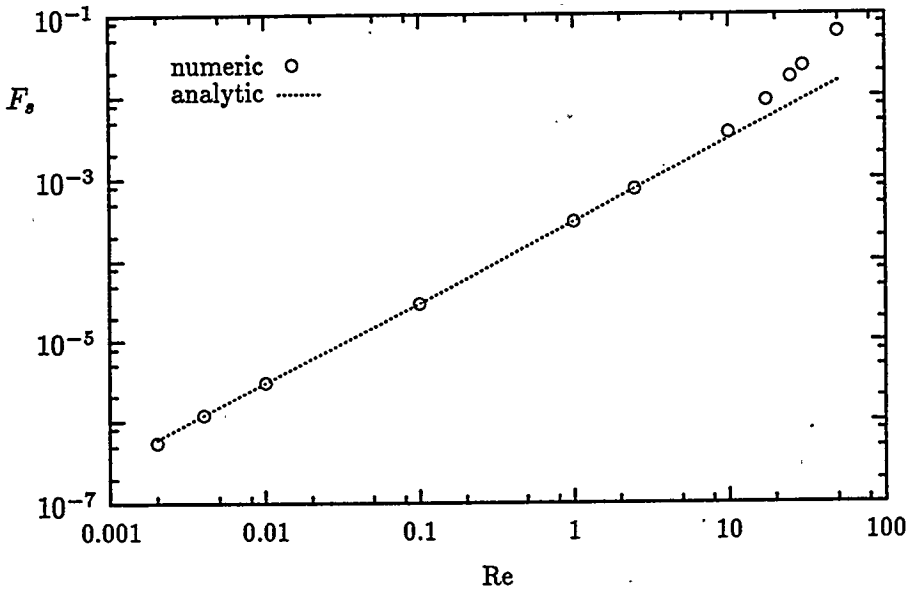


Knowing the dependence of the restitution coefficient on the material and fluid properties, one can construct an adopted numerical algorithm for granular materials in a fluid. The net effect of the surrounding fluid will be modelled by modified contact force laws and additional long range interactions model lubrication theory. Several thousand particles can be simulated and the results obtained in such a manner will be compared with simulations using a different method [6] and experiments [7] of batch settling processes. Diffusion constants can be calculated and compared as well.

## References


[1] A. Mehta (ed.), "Granular Matter" (Springer, Berlin, 1994); D. Bideau und A. Hansen (eds.), "Disorder and Granular Media" (North-Holland, Amsterdam, 1993)

[2] G.H. Ristow, "Granular Dynamics: a Review about recent Molecular Dynamics Simulations of Granular Materials", in *Annual Reviews of Computational Physics*, 275-308, D. Stauffer (ed.) (World Scientific, Singapore 1994)

[3] R.H. Davis, J.-M. Serayssol and E.J. Hinch, *J. Fluid Mech.* **163**, 479 (1986)

[4] G. Barnocky and R.H. Davis, *Phys. Fluids* **31**, 1324 (1988)

[5] R. Peyret and T.D. Taylor, "Computational Methods for Fluid Flow" (Springer, Berlin 1983); S.V. Patankar, "Numerical Heat Transfer and Fluid Flow" (Hemisphere, New York 1980)

[6] W. Kalthoff, S. Schwarzer, G.H. Ristow and H.J. Herrmann, preprint 1994

[7] H. Nicolai, B. Herzhaft, E.J. Hinch, L. Oger and E. Guazzelli, *Phys. Fluids* **7**, 12 (1995)

# ORIENTATIONAL AND CONFIGURATIONAL DIFFUSION IN THE SLOW FLOWS OF PARTICLES AND POLYMERS

*Eric S. G. Shaqfeh*

Department of Chemical Engineering, Stanford, CA 94305

Although it is well known that hydrodynamic interactions between particles in suspension can cause diffusion and dispersion of the center-of-mass, less is known about the effect of multiparticle interactions on the configuration of complex bodies – i.e. the orientation of non-spherical bodies, the stretch of added polymers, and the deformation of drops. Initial studies have demonstrated a wealth of interesting physics in these multi-phase flows and the concomitant need for new theories to describe these configurational diffusion processes. Moreover, even in dilute suspensions, the change of configuration can make an O(1) change in the effective suspension properties, and thus theories based on "cluster expansion" ideas can play a major role. However, the kinetic theory of configurational changes created by interparticle interactions is far less developed than that involving center-of-mass diffusion even without long-range hydrodynamic interactions. Thus, the construction of model equations and systems has been relatively slow.

The talk will begin by reviewing the concepts and nomenclature which is unique to this field of study via discussion of the simplest flow problem in this class — the flow of complex liquids through fixed beds.[1, 2, 8, 6, 9, 12, 11]. We shall focus on the flows through *dilute* disordered fixed beds, and examine the orientation of non-spherical particles,[1, 2, 6] the stretch of flexible polymers,[8, 9, 12, 11] and finally the deformation of drops [11] in these beds. The simplifying factors in this flow class include the fact that the configuration of the bed particles is fixed in space and the Brinkman screening in the bed acts to cut-off the long range hydrodynamic interactions. As a result of these simplifications, averaged configurational diffusion equations can be developed to describe the evolution of the configuration of these various dynamical elements.[1, 2, 8] In all cases the hydrodynamic interactions (acting in the absence of steric effects) change the configuration of these microstructural elements, and cause them to reach a highly anisotropic steady state – a steady state which would remain indeterminate in the presence of the mean "plug" flow alone. The evolution of configuration of polymers and drops in the flow through fixed beds is particularly interesting as large conformation change can be engendered by these flows even though the Eulerian mean flow is a "plug". Thus the concept of a "stochastic strong flow" and its application to suspensions will be developed. New computer simulations of the configuration of polymers and drop models in these flows will be discussed. Many of the theoretical predictions have been verified via detailed experiments and these will also be presented.[6, 9, 12]

Beyond the discussion of fixed bed flows, more complicated flow situations involving the configuration of microstructural elements will be discussed. In particular, we turn to particle (fiber) orientation in free non-Brownian suspensions subject to extensional and shear flows.[7, 5, 10] In these examples, the trajectories of the interacting particles may be complicated, and the long-range interactions require renormalization in order to obtain convergent results from any "collision integrals". In extensional flows the mean flow creates a determinate steady orientation distribution when the particles are acting alone, i.e. it aligns

nonspherical particles along the principle axis of extension. In this instance the hydrodynamic interactions act to create configurational dispersion about that axis.[5] We discuss the theories and experiments [16] designed to predict and measure that dispersion as a function of particle loading from "dilute" suspensions, through the "semi-dilute" regime. For simple shear flow, in the absence of particles interactions, the motion of a single particle does not specify a steady orientation distribution that is independent of the initial conditions. Instead, in the absence of other forces, we discuss how interparticle interactions have been shown in very recent work to specify the steady orientation distribution.[10] We also discuss the rheological consequences of this distribution.[7, 15]

Finally, we end with perhaps the most difficult flow situation in this class of problems: microstructural configuration and its development in sedimentation.[3] New results regarding the orientation of sedimenting fibers will be presented. We first demonstrate that a theoretical understanding of the sedimentation of non-spherial particles is frought with difficulties owing to the coupling of the sedimentation velocity and the particle orientation. While calculations for random suspensions are well posed and yield,[14] reasonable results for the mean sedimentation velocity, when the suspension is allowed to evolved dynamically, the the orientation-center-of-mass coupling causes the pair probability to decay very slowly. Renormalization does not allow one to calculate a mean sedimentation velocity for this system which is independent of box size.[3] Moreover, our calculations suggest that the suspension becomes inhomogeneous, and is subject to particle clustering where the concentration fluctuations scale on lengths of order $\phi^{-\frac{1}{2}}L$, where $L$ is the fiber length and $\phi$ is the particle volume fraction. Dynamic simulations of sedimenting fiber suspensions will be presented which indicate clustering, and also show that this clustering causes the sedimentation velocity to increase over its maximum possible value in unbound Newtonian fluids. These same simulations show that the orientation distribution in these sedimenting fiber suspensions achieves a steady state created by the hydrodynamic interactions, and this steady distribution is compared to the results of kinetic theory (keeping two body interactions) and very recent experimental results. In the experiments, image analysis of fibers dynamically sedimenting in an otherwise index-of-refraction matched (and therefore, transparent) suspension are presented which demonstrate that the orientation of fibers veritically – in the direction of gravity – appears to be the stable orientation as determined by hydrodynamic interactions. However, the velocity fluctuations also cause occasional "tumbling" of the fibers, thereby broadening he distribution of particle orientation.

# References


[1] Shaqfeh, E.S.G. and Koch, Donald L., "The Effects of Hydrodynamic Interactions on the Orientation of Axisymmetric Particles Flowing Through a Fixed Bed of Spheres or Fibers",*Phys. Fluids* **31**, 728 (1988)

[2] Shaqfeh, E.S.G. and Koch, Donald L., "The Combined Effects of Hydrodynamic Interactions and Brownian Motion on the Orientation of Axisymmetric Particles Flowing Through Fixed Beds", *Phys. Fluids* **31**, 2769 (1988)

[3] Koch, D.L. and Shaqfeh, E.S.G., "The Instability of a Dispersion of Sedimenting Spheroids", *J. Fluid Mech.* **209**, 521 (1989)

[4] Shaqfeh, E.S.G. and G.H. Fredrickson, "The Hydrodynamic Stress in a Suspension of Rods", *Phys. Fluids A* **2**(1), 7 (1990)

[5] Shaqfeh, E.S.G. and D.L. Koch, "Orientational Dispersion of Fibers in Extensional Flows", *Phys. Fluids A* **2**(7) 1077 (1990)

[6] Frattini, P.L., E.S.G. Shaqfeh, J.L. Levy, and D.L. Koch, "Observations of Axisymmetric Tracer Particle Orientation During Flow Through a Dilute Fixed Bed of Fibers",*Phys. Fluids A* **3**(11), 2516 (1991)

[7] Koch, D.L. and E.S.G. Shaqfeh,"The Average Rotation Rate of a Fiber in the Linear Flow of a Semi-Dilute Suspension", *Phys. Fluids A* **2**(12) 2093, (1990)

[8] Shaqfeh, E.S.G. and D.L. Koch, "Polymer Stretch in Dilute Fixed Beds of Spheres or Fibers", *J. Fluid Mech.***224**, 17–54 (1992)

[9] Evans, A.R., E.S.G. Shaqfeh, and P. L. Frattini, "Observations of Polymer Conformation During Flow Through a Fixed Fiber Bed",*J. Fluid Mech.* **281** pp 319-356 (1994)

[10] Rahnama, M., D.L. Koch, and E.S.G. Shaqfeh, "The Effect of Hydrodynamic Interactions on the Orientation Distribution of Fiber Suspensions Subject to Simple Shear Flow", *Physics of Fluids A* **7**(3) pp 487-506 (1995)

[11] Mosler, A. and E.S.G. Shaqfeh, "Polymer Conformation Change in Stochastic Flow Fields: Flow Through Fixed Beds", *J. Non-Newtonian Fluid Mech.* (in preparation)

[12] Evans, A.R. and E.S.G. Shaqfeh, "The Conformation of Semi-Rigid Polymers During Flow Through a Fixed Fiber Bed", *J. Non-Newtonian Fluid Mech.* (in preparation)

[13] Evans, A.R., E.S.G. Shaqfeh and P.L. Frattini, "Polymer Configuration During Flow Through a Fixed Bed of Fibers", *Theoretical and Applied Rheology* Vol. 2, Proceedings of XIth Int. Congr. on Rheology, Brussels, Belgium 8/17—21/92 (edited by P. Moldenauers and R. Keunings) Elsevier. pp 847–849

[14] Mackaplow, M. (speaker) and E.S.G. Shaqfeh, "*Simulations of the Sedimentation of a Fiber Suspension*", Particulate and Multiphase Flow Session, Fluid Mechanics Section, AICHE National Meeting, St. Louis, MO 11/16-19/93

[15] Stover, C.A., Koch, D.L. and Cohen, C. 1992 "Observations of fibre orientation in simple shear flow of semi-dilute suspensions", *J. Fluid Mech.* **238**, pp 277-296

[16] Rahnama, M., D.L. Koch, C.Cohen "Observations of fiber orientation in suspensions subject to plana extensions flows", *Phys. Fluids*, (to appear, Aug. 1995)

# The dynamics of semi-dilute and semi-concentrated fiber suspensions

R. R. SUNDARARAJAKUMAR DONALD L. KOCH

*School of Chemical Engineering, Cornell University, Ithaca, NY 14853*

**Abstract**

The mechanical, thermal, and electrical properties of a fiber composite are greatly influenced by the way in which the fibers are distributed within the polymer matrix. The orientation distribution and spatial configuration of the fibers are determined by the number of fibers per unit volume $n$, fiber aspect-ratio $L/d$ (where $L$ is the length and $d$ is the diameter of the fiber) and the hydrodynamics of the processing flow.

Dilute ($nL^3 \ll 1$) and semi-dilute ($nL^3 \gg 1$, $nL^2d < 1$) suspensions undergoing flows that are approximately linear have been the subject of many theoretical and experimental studies. These studies indicate that mechanical contacts are not important in these situations. This will no longer be true in the presence of nonlinear flows or solid boundaries or when $nL^2d > O(1)$—the so-called semi-concentrated regime. We discuss here the influence of mechanical contacts on the angular dispersion of fiber orientations in a semi-concentrated fiber suspension undergoing simple shear flow, and the non-hydrodynamic diffusion of a ball settling through a suspension of neutrally buoyant fibers.

In the semi-concentrated regime, we expect that a fiber can most easily rotate (disturbing a minimum number of neighboring fibers) if it remains in the plane made of the mean velocity and velocity gradient directions. This idea is supported by our simulations of the simple shear flow of a semi-dilute fiber suspension at moderate values of $nL^2d$. Thus, as a beginning, it is reasonable to model the simple shear flow of a semi-concentrated fiber suspension as that of a monolayer fiber suspension. Figure 1 shows the effect of mechanical contacts on the dispersion of particle orientations, as measured by $< p_y^2 >$ ($p_y$ being the projection of fiber orientation $\mathbf{p}$ in the velocity gradient direction $y$). The abscissa is the concentration measure $n_a L^2$, where $n_a$ is the number density and $L$ is the fiber length. It can be seen that $< p_y^2 >$ shows a nonlinear increase in the range $3.5 < nL^2 < 5.0$. This implies that the transport and mechanical properties such as conductivity in the velocity gradient direction and particle

stress show a nonlinear increase as well.

In semi-dilute fiber suspensions undergoing unbounded linear flows, the fibers rotate and translate like fluid lines so that they do not tend to collide. However, for non-linear flows or in the presence of solid boundaries, particle collisions are possible. Falling ball rheometry experiments (Milliken *et al* 1989) have established that the drag on the falling ball is significantly influenced by mechanical contacts. In addition, these mechanical contacts also lead to a *non-hydrodynamic* dispersion. Unlike hydrodynamic dispersion, which results solely from random hydrodynamic interactions among particles (Ham & Homsy 1988), the non-hydrodynamic dispersion is due to the hindered settling of the ball caused by mechanical contacts among the fibers as well as between the fibers and the ball. We present results for the variance of the time $t$ required by the ball to fall through a distance $z$ for various values of the concentration $nL^3$. This enables us to analyze the behavior of the dispersion coefficient as a function of the concentration.

## REFERENCES

J. M. HAM & G. M. HOMSY 1988 Hindered settling and hydrodynamic dispersion in quiescent sedimenting suspensions. *Int. J. Multiphase Flow*, **14**(5), 553.

W. J. MILLIKEN, M. GOTTLIEB, A. L. GRAHAM, L. A. MONDY & R. L. POWELL 1989 The viscosity volume fraction relation for suspensions of randomly oriented rods by falling ball rheometry. *J. Fluid Mech.*, **202**, 217.

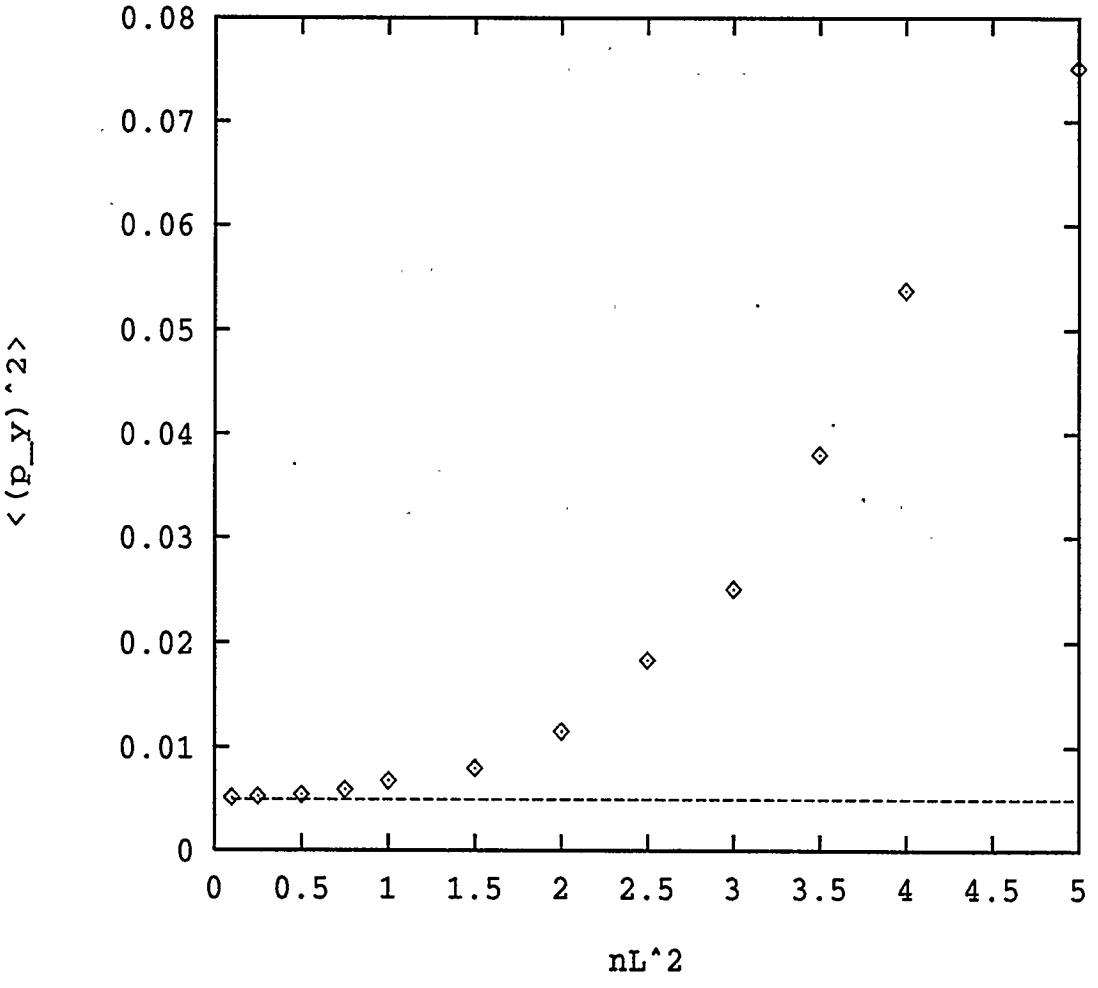


Figure 1: Schematic showing the nonlinear increase of angular dispersion due to the presence of mechanical contacts. The dotted line is the value of $< p_y^2 >$ for Jeffery orbits i.e. no collisions. The symbols ($\diamond$) are the results of our simulation.

# Fibre suspensions in dilute polymer solutions

Oliver G Harlen
Department of Applied Mathematical Studies, University of Leeds,
Leeds, LS2 9JT, UK

Donald L Koch
School of Chemical Engineering, Cornell University, Ithaca, NY 14853, USA

## 1 Introduction

Many injection moulded materials consist of polymers reinforced with short glass or carbon fibres. In this paper, we examine the behaviour of fibre suspensions in dilute polymer solutions at high Deborah numbers. In particular, we calculate the effect of hydrodynamic interactions between the fibres and polymer molecules on the orientation of the fibres and the conformation of the fibres in simple shear and purely extensional flow. A more detailed description is given in Harlen & Koch (1992, 1993).

## 2 Simple shear flow

At high Deborah numbers, the shear viscosity of polymer solution is much lower than the extensional viscosity. In a shear flow the polymer molecules stretch in the flow direction, perpendicular to the velocity gradient, and so the velocity difference across a molecule remains small. In a fibre suspension the polymers no longer experience purely simple shear flow, because of disturbances produced by the fibres. The effect of these disturbances is to rotate the polymers away from alignment with the flow direction, allowing the shear flow to stretch them further.

The polymers are modelled as elastic dumbbells with either a Hookean or Warner spring, yielding respectively the Oldroyd B and FENE constitutive models. The method of averaged equations is used to calculate the average extension of a polymer molecule in a random suspension of fibres undergoing simple shear.

For linear dumbbells, the shear viscosity in the absence of fibres is constant. With the addition of fibres the shear viscosity is given by

$$\mu_{\text{shear}} = \mu_s \left(1 + \frac{c}{1 - nl^3 \text{De}^3 M}\right),$$

where $\mu_s$, is the solvent viscosity, $c$ the volume concentration of dumbbells, $n$ the number density of fibres, $l$ the fibre half-length and De the Deborah number. $M$ is a constant that depends on the orientation distribution of the fibres. At a critical Deborah number of $(nL^3M)^{-1/3}$ the polymers undergo a coil-stretch transition similar to that found in extensional flow and the viscosity becomes unbounded.

This singular behaviour may be remedied by changing to a Warner spring, so that the dumbbells cannot stretch beyond a maximum length $R_{\max}$. With this modification the shear viscosity remains bounded and asymptotes to a constant value at high Deborah numbers.

$$\mu_{\text{shear}} \sim \mu_s \left(1 + cR_{\max}^2 (nl^3M)^{2/3}\right),$$

The orientation of an isolated fibre in a Newtonian fluid follows one of a family of closed curves called Jeffery orbits, depending upon its initial orientation. The distribution of a suspension of fibres between different Jeffery orbits cannot be found from the motion of a single fibre, but depends on secondary effects such as hydrodynamic interactions between fibres. In a weakly non-Newtonian fluid, the Newtonian stresses are expected to perturb the Jeffery rotation and may cause fibres to drift between Jeffery orbits. In the limit of low Deborah number, Leal (1975) calculated the perturbation to Jeffery orbits for a second order fluid. This predicts a drift towards the vorticity axis for fluids with a second-normal-stress difference.

We consider an alternative limit of small polymer concentration, but high Deborah number. The perturbation to the rotation of a fibre is found to be in the same direction as that found by Leal, but due to a different mechanism that does not require a second-normal-stress difference.

Experiments by Bartram *et. al.*(1975) and more recently by Iso *et. al.*(1995) see a drift of fibre orientation towards the vorticity axis for weakly viscoelastic fluids, in qualitative agreement with both theories. One of the fluids studied by Iso has a negligible second-normal-stress difference and the fibre orientation is also observed to drift towards the vorticity axis in this fluid, suggesting that a second-normal stress difference is not essential for this behaviour. However, at higher polymer concentrations Iso observed qualitatively different behaviour, that is not explained by either theory.

## 3 Extensional flow

In a steady uniaxial extensional flow at a Deborah number greater than unity, the polymer molecules become highly extended and oriented with the extensional axis. The fluid behaves as anisotropic viscous fluid with a high extensional viscosity, so that the fluid stress is of the form

$$\sigma_{ij} = \mu \left( \frac{\partial u_i}{\partial x_j} + \frac{\partial u_j}{\partial x_i} + \alpha \delta_{1i} \delta_{1j} \frac{\partial u_1}{\partial x_1} \right),$$

where 1 denotes the extensional axis. The parameter, $\alpha$, determines the magnitude of the extensional viscosity, and is proportional to the effective volume concentration of of extended polymers.

Provided $\alpha$ is small compared to the square of the aspect ratio, $r$, the velocity disturbance generated by a slender fibre in this medium can be calculated using slender body theory (Acrivos & Shaqfeh 1988). The high extensional viscosity produces only a logarithmic change to the fibre stress, which would be swamped by any shear-thinning of the fluid. If $\alpha \geq r^2$ the flow cannot be analysed using slender body theory. However, for spheroidal fibres it is possible to obtain an analytical solution in the limit $\alpha \gg r^2 \gg 1$. In this limit, the contribution from the fibres is found to be negligible in comparison to contribution from the polymers.

A single fibre in an extensional flow will align perfectly with the extensional axis, however, hydrodynamic interactions between fibres will produce a small dispersion of orientations about this direction. The effect of adding polymers is to decrease the degree of dispersion from that calculated by Shaqfeh & Koch (1990) for a Newtonian fluid. This is because the anisotropy of the fluid screens the velocity disturbances between fibres, with a radial screening length of $L/\sqrt{\alpha}$. This is confirmed by recent experiments by Rahnama *et. al.*(1995) on fibre alignment in a four-roll mill that show a decrease in fibre dispersion with the addition of polymer.

# 4 References


A. Acrivos and E.S.G. Shaqfeh (1988) Physics of Fluids **31**, 1841.
E. Bartram, H.L. Goldsmith and S.G. Mason (1975) Rheologica Acta **14**, 776.
O.G. Harlen and D.L. Koch (1992) Physics of Fluids A **4** 1070.
O.G. Harlen and D.L. Koch (1992) Journal of Fluid Mechanics **252** 187.
Y. Iso, D.L. Koch and C.Cohen (1995) submitted to the Journal of non-Newtonian Fluid Mechanics.
L.G. Leal (1975) Journal of FLuid Mechanics **69**, 305
M. Rahnama, D.L. Koch and E.S.G. Shaqfeh (1995) submitted to Physics of Fluids.
E.S.G. Shaqfeh and D.L. Koch (1990) Physics of Fluids A **2**, 1077.

# Exploitation of Brownian motions for the optimal control of fiber orientation distributions

Andrew J. Szeri*

The nonlinear dynamics of Brownian suspensions of orientable particles are considered in unsteady flows. Suspensions of orientable particles are interesting microstructured fluids that store information about their flow prior to an instant of time in their current orientation distribution. The distinguishing feature of *Brownian* suspensions of orientable particles is that they tend to have fading memories; in other words Brownian motions cause these materials to have a more vivid memory of the recent past than of the more distant past. This phenomenon is explored in some detail. These explorations will make possible the *optimal control* of orientation distributions by exploitation of fading memory.

In a dilute, non-Brownian suspension of rods, the motion of a particle may be conveniently understood in terms of the deformation $\boldsymbol{u}(t, \boldsymbol{u}_0) = \boldsymbol{Q}(t)\boldsymbol{u}_0/\|\boldsymbol{Q}(t)\boldsymbol{u}_0\|$, where $\boldsymbol{Q}$ is a second rank tensor that depends on time, $\boldsymbol{u}$ is the (normalized) direction-vector of a rod-like particle, and $\boldsymbol{u}_0$ is an initial orientation. For a dilute non-Brownian suspension of rod-like particles in a flow, the deformation is exact, with $\mathrm{d}\boldsymbol{Q}/\mathrm{d}t = \boldsymbol{\kappa}(t)\boldsymbol{Q}$ and initial condition $\boldsymbol{Q}(0) = \boldsymbol{I}$; see Bretherton [2]. Here $\boldsymbol{\kappa}$ is the "equivalent velocity gradient tensor" of the flow, evaluated at the location of the material point in question ($\boldsymbol{\kappa} = \boldsymbol{\Omega} + G\boldsymbol{E}$, where $\boldsymbol{\Omega}$ is the vorticity tensor, $G$ is the shape factor of particles, and $\boldsymbol{E}$ is the rate-of-strain tensor). If $G = 1$ then $\boldsymbol{Q}$ is simply the deformation gradient tensor for the underlying fluid flow.

*University of California, Irvine, Department of Mechanical and Aerospace Engineering, Irvine, California 92717-3975. Internet: szeri@uci.edu

A simple example shows that the deformation can become become arbitrarily sharply peaked about some favored direction. Consider a uniaxial extensional flow. The dynamical equation for $Q$ may be written in coordinates in the form $\dot{Q}_{11} = G\dot{\epsilon}Q_{11}$ where $\dot{\epsilon}$ is the rate-of-strain in the 1-direction. If $\dot{\epsilon} > 0$ and steady, then clearly $Q_{11}$ increases with time exponentially. Hence, an initial orientation distribution becomes arbitrarily sharply peaked about the 1-axis, provided one waits long enough. Simply allowing for Brownian motions will cause the deformation to saturate at some point so that $Q$ remains finite.

A modification of the previous construction has been developed [5] for the influence of Brownian motions on the orientation distribution. The addition of another term to this model corresponding to an excluded-volume potential yields a model for liquid crystalline polymers [4]. The Brownian terms in the model lead to nonlinear saturation of the deformation $Q$ in any (time-dependent, three-dimensional) flow. Hence, so long as there are Brownian motions the deformation $Q$ cannot become arbitrarily sharply peaked about some favored direction.

A special class of unsteady flows is studied in the present work. These are termed *closed flows*: in a closed flow material points of the carrier fluid experience no net deformation over the interval of the closed flow. However, during the closed flow, material points of the carrier fluid may experience arbitrarily large excursions —the point is that they return to their initial locations. The class of closed flows includes general shear-free flows and simple shear flow, provided the components of the rate-of-strain tensor in these flows integrate to zero.

It is of interest to study suspension dynamics in these flows because in some sense there is no 'net' history experienced by particles suspended in such a flow. What this means precisely is that a non-Brownian suspension, with perfect memory, will return to its initial orientation distribution after such a closed flow. In contrast, a non-Brownian suspension will not. Because its memory is fading, the first part of the closed flow will produce an effect on the orientation distribution that is forgotten as the flow 'reverses' and returns to its initial state. At the end of the closed flow, there is a net change to the orientation distribution that arises from the more vivid memory the material has of the more recent part of the flow.

These simple ideas lead to a class of control problems that are formulated and solved in the present work. Within the class of closed flows, the task

is to identify what closed flow will have the greatest 'net' history on the orientation distribution of a *Brownian* suspension. These problems open up new possibilities for the control of the orientation distribution. For example, in a non-Brownian suspension, if one wants to align the particles with the flow direction, the most effective way is to contract the conduit through which the material flows [3]. Similarly, to align particles across the streamlines, one expands the cross-section of the flow [1]. In a Brownian suspension, optimal control theory demonstrates that it is possible to align particles with the flow direction without any net contraction of the flow domain normal to the flow direction. Such a capability can improve industrial processes such as fiber spinning and injection molding.

# References


[1] ALTAN, M. C. AND B. N. RAO Closed-form solution for the orientation field in a center-gated disk *J. Rheology* **39** (1995), 581–599.

[2] BRETHERTON, F. P. The motion of rigid particles in a shear flow at low Reynolds number. *J. Fluid Mech.* **14** (1962), 284–304.

[3] DOSHI, S. R. AND J.-M. CHARRIER A simple illustration of structure-properties relationships for short fiber-reinforced thermoplastics *Polym. Comp.* **10** (1989), 28–38.

[4] SZERI, A. J. A deformation tensor model for liquid crystalline polymers *J. Rheol.*, to appear.

[5] SZERI, A. J. AND D. J. LIN A deformation tensor model of Brownian suspensions of orientable particles —the nonlinear dynamics of closure models *J. non-Newt. Fluid Mech.*, submitted.

# Theoretical and experimental study of hydrodynamic interactions between several spheres

J. Bławzdziewicz[1,2], F. Feuillebois[1],
N. Lecoq[3], R. Anthore[3], and C. Petipas[3]

[1]PMMH, URA 857, ESPCI, 10 rue Vauquelin, 75231 Paris cedex 05, France.
[2]Permanent address: Institute of Fundamental Technological Research,
Polish Academy of Sciences, Świętokrzyska 21, 00-049 Warsaw, Poland.
[3]URA 808, BP 118, 76134 Mont Saint Aignan, France.

A detailed knowledge of the hydrodynamic interactions between many spheres in a Stokes flow is essential in the analysis of complex processes that occur in a suspension flow. In particular, understanding of the hydrodynamic interactions may provide an important insight into mechanisms of hydrodynamic diffusion. In this paper we address the problem of precise experimental and theoretical evaluations of the hydrodynamic interactions between several spheres.

A recently developed laser interferometric technique [1] has been used to measure the velocity of a sphere settling vertically towards a fixed cluster of spheres. Our equipment permits measurements of the vertical motion of a sphere with a sensitivity of about 50 nm. Clusters of one to four fixed spheres were considered. The fixed spheres had the same diameter as the moving one. The spheres were millimeter size steel balls. They were enclosed in a cylindrical container 5 cm in diameter and 4 cm in height containing silicon oil. The oil was very viscous (100 Pa.s), so that the Reynolds number relative to the moving sphere was small. The influence of the container walls was estimated by changing the diameter of the set of spheres.

The experimental results have been compared with the numerical calculation of the mobility matrix for a group of spheres in an infinite fluid. To this end the algorithm recently developed by Cichocki at al. [2] has been used. The algorithm is based on a systematic expansion of the force distribution induced at the particle surface into the irreducible multipole moments and includes a correction for the lubrication layer. A moderate number of multipoles is sufficient to obtain accurate results.

The techniques were first validated for a settling sphere approaching another equal fixed sphere: The theory, which for the two particle case gives a more accurate result than the earlier theory for two spheres by Jeffrey and Onishi [3], was in good agreement with experiment for small gaps, less than 0.01 when normalized by the sphere radius. The deviation of the theory from the experiment for larger gaps was decreasing with a decreasing particles diameter (the largest spheres were 6.35 mm in diameter) and was thus attributed to wall effects. The effects of the walls on the particle mobility matrix were estimated by introducing correction terms in the theoretical approach. The effect of the support of the fixed cluster was also modeled by a vertical line of spheres. The calculation showed that this effect is negligible.

Cluster of two to four fixed spheres were then considered. Comparison between experiment and theory was found to be good, although a more detailed analysis of the wall effect is still needed.

Experimental and theoretical results show that in some cases a very precise determination of the positions of the fixed spheres is critical. This happens when the hydrodynamic interactions of the falling sphere with four fixed spheres, or more, occur simultaneously in the lubrication regime. For example, we have considered a cluster of four spheres with their centers forming a horizontal square. When two spheres located along the diagonal were moved up by about 30 to 50 $\mu$m (the sphere diameter being 6.35 mm), the dependence of the mobility of the falling sphere on the distance from the touching configuration changed significantly for small gaps (less than 200 $\mu$m). The sensitivity of the results to small displacements of the fixed spheres was much smaller for clusters of two and three spheres. This effect has been observed both theoretically and in the experiment. Our result suggests that in some cases a small change of the suspension microstructure may result in a significant change of the hydrodynamic interactions.

# References


[1] N. Lecoq, F. Feuillebois, N. Anthore, R. Anthore, F. Bostel and C. Petipas, Phys. Fluids A **5**, 3 (1993).

[2] B. Cichocki, B.U. Felderhof, K. Hinsen, E. Wajnryb, and J. Bławzdziewicz, J. Chem. Phys. **100**, 3780 (1994).

[3] D.J. Jeffrey and Y. Onishi, J. Fluid Mech. **139**, 261 (1984).

# Diffusion and coalescence due to pair interactions in a suspension of bubbles in potential flow

V. Kumaran,
Department of Chemical Engineering,
Indian Institute of Science,
Bangalore 560 012 India

The calculation average properties of a suspension of bubbles rising due to gravity in the high Reynolds number, low Weber number limit (Kumaran and Koch [1,2]) is discussed. In the high Reynolds number limit, the viscous forces are small compared to the inertial forces and the fluid flow is described by the potential flow equations, while in the low Weber number limit the surface tension forces are large and the bubbles can be considered to be spherical. The calculation involves two steps — determination of the effect of pair interaction on the motion of the bubbles, and an ensemble averaging procedure to determine macroscopic properties from a knowledge of the details of the interactions.

The interaction between a pair of bubbles of radii $a_1$ and $a_2$ with velocities $\mathbf{U}_1$ and $\mathbf{U}_2$ in potential flow (Figure 1) is determined using the method of twin spherical expansions[1]. The fluid velocity field is expressed in terms of the velocity potential $\mathbf{u} = \nabla\phi$. The governing equation for the velocity potential $\phi$ is the Laplace equation:

$$\nabla^2\phi = 0, \tag{1}$$

and the pressure in the fluid is given by the Bernoulli equation:

$$p = -\frac{\partial\phi}{\partial t} - \frac{1}{2}\mathbf{u}^2. \tag{2}$$

The boundary conditions are the zero normal velocity at the surface of the bubbles:

$$\mathbf{u}.\mathbf{n} = \mathbf{U}_i.n \tag{3}$$

at the surface. In addition, the bubbles are considered to be massless, so the net force on each bubble is zero:

$$-\int_{A_i} p\,\mathbf{n}_i\,dA_i + \mathbf{F}_i = 0, \tag{4}$$

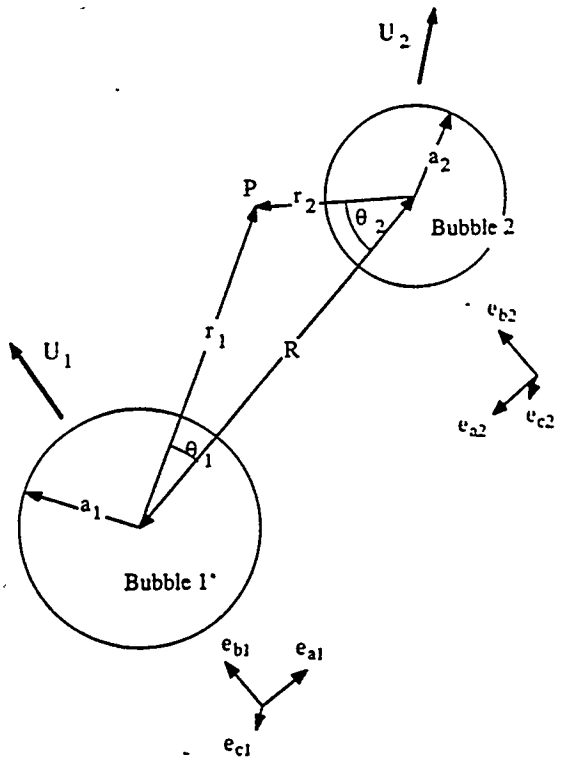


FIG. 1: Definition of coordinate system for analyzing the interactions between non - deformable bubbles.

where $A_i$ is the surface of the bubble $i$ and $\mathbf{n}_i$ is the outward unit normal to this surface. $\mathbf{F}_i$, the sum of the buoyancy and drag forces, is $12\pi\mu a_i(\mathbf{U}_i - \mathbf{U}_{it})$, where $\mathbf{U}_{it}$ is the terminal velocity of a bubble of radius $a_i$.

The fluid velocity field is expressed in terms of the bubble velocities using the method of twin spherical harmonics[1], and the acceleration of the bubbles is determined as an expansion in $(a_1/R)$ using the zero net force condition (4). The equations of motion are non - linear due to the presence of the $(\mathbf{v}^2/2)$ term in the Bernoulli equation. The acceleration of bubble

1 due to potential flow interactions is:

$$\frac{dU_1^{\parallel}}{dt} = \frac{9a_2^3}{2R^4}[U_1^{\perp}U_2^{\perp} - 2U_2^{\parallel 2}] + \frac{F_1^{\parallel}}{(2/3)\pi\rho a_1^3}, \quad (5)$$

$$\frac{dU_1^{\perp}}{dt} = \frac{9a_2^3}{2R^4}U_2^{\parallel}(U_1^{\perp} + U_2^{\perp}) + \frac{F_1^{\perp}}{(2/3)\pi\rho a_1^3}, \quad (6)$$

and the acceleration of bubble 2 is given by symmetrical relations, where $U_i^{\parallel}$ and $U_i^{\perp}$ are the velocities along and perpendicular to the line joining the centres of the bubbles respectively. The leading order acceleration due to the potential flow interaction is proportional to $(1/R)^4$. Due to this strong decay, no divergences are encountered in the pair averaging procedure.

The interaction between a pair of bubbles rising due to gravity, which initiated by the approach of the larger bubble from below, can be determined by a numerical integration of the equations (5) and (6)[1]. The result of an interaction is strongly dependent on the ratio of their sizes $s = (a_2/a_1)$ (here, $a_1$ is assumed to be the radius of the smaller bubble). If the ratio of sizes is larger than a critical value, $s_c$, the bubbles repel each other during an interaction and their surfaces do not touch, as shown in Figure 2. If the ratio is less than the critical value $s_c$, the bubble collide along the horizontal plane if their initial horizontal separation $b$ is less than a critical value $b_c$ as shown in Figure 3. If the trajectories are continued assuming that the collision is elastic, the bubbles collide repeatedly and coalesce. The empirical relation for $s_c$

$$(s_c - 1) = 1.73Re^{-3/5} \quad (7)$$

is applicable in the range $Re = 100$ to 400[1]. The numerical calculations[1] indicate that there are two scaling regimes for $b_c$:

$$b_c = 0.85(Re/(s-1))^{1/4} \quad \text{for} \quad b_c < \tau_v \Delta U_t, \quad (8)$$

$$b_c = 0.8(s-1)^{-2/3} \quad \text{for} \quad b_c > \tau_v, \Delta U_t \quad (9)$$

where $\Delta U_t$ is the difference in terminal velocities, and $\tau_v = (Re/18)(a_1/U_{1t})$ is the viscous relaxation time.

The interaction between bubbles with size ratio $s > s_c$[1] results in a vertical and horizontal displacement of their positions in a reference frame moving

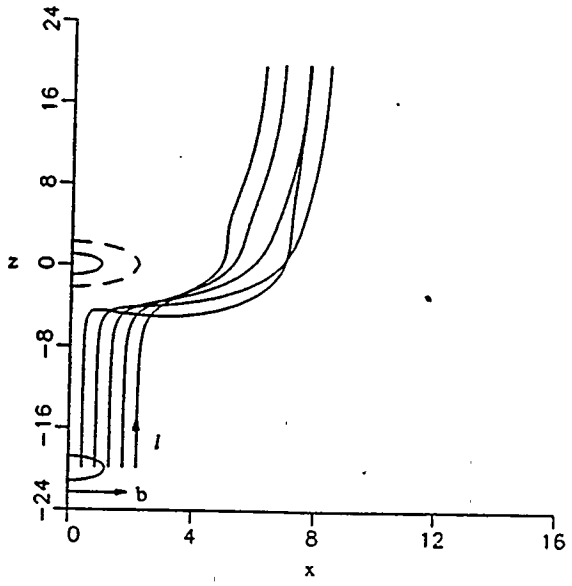


FIG. 2: Trajectories of bubbles of different sizes rising due to gravity. The size ratio $s$ is 1.2, the Reynolds number based on the radius and terminal velocity of the smaller bubbleis 200 and the position of the larger bubble is tracked in a reference frame moving with the smaller one. The broken line represents a circle of radius $(s+1)$; when the center of the larger bubble is on the broken line, the surfaces touch.

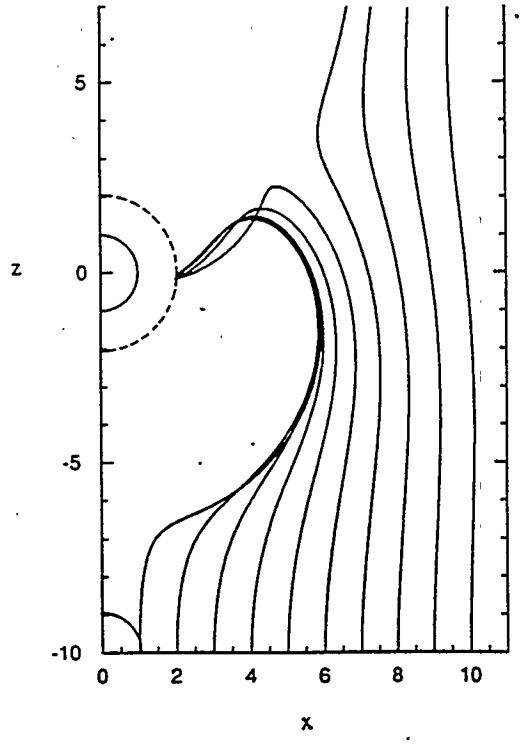


FIG. 3: Interaction between bubbles of nearly equal size. The size ratio is 1.05, and the Reynolds number based on the radius of the smaller bubble is 200. The broken line represents a circle of radius $(s+1)$, when the center of the larger bubble is on the broken line, the surfaces touch.

at the terminal velocity, and this results in a flux ofbubbles in a non - uniform suspension. The flux of bubbles of species $i$ due to interaction with bubbles of species $j$ in the horizontal and vertical directions can be expressed as:

$$J_x^i = D_x^{ij}\frac{\partial n_j}{\partial x}, J_z^i = D_z^{ij}\frac{\partial n_j}{\partial z}, \qquad (10)$$

where $n_i$ and $n_j$ are the number densities of the two species. Note that there could be diffusion of a bubble of species $i$ due to gradients in the densities of both $i$ and $j$. The diffusion coefficient for small gradients in the number density is given by[1]:

$$D_x^{ij} = \frac{\pi}{2}|U_{1t} - U_{2t}|n_{3-j}\int_b x_{ci}^2\, bdb \qquad (11)$$

$$D_z^{ij} = \pi|U_{1t} - U_{2t}|n_{3-j}\int_b z_{ci}^2\, bdb \qquad (12)$$

where $x_{ci}$ and $z_{ci}$ are the horizontal and vertical deflections of the bubble $i$ due to an interaction with a bubble of species $j$ in which the horizontal distance between the trajectories before the interaction is $b$. Typical diffusion coefficients are shown as a function of $Re$ and $s$ in Figures 4 and 5. An interesting feature of these results is that the horizontal and vertical coefficients are nearly equal. This is very different from an isotropic medium. in which $D_x$ is twice $D_z$, indicating that the diffusion due to interactions is highly anisotropic.

The interaction between a pair of bubbles with size ratio $s < s_c$ results in coalescence[2]. The frequency of coalescence can be determined using relations (7) for $s_c$ and (8) and (9) for $b_c$. This calculation shows that the rate of coalescence decreases $\propto Re^{-2/5}$, where $Re$ is the Reynolds number.

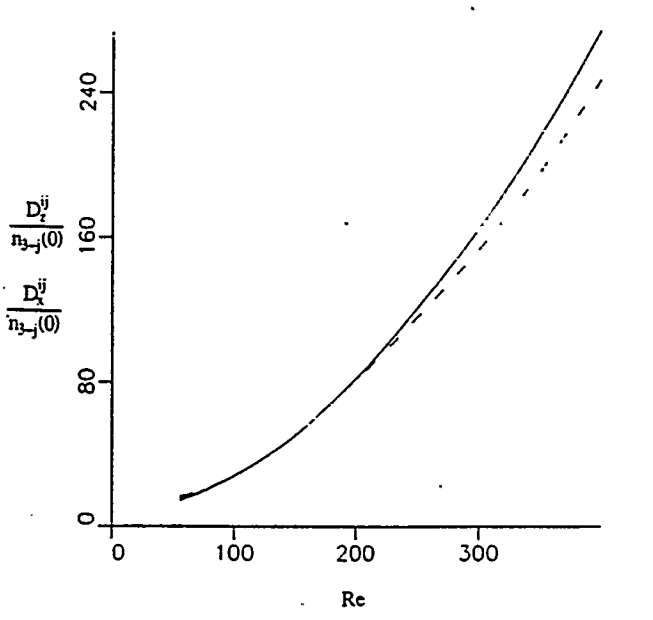


FIG. 4: $[D_z^{ij}/n_{3-j}]$(broken line) and $[D_z^{ij}/n_{3-j}]$ (solid line) as a function of Reynolds number based on radius and terminal velocity of species 1. The size ratio $s$ is 1.25

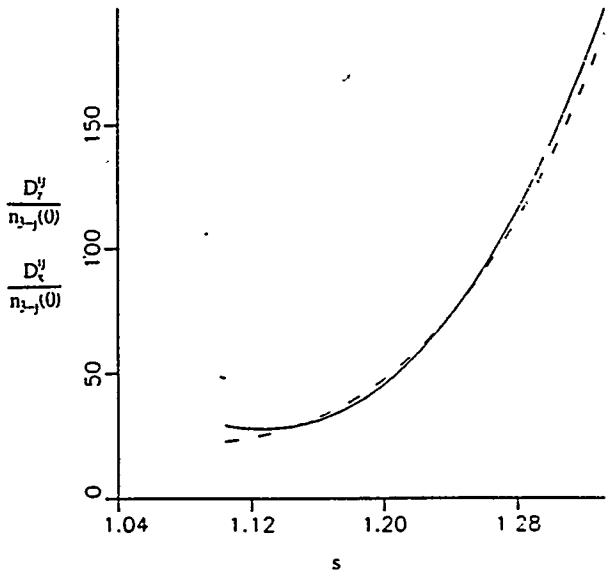


FIG. 5:$[D_z^{ij}/n_{3-j}]$(broken line) and $[D_z^{ij}/n_{3-j}]$ (solid line) as a function of soze ratop $s$.The Reynolds number based on radius and terminal velocity of species 1 is 200.

## References


[ 1 ] V. Kumaran and D. L. Koch, 'The effect of interactions on the average properties of a bidisperse suspension of high Reynolds number, low Weber number bubbles', *Phys. Fluids A*, **5**, 1123, (1993).

[ 2 ] V. Kumaran and D. L. Koch, 'The rate of coalescence in a suspension of high Reynolds number, low Weber number bubbles', *Phys. Fluids A*, **5**, 1135, (1993).

# The nature of particle contacts in sedimentation

Shulin Zeng, Todd Kerns, Alexander Zinchenko, and Robert H. Davis
Department of Chemical Engineering
University of Colorado at Boulder
Boulder, CO 80309-0424

The macroscopic properties of a suspension of particles in a fluid depend on the nature of the relative motion of particles. For example, extending Einstein's classical expression for the effective viscosity of a dilute suspension of rigid spheres to more concentrated suspensions requires an understanding of particle interactions (Batchelor and Green, 1972; Nir and Acrivos, 1973). Previous analyses have dealt with the interaction of two smooth spheres which, according to classical lubrication theory, do not come into physical contact under the action of finite forces. However, in the cases where the interacting spheres are not smooth but have microscopic roughness elements on their surfaces, experimental evidence shows that physical contact does occur and significantly affects the relative motion of the spheres (Arp and Mason,1977; Parsi and Gadala-Maria,1987; Barnocky and Davis,1988; Smart and Leighton, 1989). Moreover, particle contact due to surface roughness breaks the symmetry of the relative trajectory of two spheres in shear flow, or of two unequal spheres in sedimentation. This gives rise to a non-zero transverse hydrodynamic diffusivity for dilute suspensions, as well as modifying the longitudinal hydrodynamic diffusivity (Davis, 1992; da Cunha and Hinch, 1995).

Although spheres with small roughness do make physical contact in suspensions, the nature and role of this contact are not understood. Davis (1992) developed two models for the nature of this contact. One is a "stick/rotate" model in which the roughness elements on the surfaces of the two spheres lock together so that the two spheres move in rigid-body translation and rotation. The other is a "roll/slip" model in which one sphere rolls around the surface of the other with slip occurring if the maximum tangential force allowed by solid-solid friction is exceeded. In this paper, experimental observations of the contact of two unequal sedimenting spheres are described and compared to the models of Davis (1992).

The system under consideration involves a neutrally buoyant nylon sphere of diameter 6.35 mm and density 1.11g/cm$^3$ in a Newtonian fluid of density 1.11g/cm$^3$ and viscosity 25 kg/m-s. This fluid is a mixture of 97.4% polyalklene glycol and 2.6% tetrabromoethane by weight. A single teflon sphere of diameter 6.35 mm and density 2.30 g/cm$^3$ sediments due to gravity through the fluid and interacts with the neutrally buoyant one in this fluid. The heights of the roughness elements on nylon and teflon spheres from microscopic analysis are approximately 20 and 8 microns, respectively. The fluid is contained in a rectangular vertical glass chamber, which has dimensions 25cm*25cm in horizontal cross section and is 30 cm in depth. The interaction of the two spheres is observed by a video camera and recorded on a video tape. The interaction message on the video tape is transformed into a computer data file by Global Lab Image software.

Results for a typical experiment are shown in Figures 1-3. The relative trajectory (representing the location of the center of the heavy sphere relative to the center of the neutrally buoyant sphere, made dimensionless with the sphere radius) is depicted in Figure 1. The theory was calculated in three parts: (i) an upstream noncontact interaction using complete two-sphere mobility functions starting with an initial horizontal offset of 0.26 found by a best-fit of the data; (ii) a contact interaction described by the stick/rotate and roll/slip models of Davis (1992), which give indistinguishable results in this case; and (iii) a downstream non-contact interaction starting when the line-of-centers is horizontal and with a best-fit initial separation of 0.00315, which represents the minimum dimensionless separation of the nominal sphere surfaces supported by the roughness elements. Note that the symmetry of the trajectory is broken by the contact.

Figure 2 is a plot of the angle of the line-of-centers from the vertical versus time made dimensionless by the heavy sphere radius divided by its isolated velocity corrected for wall effects by a best fit of the measured time dependence of the relative trajectory to theory. The angle of the line-of-centers rotates more slowly for the stick/rotate model than for the roll/slip model, and the latter provides a better fit of the data; a best-fit value of 35° is found for the critical angle at which friction is no larger able to prevent slip at the surface. This corresponds to a friction coefficient of 0.30. The individual spheres were observed to rotate at different angular velocities, providing further support for the roll/slip model over the stick/rotate model.

Figure 3 shows the transverse mobility function (representing the dimensionless relative velocity normal to the line-of-centers) for the two-sphere interaction. Again, the roll/slip model with a critical slip angle of 35° provides an excellent fit of the data, whereas the stick/rotate model and the roll/slip model with no slipping underpredict the relative velocity during contact.

Additional experiments were carried out using different initial horizontal offsets. It was found that the critical impact parameter is 0.62 (Figure 4), beyond which contact does not occur and the relative trajectories are symmetric. This value agrees with theory for a contact separation of 0.00315.


1. A. P. Arp and S. G. Mason(1977), "The kinetics of flowing dispersions, IX, Doublets of rigid spheres(experimental)", J. Colloid Interface Sci., **61**, 44.
2. G. Barnocky and R. H. Davis(1988), "Elastohydrodynamic collision and rebound of spheres: Experimental verification", Phys. Fluids **31**, 1324.
3. G. K. Batchelor and J. T. Green(1972), "The determination of the bulk stress in a suspension of spherical particles to order $c^2$", J. Fluid Mech. **56**, 401.
4. F. R. da Cunha and E. J. Hinch(1995), "Shear-induced dispersion in a dilute suspension of rough spheres", submitted to Physics of Fluids.
5. R. H. Davis(1992), "Effects of surface roughness on a sphere sedimenting through a dilute suspension of neutrally buoyant spheres", Phys. Fluid A, **4**, 2607.
6. A. Nir and A. Acrivos(1973), "On the creeping motion of two arbitrary-sized touching spheres in a linear shear field", J. Fluid Mech., **59**, 209.

7. F. Parsi and F. Gadala-Maria(1987), "Fore-and-aft asymmetry in a concentrated suspension of solid spheres", J. Rheol., **31**, 725.
8. J. R. Smart and D. T. Leighton(1989), " Measurement of the hydrodynamic surface roughness of noncolloidal particles", Phys. Fluids A, **1**, 52.
9. M. Tabatabaian and R. G. Cox(1991),"Effect of contact forces on sedimenting spheres in Stokes flow", Int. J. Multiphase Flow, **17**, 395.

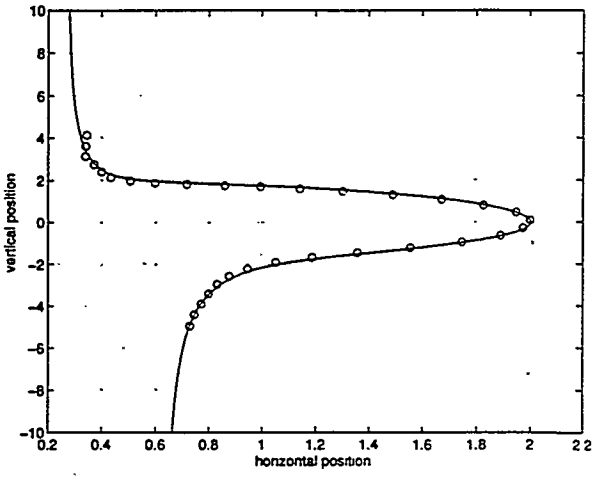


Figure 1. Trajectory of the falling sphere relative to the neutrally buoyant one from experiment(circles), stick/rotate model(solid line), rolling without slipping model (dashed line, covered by solid line), and roll/slip model with slip angle of 35°(dashed-dotted line, also covered by solid line )

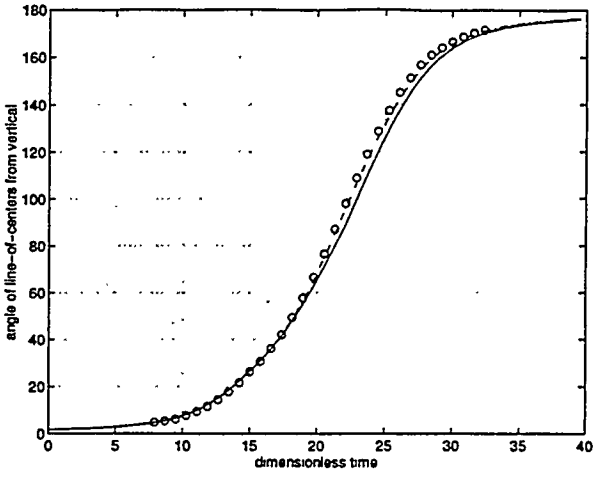


Figure 2. Angle of the line of centers versus dimensionless time from experiment(circles), stick/rotate model(solid line), rolling without slipping model(dashed line, covered by solid line), and roll/slip model with slip angle of 35°(dashed-dotted line).

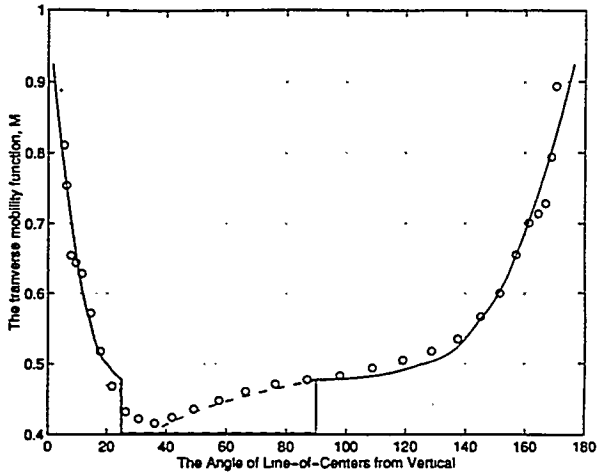


Figure 3. Transverse relative mobility function versus the angle of line of centers from experiment(circles), stick/rotate model(solid line), rolling without slipping model (dashed line, covered by solid line), and roll/slip model with slip angle of 35°(dashed-dotted line).

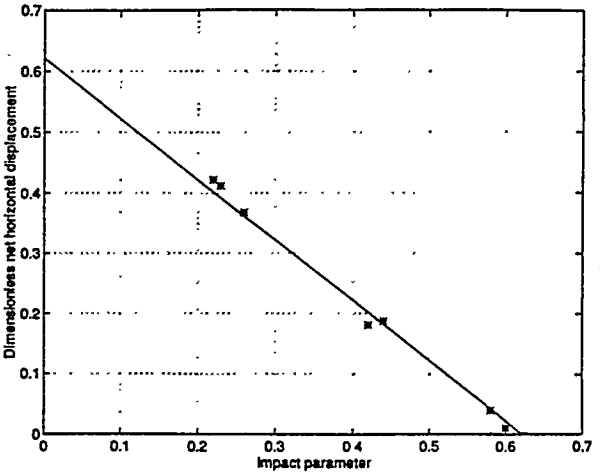


Figure 4. Net horizontal displacements versus the initial horizontal offset or impact parameter from experiments(stars) and theory(solid line)

# Deformation-Induced Drop Dispersion

Michael Loewenberg
Department of Chemical Engineering
Yale University

Dispersion of nonBrownian particles and drops in suspensions and emulsions is important because it provides a mechanism for mixing. In a sheared suspension of spherical particles, dispersion arises due to the irreversibility of multiparticle interactions. In dilute suspensions, particle dispersion is a weak, $O(\phi^2)$ effect, where $\phi$ is the particle volume fraction, because pairwise interactions are reversible under low-Reynolds number, viscous flow conditions.

By contrast, pairwise interactions between deformable drops are intrinsically irreversible so that dispersion has a more pronounced, $O(\phi)$ effect. There are two sources of this irreversibility: the nonspherical shape of an isolated, deformable drop in a shear-flow and the nonlinear behavior of interacting, deformable drop interfaces. The first source of irreversibility relates to any nonspherical but fixed shapes, including rigid particles; the second is a dynamic effect that is unique to deformable drops.

Self-diffusion refers to the random walk of a single marked particle or drop which can be described in terms of a dispersion coefficient, $D_\alpha$, where $\alpha$ is a coordinate direction. Here, we consider the two cross-flow components of self-diffusion in the direction of the velocity gradient and the vorticity, denoted by $\alpha = \| \ , \ \perp$. In a dilute system, the dispersion coefficient may be computed from pairwise interactions:

$$D_\alpha = \frac{3}{2\pi} \phi \dot{\gamma} a^2 \int_0^\infty \int_0^\infty \Delta_\alpha^2 \, x_\| \, dx_\| dx_\perp \ ,$$

where $\dot{\gamma}$ is the shear-rate and $a$ is the undeformed drop radius and the characteristic length of the problem; $\Delta_\alpha(x_\|, x_\perp)$ is the net cross-flow displacement between a pair of interacting drops that is obtained by integrating along the relative trajectory from an initial, widely separated location $(x_\|, x_\perp)$ on a plane perpendicular to the flow direction. The dispersion coefficient is obtained by integrating over all initial locations.

Neglecting surfactant effects, the dispersion coefficients depend on the drop viscosity ratio, $\lambda$ and the Capillary number, $Ca = \mu \dot{\gamma} a / \sigma$, where $\sigma$ is the interfacial tension. The Capillary number is the dimensionless shear-rate and the ratio of deforming viscous stresses to surface tension. Three-dimensional boundary integral calculations were used to compute the net displacements, $\Delta_\alpha$. A portion of a typical trajectory is illustrated below; the net cross-flow displacement resulting from the drop interaction is apparent.

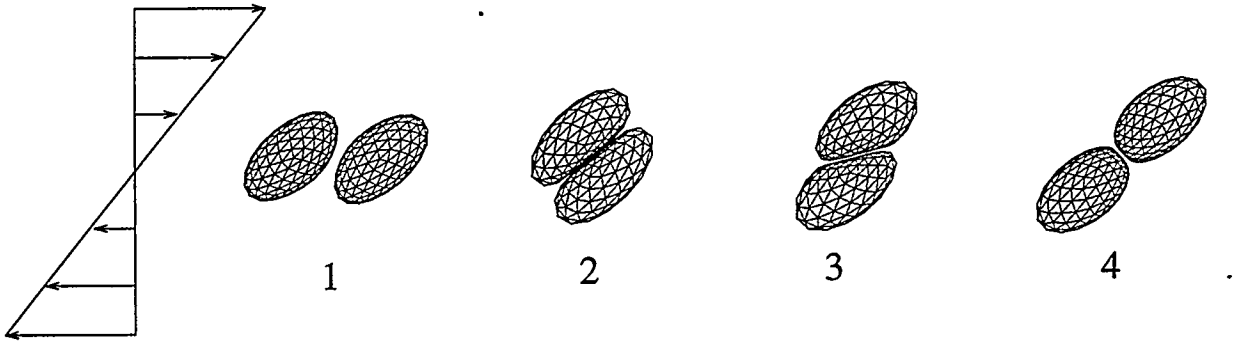


Figure 1: Sequence of interacting drops in shear-flow; $Ca = 0.3$, $\lambda = 1$.

A reflection-type analysis shows that $\Delta_\alpha \sim r^{-2}$ as $r \to \infty$ where $r^2 = x_{\|}^2 + x_{\perp}^2$. It follows that a large number of trajectory calculations are needed to accurately evaluate the 2-dimensional integral shown above. Fortunately, however, our results indicate that the net contribution from all trajectories with $r > 2$ is only about 1% of the total value for the dispersion coefficients. This unexpected finding greatly speeds evaluation of the dispersion coefficients.

A sample of the results, shown below, predict that the dispersion coefficient is highly anisotropic: dispersion in the direction of the velocity gradient is an order-of-magnitude larger than dispersion in the vorticity direction. At vanishingly low shear-rates, drop deformation is negligible so that pairwise interactions are reversible and do not produce dispersion. At moderate shear-rates, $Ca \geq 0.1$, the results predict that dispersive effects attain a rather constant value. A slight tendency for the dispersion coefficients to decrease at the highest shear-rates (drop breakup occurs for $Ca > 0.4$) may be a consequence of greater drop deformation and alignment into the flow direction which reduces the cross-section for pairwise interaction between drops. Similar calculations reveal that dispersive effects are weakly dependent on the drop viscosity.

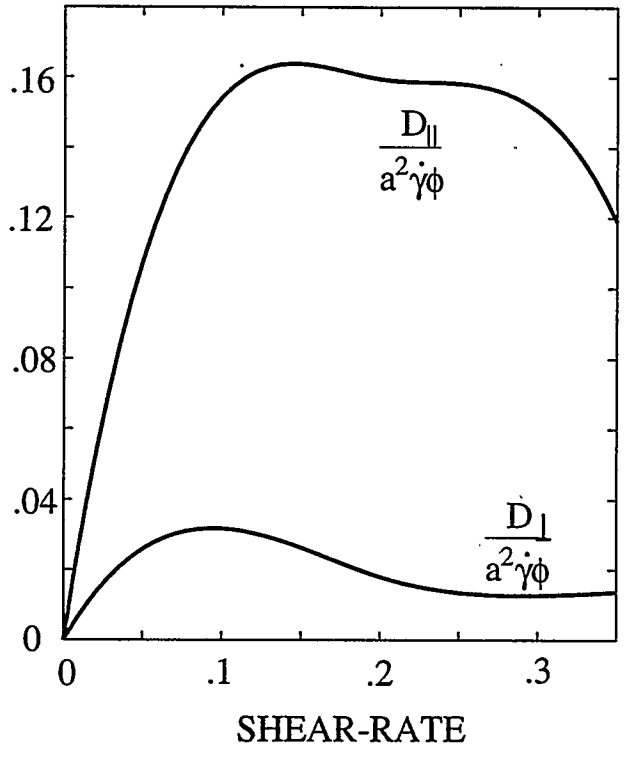


Figure 2: Dispersion coefficients as a function of Capillary number for $\lambda = 1$.

# Shear-induced structure in bidisperse suspensions

Gokul P. Krishnan * David T. Leighton, Jr. †

Department of Chemical Engineering
University of Notre Dame
Notre Dame, IN 46556

In this paper, we present results from our flow-visualization experiments with 40% (by volume) concentration bidisperse suspensions. The particles ($3175\mu m$ and $6350\mu m$ diameter) were ground PMMA spheres suspended in a solution of Triton X-100, water, and zinc chloride with a viscosity of about $53p$ at $22.5°C$. Relative concentrations (denoted by $X_s$ and $X_l$ respectively) were varied over three different values namely (a) $X_s = 0.25, X_l = 0.75$ (b) $X_s = 0.5, X_l = 0.5$ and (c) $X_s = 0.75, X_l = 0.25$. The suspensions were sheared in the interior of a rotating film belt and floated on a layer of mercury to provide a stress-free lower boundary. The sheared region measured approximately $10cm \times 50cm$ , and the resultant flow-field closely approximated a simple shear flow. In our study of these suspensions, we have focussed our attention on both the evolution of the microstructure as a function of the distance away from the wall and the pair distribution functions for small-small, small-large and large-large pairs of particles.

In general, it was found that particles in the suspension tended to segregate by size with the smaller particles being concentrated near the solid boundaries and the large particles being displaced away from the boundaries towards the center of the device. The relative enrichment of small particles at the wall was found to be much larger for the suspension with a dilute concentration of the small particles as compared to the other cases. Beyond a distance of $r/a = 2$ based on the small sphere radius, however, the concentration distribution of the small particles became more uniform and approached the bulk concentration distribution at about $r/a = 4$.

*current address: Department of Chemical Engineering, Massachusetts Institute of Technology, 25 Ames St., Cambridge, MA 02139

†Address for correspondence

In experiments with concentrated monodisperse suspensions, Rampall (1992) showed that particles in the vicinity of a wall tend to be highly ordered. This ordering persisted upto 4 particle diameters away from the wall as can be seen from figure 1. (figure 1). In concentrated bidisperse suspensions also, a maximum is observed in the

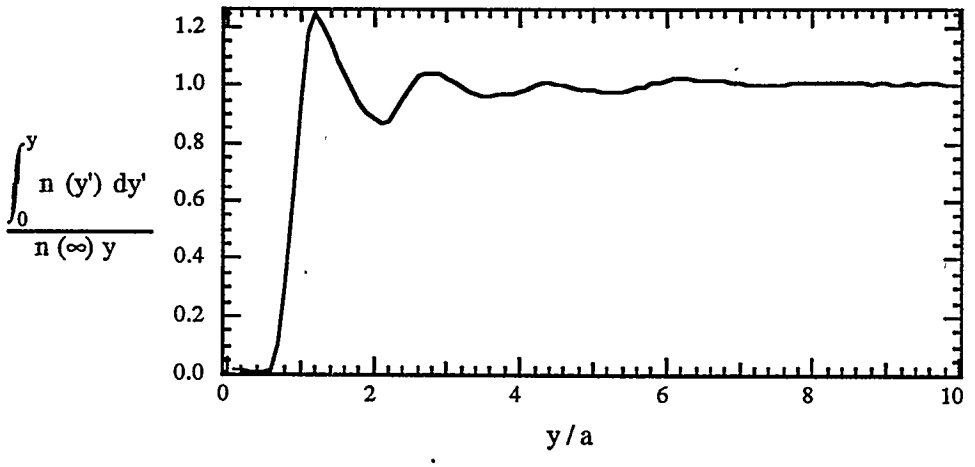


Figure 1: Integrated concentration distribution for $3175\mu m$ diameter spheres near the wall. Data were for 50% concentration suspension. The peak at the wall corresponds to a concentration of about 60%, which is close to the theoretical value of 60.7% for a close packed layer.

small particles concentration right at the wall, however, the presence of large particles disrupted the structure causing the distribution of small particles to be more homogeneous. The large particles exhibited a corresponding depletion in the near–wall region. This behavior is depicted in figures 2 and 3.

It has been demonstrated that in a concentrated suspension of monodisperse particles undergoing simple shear flow, particles tend to accumulate along the compression axis of the shear and be depleted along the recession axis (Parsi and Gadala-Maria, 1987; Leighton and Rampall, 1993). Our experiments indicate that this structure is significantly modified in bidisperse suspensions. The presence of large particles causes an agregation of the small particles in the compression quadrant of the shear flow, resulting in an observed maximum around $r/a = 2$ in the integrated pair-distribution funtions for small-small pairs of particles over what would be expected for a monodisperse suspension of small spheres at the same concentration. The magnitude of this effect diminished as $X_s$ increased (figure 4).

The large particles behaved quite differently. In the case where large spheres were in excess, the large-large pairs behaved as a concentrated monodisperse suspension, except that the small particles tended to randomize the structure. In the case of a large excess of small particles, however, the large spheres exhibited the same structure

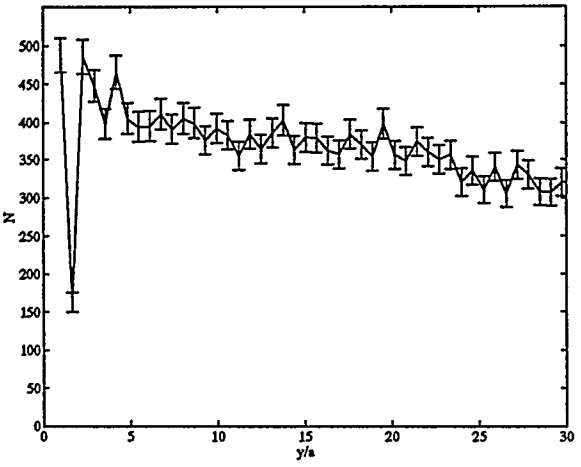


Figure 2: The actual number density of small particles in a 40% suspension with $X_s = 0.75$ and $X_l = 0.25$ with $1\sigma$ errorbars. Notice the preferential accumulation of small particles in the near wall region and a relatively homogeneous profile farther away.

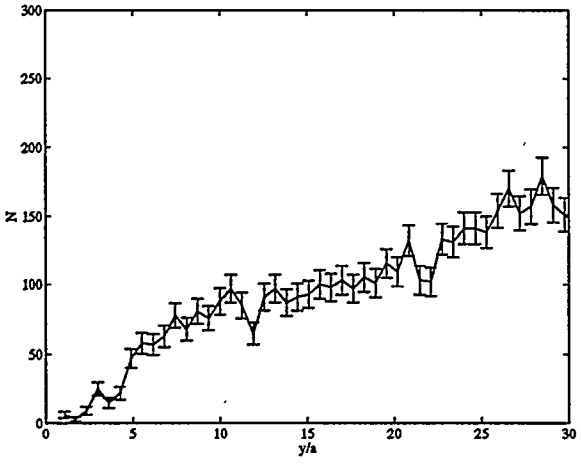


Figure 3: The actual number density of large particles in a 40% suspension with $X_s = 0.75$ and $X_l = 0.25$ with $1\sigma$ errorbars. Notice the relative depletion of large particles in the near wall region and an accumulation towards the center of the device.

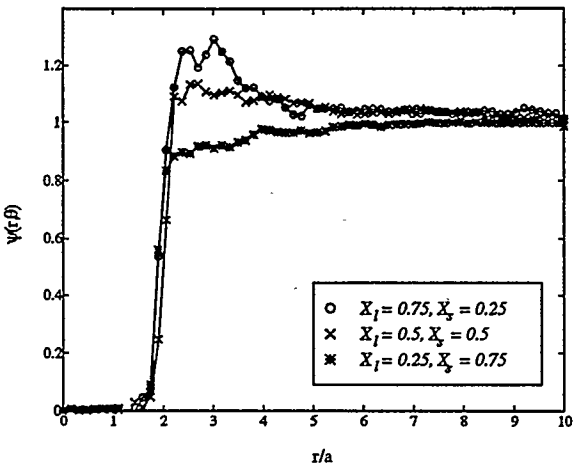


Figure 4: Radially integrated pair distribution functions for small-small pairs on the compression side. When $X_s = 0.25$, a preferential accumulation of small particles is observed. This is noticeably absent when $X_s = 0.75$ which behaves more as a concentrated suspension.

as a dilute monodisperse suspension of large spheres with a depletion in the pair distribution function in the flow-wise direction in both the compression and recession quadrants. These measurements suggest that, with at least some justification, the behavior of large particles in a bidisperse suspension may be modeled as a suspension of particles at reduced concentration moving in an effective continuum. The reverse model, however, is not valid for the smaller particles.

# References

Leighton, D. T. and Rampall, I., "Measurement of the shear-induced microstructure of concentrated suspensions of non-colloidal particles" in Particulate Two-Phase Flow, M. C. Roco, (ed.), Butterworth, Boston, (1993).

Parsi, F. and Gadala-Maria, F., "Fore-and-aft asymmetry in a concentrated suspension of solid spheres", *J. Rheol.*, **31**, 725–732 (1987).

Rampall, I., "Shear-induced structure and migration in non-colloidal suspensions", Ph.D thesis, University of Notre Dame (1992).

# The Longitudinal Shear-Induced Gradient Diffusivity of a Monodisperse Dilute Suspension of Spheres

by

**Yongguang Wang, Andreas Acrivos** and **Roberto Mauri**

The Levich Institute and Department of Chemical Engineering,
City College of CUNY, New York, NY 10031

**Abstract**

We present the calculation of the particle volumetric flux of a dilute, neutrally buoyant suspension of spheres under the action of shear when inertia and Brownian effects are negligible. This mass flux, which is the product of the local particle volume fraction $\varphi$ times the mean particle velocity, results from the effect of an imposed concentration gradient. Using a renormalization technique first employed by Batchelor [J. Fluid Mech., **52**, 245 (1972)], we found that the particle volumetric flux is proportional to the concentration gradient through a shear-induced gradient diffusivity, $\mathbf{D} = \alpha\phi a^2\mathbf{E}$, where $a$ is the radius of the spheres and $\mathbf{E}$ is the fluid rate of strain, while $\alpha = 2.50$ for simple shear flow, and $\alpha = 3.12$ for pure straining flow.

Consider a dilute, monodisperse suspension of force-free and couple-free spherical particles immersed in a fluid with a concentration gradient along the $\hat{\mathbf{e}}_2$-direction. That means that the probability of finding a particle at location $\mathbf{r} = (x_1, x_2, x_3)$ is equal to $n_o P(\mathbf{r})$, with:

$$P(\mathbf{r}) = 1 + \frac{1}{o_o}\left\langle\frac{\partial o_o}{\partial x_2}\right\rangle x_2. \tag{1}$$

Here $n$ is the number density. $\langle\partial\phi/\partial x_2\rangle$ is the imposed mean gradient in the $\hat{\mathbf{e}}_2$-direction of the particle volume fraction $\phi = \frac{4}{3}\pi a^3 n$, and the subscript "$o$" refers to the value of $n$ and $o$ at the origin. In addition, we assume that the spheres have a radius $a$ small enough that inertia effects can be neglected, while the fluid is incompressible, has viscosity $\mu$, and undergoes a uniform shear flow with velocity $\mathbf{v}(\mathbf{r}) = \gamma x_2\hat{\mathbf{e}}_1$ along the $\hat{\mathbf{e}}_1$-direction. Clearly, in writing Eq. (1) we have assumed that the concentration gradient is small, or, conversely, that $x_2 << l = \phi_o\langle\partial\phi/\partial x_2\rangle^{-1}$.

The goal of this calculation is to find the mean volumetric flux $\mathbf{J}$ of the suspended particles in terms of the concentration gradient. Now, by definition, $\mathbf{J}$ at the origin is the product of the local concentration $\phi_o$ times $\langle\mathbf{U}\rangle$, the instantaneous mean velocity of a test sphere at the origin. In turn, $\langle\mathbf{U}\rangle$ is given by:

$$\langle\mathbf{U}\rangle = n_o\int\mathbf{U}(\mathbf{0}|\mathbf{r})\,P(\mathbf{r}|\mathbf{0})\,d^3\mathbf{r} + O(n_o^2), \tag{2}$$

where $\mathbf{U}(\mathbf{0}|\mathbf{r})$ is the instantaneous velocity of the test sphere at the origin in the presence of a second sphere at position $\mathbf{r}$, and $P(\mathbf{r}|\mathbf{0})$ denotes the normalized conditional probability of finding the second sphere at $\mathbf{r}$, provided that the test sphere is located at the origin.

As shown by Batchelor and Green [2], the velocity $\mathbf{U}(\mathbf{0}|\mathbf{r})$ may be written as:

$$U_i(\mathbf{0}|\mathbf{r}) = \frac{1}{2}E_{jk}x_k\left[A(r)\frac{x_i x_j}{r^2} + B(r)\left(\delta_{ij} - \frac{x_i x_j}{r^2}\right)\right]. \tag{3}$$

where $r = |\mathbf{r}|$, $E_{jk} = \frac{1}{2}\gamma(\delta_{j1}\delta_{k2} + \delta_{j2}\delta_{k1})$ is the uniform rate of strain tensor, while $A(r)$ and $B(r)$ are known scalar functions of $r$, decaying as $r^{-3}$ and $r^{-5}$ as $r \to \infty$, respectively.

Clearly, Eqs. (2) and (3) show that the mean velocity of the test sphere in a uniformly distributed suspension, i.e. with $P(\mathbf{r}|\mathbf{0}) = 1$, is identically zero, so that $\langle\mathbf{U}\rangle$ is determined only by the deviation of $P(\mathbf{r}|\mathbf{0})$ from a constant value. Now, the conditional probability $P(\mathbf{r}|\mathbf{0})$ is not known *a priori*, as it is the solution of a two-particle convection problem, and can be determined following the method of Batchelor and Green [3], finding:

$$p(\mathbf{r},t) = P(\mathbf{r}|\mathbf{0}) = q(r)\,P_\infty(\mathbf{r}|\mathbf{0}), \tag{4}$$

where $q(r)$, with $q(\infty) = 1$, is Batchelor and Green's [3] pair distribution function, while

$$P_\infty(\mathbf{r}|\mathbf{0}) = \left[1 + \frac{1}{\phi_o}\left\langle\frac{\partial\varphi}{\partial x_2}\right\rangle x_2\right]H(r-2a). \tag{5}$$

Here $H(y)$ denotes the step function, with $H(y) = 1$ when $y > 0$, and $H(y) = 0$ when $y < 0$.

Now, when we substitute Eqs. (4) and (3) into (2) we find a diverging integral. This singularity can be removed applying the renormalization technique introduced by Batchelor [4], namely considering that the ensemble average velocity and pressure gradient at the origin must be zero. Finally, after a straightforward calculation, where the integration in (2) is taken outside the region of closed trajectories (Batchelor [3]), we find that the volumetric flux at the origin in the longitudinal direction, $J_1 = \phi_o\langle U_1'\rangle$, is given, up to terms of $O(o^2)$ and $O(|a\nabla\phi|^2)$ by the following expression:

$$J_1 = D\left\langle\frac{\partial\phi}{\partial x_2}\right\rangle, \tag{6}$$

where

$$D = \alpha\,\gamma a^2\phi_o, \tag{7}$$

with $\alpha = 1.25 \pm 0.01$.

The case of pure straining flow with rate of strain $\mathbf{E}$ can be solved following the procedure described above. Here, however, as all the trajectories of one sphere relative to another come from infinity and are open, we are led to solve the integral in (2) for $\hat{r} > 2$, which leads to the following result for the longitudinal volumetric flux:

$$\mathbf{J} = \mathbf{D}.\nabla\phi, \tag{8}$$

where

$$\mathbf{D} = \beta\,a^2\phi_o\mathbf{E}, \tag{9}$$

with $\beta = 3.12 \pm 0.01$, is the longitudinal shear-induced particle diffusivity.

Perhaps the most important characteristics of the expressions (7) and (9) for the longitudinal gradient diffusivity is that they depend linearly on the local volume fraction. unlike the coefficient of self diffusivity calculated in Ref. [1], which is proportional to $\phi \log \phi$. The reason of this difference is that the coefficient of self-diffusion is proportional to the temporal growth of the mean square displacement of the test sphere, due to its hydrodynamic interactions with the other particles. Now, summing over the contributions of all possible interactions, led to a logarithmically diverging integral. This singularity was due to the very weak but long-lasting interactions betweeen the test sphere and a very slowly moving second sphere, when the latter is at great distances from the origin and close to the $(x_1, x_3)$-plane. The diverging integral was made finite by allowing for the cut-off due to the occasional presence of another pair of particles.

On the other hand, the calculation of the gradient diffusivity consists in evaluating the *instantaneous* mean velocity of the test sphere immersed in a sheared suspension, due to the effect of an externally imposed particle concentration gradient. In this case, no singularity arises. so that the resulting diffusivity in the direction of the flow is proportional to $\dot{\phi}$.

# References


[1] A. Acrivos, G.K. Batchelor, E.J. Hinch, D.L. Koch and R. Mauri, "Longitudinal sher-induced diffusionn of spheres in a dilute suspension," *J. Fluid Mech.* **240**, 651 (1992).

[2] G.K. Batchelor and J.T. Green, "The hydrodynamic interaction of two small freely-moving spheres in a linear shear flow," *J. Fluid Mech.* **56**, 375 (1972).

[3] G.K. Batchelor and J.T. Green, "The determination of the bulk stress in a suspension of spherical particles to order $c^2$," *J. Fluid Mech.* **56**, 401 (1972).

[4] G.K. Batchelor, "Sedimentation in a dilute dispersion of spheres," *J. Fluid Mech.* **52**. 245 (1972).

# APPLICATION OF LASER-DOPPLER ANEMOMETRY IN HIGHLY CONCENTRATED SUSPENSIONS

A. Averbakh, A. Shauly, A. Nir and R. Semiat
Department of Chemical Engineering, Technion, Haifa 32000, Israel

The measurement of velocities in concentrated suspensions using laser-Doppler anemometry requires penetration of the laser beams into the flow field and collection of light scattered from the flow. In this work, velocity in highly concentrated suspensions, up to 50%, was measured. A match between the refractive indices of the solid and liquid phases, which creates a transparent suspension, facilitates the light penetration. The solid phase of the transparent suspension was PMMA spheres with an average diameter of 90 μm. The liquid phase was composed of a mixture of tetrabromoethane, UCON oil H-450, and Triton X-100. The match between the refractive indices was achieved via accurate temperature control, and was monitored on-line. It is assumed that Doppler signals in the transparent suspension were generated by various sources: the particles, defects in the particles and dust carried with the liquid.

The refractive indices match was monitored on-line using an optical unit designed for this purpose. In this unit one of the laser beams that passes through the flow field is collected and spread into a sheet of light. The light sheet illuminates a bench of photocells. Light intensity collected by the photocells is amplified and processed using a PC486. The criterion for the best match between the refractive indices was the narrowest light distribution achievable on the photocells bench. During the experiments the light distribution on the photocells bench was recorded while the suspension temperature was varied. Velocity measurements were made at the temperature which gave the best match. Temperature was controlled with an accuracy of 0.1°C during each run. In addition to defining the quality of the refractive index match, the average concentration of the suspension, illuminated by the laser beam, may be found. This concentration is interpreted from the intensity of light collected at the central photoreceiver at the temperature which gives the best match.

In this work velocity was measured in a closed rectangular channel. The dimensions ratio of cross section was 1:6.25. Velocities in two perpendicular directions were measured: velocity along the flow channel and velocity toward the center of the channel along the wide axis. At each point in the flow field 2000 Doppler signals were collected. The velocity was calculated from the average of those signals. The standard deviation of the 2000 data points was also evaluated.

Longitudinal velocity profiles measured in relatively low concentration suspensions (10%, 30%) were flat, similar to a Newtonian velocity profile typical to the flow of a homogenous fluid in such a channel. At higher suspension concentrations (40%, 45%, 50%) the profiles deviated from the Newtonian distribution and were slightly rounded. Lateral velocity profiles measured in the suspensions with higher concentration showed net velocities towards the center of the closed channel. These are due to particles drift resulting from shear-induced particle diffusion in the concentrated suspensions.

Standard deviation in velocity calculation may be related to various causes: frequency detection error, optical noise, rotation of particles in the flow field, and shear induced self diffusion in the concentrated suspensions.

In conclusion this work shows that velocity measurements in highly concentrated suspensions, up to 50%, is possible. The measurements were made in transparent suspensions. Transparency was monitored on line and maintained with careful temperature control, with accuracy of $0.1^{o}C$. Velocity profiles measured in concentrated suspensions are different from Newtonian velocity profiles typical to this flow channel.

# A NEWTONIAN MODEL FOR PROPPANT TRANSPORT IN AN INCLINED CHANNEL

S.J. MCCAFFERY, L. ELLIOTT, D.B. INGHAM, A.T. UNWIN*
Department of Applied Mathematical Studies, University of Leeds, Leeds, LS2 9JT, England
*Schlumberger Cambridge Research Limited, P.O. Box 153, Cambridge, CB3 0HG, England

## ABSTRACT

In a hydraulic fracturing treatment, a fracture is created from the wellbore by means of a non-Newtonian fracturing fluid. Sand particles, or 'proppants', are carried by the fracturing fluid into the induced fracture channel where they form a packed bed which props the fracture open. In practice particles sediment much faster in an inclined fracture than in one that is vertical . This phenomenon is known as the 'Boycott Effect'. A two-dimensional model for the settling of proppants within a channel is presented in this paper, and using this model the effect on the sedimentation process of the angle of inclination of a channel is illustrated.

## INTRODUCTION

This paper presents a Newtonian model for the two-dimensional sedimentation of proppant particles in a hydraulic fracturing treatment, and by numerically solving the underlying equations the Boycott effect is demonstrated. The sedimentation process considered consists of rigid spherical particles, which are of equal size and density and do not aggregate, settling at very small particle Reynolds numbers from a suspension comprised of an incompressible Newtonian fluid. The problem addressed is temperature independent and, by assuming that there is no main (primary) flow along the fracture, the situation is equivalent to the stage when the pumping of material has ceased but the fracture is still open.

## GOVERNING EQUATIONS

The geometry employed is illustrated in figure 1, where $y$ and $z$ represent non-dimensional spatial variables. The non-dimensional equations governing two-dimensional sedimentation in a fracture are

$$\frac{\partial C}{\partial t} + \frac{\partial}{\partial y}(CV_{py}) + \frac{\partial}{\partial z}(CV_{pz}) = 0 \qquad (1)$$

$$-\lambda k_1 \frac{\partial p}{\partial y} + \sin\theta \lambda C_m B C + \frac{\partial}{\partial y}\left\{\frac{1}{(1-C)^\alpha}\frac{\partial V_y}{\partial y}\right\} + \frac{\partial}{\partial z}\left\{\frac{1}{(1-C)^\alpha}\frac{\partial V_y}{\partial z}\right\} = 0 \qquad (2)$$

$$-\lambda k_1 \frac{\partial p}{\partial z} + \cos\theta \lambda C_m B C + \frac{\partial}{\partial y}\left\{\frac{1}{(1-C)^\alpha}\frac{\partial V_z}{\partial y}\right\} + \frac{\partial}{\partial z}\left\{\frac{1}{(1-C)^\alpha}\frac{\partial V_z}{\partial z}\right\} = 0 \qquad (3)$$

$$\frac{\partial V_y}{\partial y} + \frac{\partial V_z}{\partial z} = 0 \qquad (4)$$

where $C$ is the concentration of particles normalised with respect to the concentration, $C_m$, of particles in the state of close packing, $V_y$, $V_{py}$ and $V_z$, $V_{pz}$ are the $y$- and $z$-components of the non-dimensional bulk average velocity, particle velocity, respectively, $p$ is the non-dimensional pressure, $t$ is non-dimensional time and $\lambda$, $k_1$, $B$ and $\alpha$ are constants. Expressions for $V_{py}$, $V_{pz}$ in terms of $C$ and $V_y$, $C$ and $V_z$, respectively, are obtained from a slip velocity law.

The boundary conditions on $C$ were taken to be

$$C = 0 \text{ on } y = -1 \text{ and } \frac{\partial C}{\partial z} = 0 \text{ on } z = -2 \qquad (5)$$

$$C = 1 \text{ on } y = 1 \ , \ z = 2 \qquad (6)$$

while those enforced on $V_y$ and $V_z$ were, respectively,

$$V_y = 0 \text{ on } y = \pm 1 \ , \ z = 2 \text{ and } \frac{\partial V_y}{\partial z} = 0 \text{ on } z = -2 \qquad (7)$$

$$V_z = 0 \text{ on } y = \pm 1 \ , \ z = 2 \text{ and } \frac{\partial V_z}{\partial z} = 0 \text{ on } z = -2 \qquad (8)$$

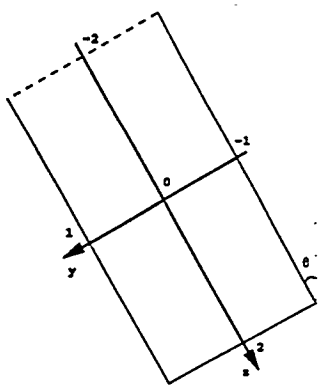

Figure 1. Geometry for two-dimensional sedimentation in an inclined channel.

## SOLUTION PROCEDURE

To determine the solution of the governing equations (1)-(4), the following procedure was repeated iteratively for successive times. For the known distributions of concentration, $C$, and bulk average velocity, $\underline{V}$, at the current time, $t$, equation (1) was solved using a Godunov-type scheme, Hirsch [1], to produce $C$ at the next time, $t + \triangle t$. Employing this distribution of $C$, a control-volume formulation, Patankar [2], was then applied to equations (2)-(4) to yield $\underline{V}$ and $p$ at the same time, $t+\triangle t$.

## RESULTS

Equations (1)-(4) were solved as described above for a progression of times subject to several different values, in turn, of the angle of inclination, $\theta$. For each value of $\theta$, the distributions of $C$ and $\underline{V}$ at a selection of times were displayed graphically in the form of contour plots and vector plots, respectively. Examples of such contour plots and vector plots are illustrated, respectively, in figures 2 and 3 for the case when $\theta = 80°$, $C|_{t=0} = 0.5$, $C_m = 0.67$, $\lambda = 9000$, $k_1 = 1$, $B = 2$, $\alpha = 1$.

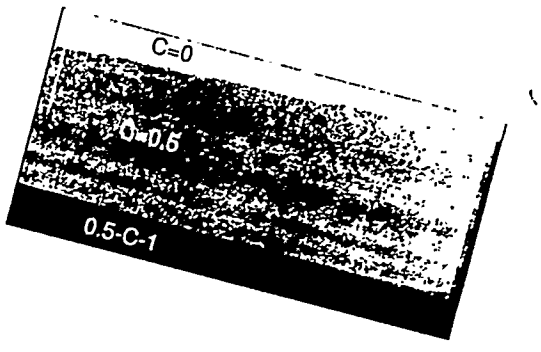


Figure 2. $C$ after 100 time steps when $\theta = 80°$.

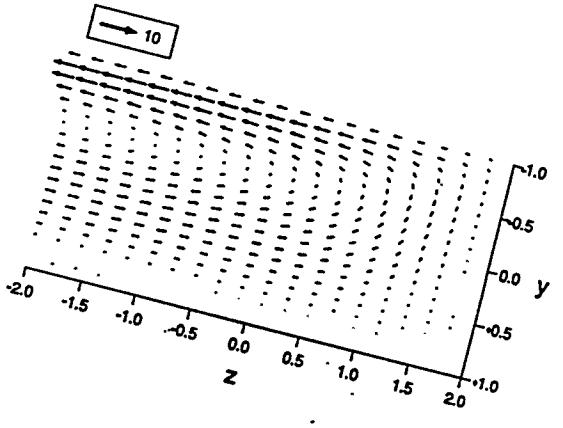


Figure 3. $\underline{V}$ after 100 time steps when $\theta = 80°$.

## CONCLUSION

A two-dimensional Newtonian model for proppant transport in an inclined channel has been presented in this paper, and by solving the governing equations (1)-(4) of the model for a variety of angles of inclination it has been shown that the greater the angle of the channel to the vertical, the greater the rate of sedimentation of the proppant.

## REFERENCES

1. Hirsch, C., 1988, Numerical computation of internal and external flows , John Wiley and Sons Ltd.
2. Patankar, S. V., 1980, Numerical Heat Transfer and Fluid Flow, Hemisphere Publishing Corporation.

# Self -Diffusion in Vibrated Granular Beds

Yidan Lan and Anthony D. Rosato
Mechanical Engineering Department
New Jersey Institute of Technology
Newark, NJ. 07102

Self-diffusion in a vertically vibrated bed of smooth, inelastic uniform spheres has been investigated in a three-dimensional discrete element simulation. The computational cell is a parallelepiped with a flat vertically oscillating floor, lateral periodic boundaries and an open top. A right-handed Cartesian coordinate system is established, such that the origin of the $x$ and $z$ axes coincides with a corner of the floor, while gravity acts in the $-y$ direction. Self-diffusion coefficients are computed from both the ensemble-averaged velocity autocorrelation functions and the mean-square displacements.

In terms of velocity autocorrelations, the trace of the self-diffusion tensor $D$ is computed using

$$D = \frac{1}{3}\int_0^\infty \langle \mathbf{v}(\tau)\cdot\mathbf{v}(0)\rangle d\tau = \frac{1}{3}\left[D_{xx}+D_{yy}+D_{zz}\right] \text{ where } D_{kk} = \int_0^\infty \langle \mathbf{v}_k(\tau)\cdot\mathbf{v}_k(0)\rangle d\tau, \text{ where } k = x, y, z.$$

The Einstein relation $D = \lim_{t\to\infty}\frac{1}{6t}\left\langle[\mathbf{r}(t)-\mathbf{r}(0)]^2\right\rangle$ provides an alternative method to compute $D$ in terms of the particle displacement r. where $\langle\ \rangle$ represent the ensemble average. We use this method as a comparison with the result obtained from the autocorrelation.

Particles are modeled as smooth spheres of diameter $d = 0.1\ m$ and density $\rho = 1200\ kg/m^3$. The soft sphere contact model of Walton and Braun [3] is used, where the normal force acting between two overlapping spheres is governed by linear loading and unloading springs of stiffness $K_1$ and $K_2$, respectively. This produces a constant effective restitution coefficient $e = \sqrt{K_1/K_2}$. The loading stiffness $K_1$ =2.8 x $10^6$ is chosen to ensure a maximum overlap of approximately less than $0.01d$, and produces a time step $dt \sim 10^{-5}$ seconds. Diagnostic quantities are accumulated after the system has reached steady state to compute $D$. In all studies discussed below, $e = 0.9$.

In the regime of large floor accelerations $\Gamma = a\omega^2$, where $a$ is displacement amplitude and $\omega$ the frequency of the sinusoidally oscillating floor, the autocorrelation functions in the three coordinate directions are exponentially decaying. This produces a value of D in agreement with the value obtained from kinetic theory predictions of Savage and Dai [2], that is, $D = \dfrac{d\sqrt{\pi T}}{8(1+e)\nu g_o(\nu)}$. Here, $T$ is the granular temperature, $\nu$ is the solids fraction and $g_o(\nu)$ is the Carnahan-Starling approximation to the contact radial distribution function given by $g_o(\nu) = (2-\nu)/2(1-\nu)^3$. Fig. 1a,b shows a typical velocity autocorrelation function and mean square displacement $\left\langle[\mathbf{r}(t)-\mathbf{r}(0)]^2\right\rangle$ while Table 1 summarizes results for two different values of $\Gamma = a\omega^2$ at a fixed frequency $f$ = 50 Hz.

| Parameters | $D$ ($m^2/s$) (Simulation) | $D$ ($m^2/s$) (Savage) | $D^*$ ($m^2/s$) | $\nu$ | $T$ (cell average) |
|---|---|---|---|---|---|
| $\Gamma = 90g,\ a = 0.09d$ | 0.00544 | 0.00532 | 0.00530 | 0.44 | 0.7950 |
| $\Gamma = 483g,\ a = 0.5d$ | 0.2676 | 0.2116 | -- | 0.14 | 13.80 |

* Computations from mean-square displacement method

At low acceleration levels, it was not possible to compute $D_{yy}$ since the $y$-velocity autocorrelatoin function (Fig. 2) did not exponentially decay, but showed oscillations about zero with a frequency equal to that of the vibrating floor. This provides evidence that the vertical motion of the bed was well-correlated with the floor oscillations, as was also seen in other recent simulations by the authors [1]. In an attempt to uncover possible scaling behavior, a series of investigations was performed in which $\Gamma$ was varied at fixed amplitude $a = 0.5d$. Since it was not possible to determine $D_{yy}$ for low $\Gamma$'s for the reason described above, only $D_{zz}$ and $D_{xx}$ could be computed. The results shown in Fig. 3 indicate that these components increase with $\Gamma$. Several cases have also been completed where the quantity $a^2\omega$ is fixed while varying its constituents.

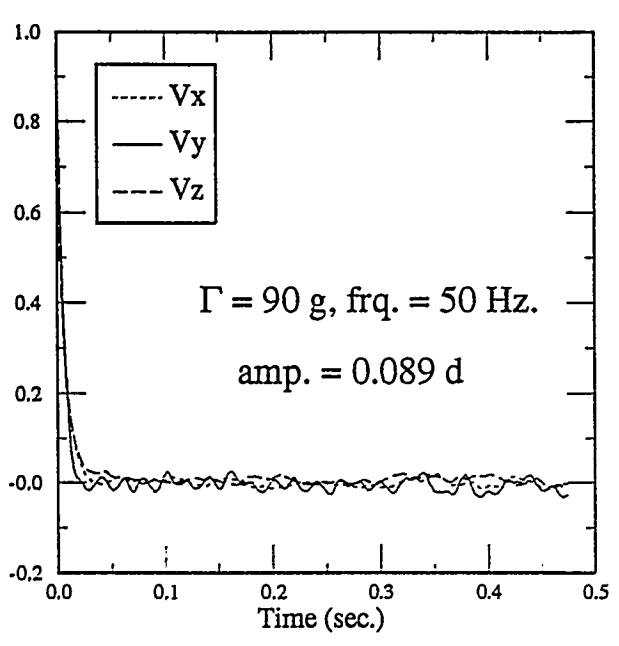


Fig. 1a: Typical velocity autocorrelation at high $\Gamma$.

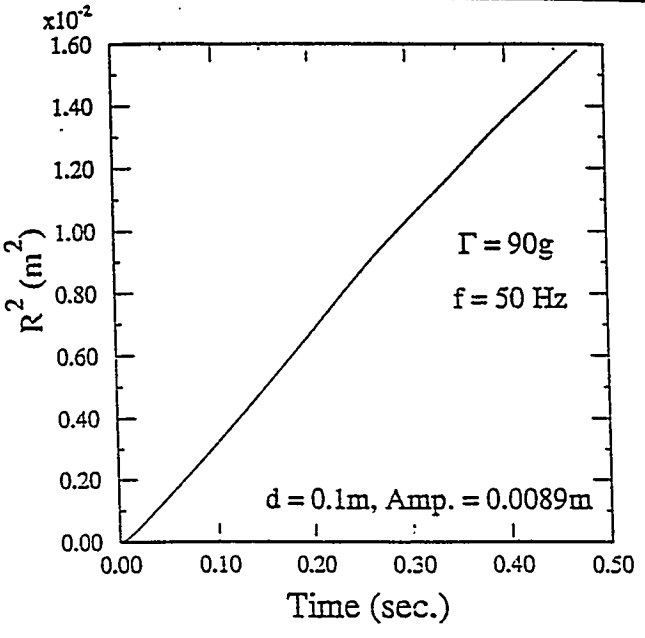


Fig. 1b: Corresponding mean square displacement.

**Acknowledgments**

Partial support for this work was provided by the Pittsburgh Energy Technology Center of the US Department of Energy. We are grateful to Dr. Otis R. Walton (Lawrence Livermore National Laboratory) for his interest in our work and for providing an original discrete element uniform shear code, which was modified for the purposes of this study.

**References**

1. Y. Lan and A. D. Rosato. *Physics of Fluids*. in press (1995).
2. S. B. Savage and R. Dai, *Advances in Micromechanics of Granular Materials* (eds. H. H. Shen et al.), Elsevier, Amersterdam (1991).
3. O. R. Walton and R. L. Braun, *Acta Mech.* 63, 73 (1986).

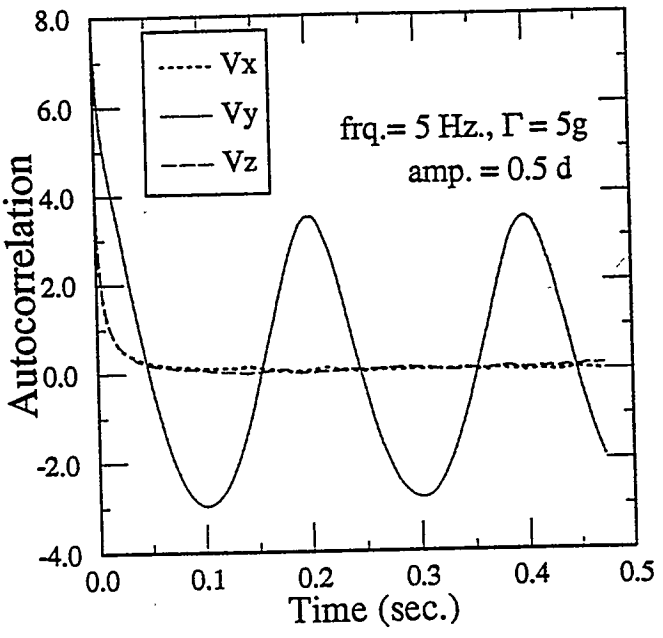


**Fig. 2:** Y-velocity autocorrelation at $\Gamma = 5g$

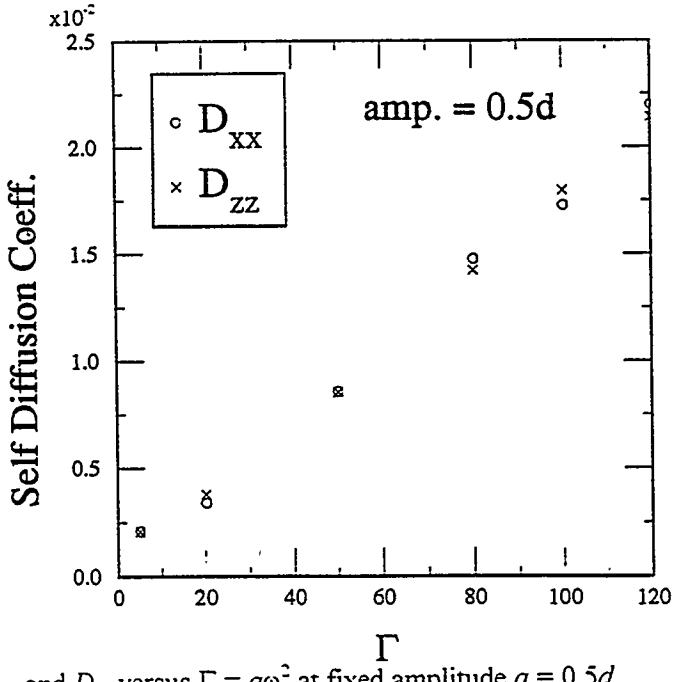


**Fig. 3:** $D_{xx}$ and $D_{zz}$ versus $\Gamma = a\omega^2$ at fixed amplitude $a = 0.5d$.

# Application of a novel algorithim to Hydrodynamic Diffusion in Sedimenting Systems

**W. Kalthoff[1], S. Schwarzer[1], G. H. Ristow[2] and H. Herrmann[1]**

## Introduction

We want to focus on the application of a novel computer simulation method [6] for particulate multiphase flow to the problem of sedimentation. Our aim is to capture the large scale collective processes of the combined particle-liquid system. To this end we solve the Navier-Stokes equation for the liquid, giving us the correct long-range interactions, and use molecular dynamics to simulate particle motion. A particle-fluid interaction force entering both the Navier-Stokes and the molecular dynamics equations is used as a coupling term.

## Simulation Technique

To be able to simulate large systems in a reasonable amount of time, we make the assumption that we can represent the fluid-particle interaction by a drag force instead of evaluating and integrating the stress tensor on each particle surface. For low Reynolds numbers it seems reasonable to use a Stokes-like drag force $F_d = C_d \eta r_i (\vec{V}_i - \vec{v}_i)$, where $\vec{v}_i$ is the particle and $\vec{V}_i$ the liquid velocity. As we cannot access the liquid velocity at infinity, we have to use the local average liquid velocity $\vec{V}_i$. The resulting error is accounted for by the drag coefficient $C_d$ which is fitted so that a single Sphere falls with Stokes velocity. In most simulations, $C_d$ differs by a factor of less than 2 from the expected $6\pi$. Since lubrication effects are not properly represented by this force ansatz, we replace them by particle contact forces. These together with gravitation and the drag force enter into the molecular dynamics equations used to describe particle motion. The fluid itself is modeled by solving the Navier-Stokes equation on a quadratic MAC-grid using the Chorin scheme. There is no limitation due to inertial effects, neither by the particles nor by the liquid.

## Results and Discussion

Our approximation described above delivers acceptable results when applied to sedimentation. In a first step we apply the method to a two dimensional sedimenting system at low Reynolds numbers, looking at the diffusion constants, settling velocities and velocity fluctuations as a function of the solid volume fraction. We find a strong isotropy of the diffusion constants in horizontal and vertical direction, in good agreement with experimental results (Fig. 1). Our simulations also showed a decrease of the mean settling velocity as a function of the volume fraction $\Phi$. The observed decrease is however slightly

[1]PMMH, ESPCI, 10 rue Vauquelin, F-75231 Paris Cedex 5, France.
[2]Fachbereich Physik, Philipps-Universität Marburg, 35032 Marburg, Germany.

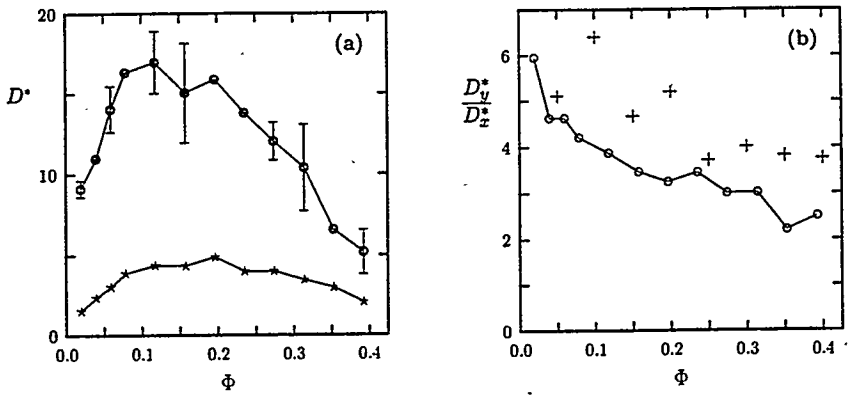


Figure 1: **(a)** Dimensionless particle self-diffusion constants $D_x^*$ ($\star$) and $D_y^*$ ($\bigcirc$) as a function of solid fraction $\Phi$. **(b)** Dimensionless ratio $D_y/D_x$ of self-diffusivity parallel ($D_y$) and perpendicular ($D_x$) to settling direction ($\bigcirc$) and the experimental data from Nicolai et al. [2] (+).

smaller than that found in experimental and theoretical results. One reason is our drag-force ansatz, which does not produce as much back flow as a complete treatment of the particles as internal liquid boudaries would.

## Conclusions and Outlook

The presented algorithm is both fast and capable of reproducing many known results at low Reynolds numbers, while being applicable to larger Reynolds and Stokes numbers. An extension to three dimensions has already been done. The greatest drawback seems to be the drag-force ansatz for the liquid-particle interaction, which will be replaced by an evaluation of the stress-tensor and the treatment of the particles as liquid boundaries in the near future.

## References

[1] G. K. Batchelor, *J. Fluid Mech.* **52**, 245 (1972).

[2] H. Nicolai, B. Herzhaft, E. J. Hinch, L. Oger and E. Guazzelli *Phys. Fluids*, **7**, 12 (1995).

[3] Koch and Shaqfeh, *J. Fluid Mech.*, 224, 275 (1991).

[4] A.J.C. Ladd, *J. Fluid Mech.* 271, 311 (1994); A.J.C. Ladd,*J. Fluid Mech.* 271, 285 (1994).

[5] J. F. Brady and G. Bossis, *Ann. Rev. Fluid Mech.* **20**, 111 (1988).

[6] S. Schwarzer *Phys. Rev. E* to be published.

# Velocity and fluid fraction measurements in suspensions flowing through abrupt contractions and expansions

S. Altobelli, E. Fukushima
The Lovelace Institutes, Albuquerque, NM
L. A. Mondy
Sandia National Laboratory, Albuquerque, NM

## Abstract

Nuclear Magnetic Resonance Imaging (NMRI) was used to study two neutrally buoyant suspensions flowing through an axially symmetric, 4:1:4 (diameter) contraction/expansion model. The suspensions were 50% solids (100 and 675 μm) in a viscous synthetic oil. NMRI was performed while the suspensions were piston-driven through the model. The fluid fraction and the axial component of liquid-phase velocity were measured in the small tube and fluid fraction, axial, and radial velocities were measured in the expansion region, using a phase method. Fluid fraction was measured near the driving piston face in a series of static images. The average velocity in the small tube was 1 cm/s and the total duration of flow was 6-8 minutes. Particle migration was observed in the suspension prepared with larger particles: the particle concentration was lower near the wall of the small tube and suspension which was relatively low in particles accumulated immediately downstream of the expansion. In the suspension of smaller particles, no migration was observed in a single pass, but repeated processing produced accumulations of particles in the sections of the large tube adjacent to the small tube. Observations of the driven piston show that a region of relatively high fluid fraction rapidly develops along the tube axis adjacent to the piston.

## Extruder

The extruder consists of a reservoir pipe, a four-to-one contraction into a smaller pipe and a one-to-four expansion into another larger pipe (Figure 1.) The larger diameter pipe is 6.35 cm OD polymethyl methacrylate (PMMA) tubing with 0.635 cm walls. The smaller pipe is made from 6.35 cm OD PMMA stock with a 1.27 cm hole bored through the center. Each section is 38 cm long. The contraction and expansion are abrupt. Two pistons, sealed with O-rings, slide in the larger pipes. A 2 m rod connects the reservoir side piston to a digitally controlled screw drive, which forces the suspension into the contraction at a steady 0.0625 cm/s, yielding a 1.0 cm/s average velocity in the small pipe.

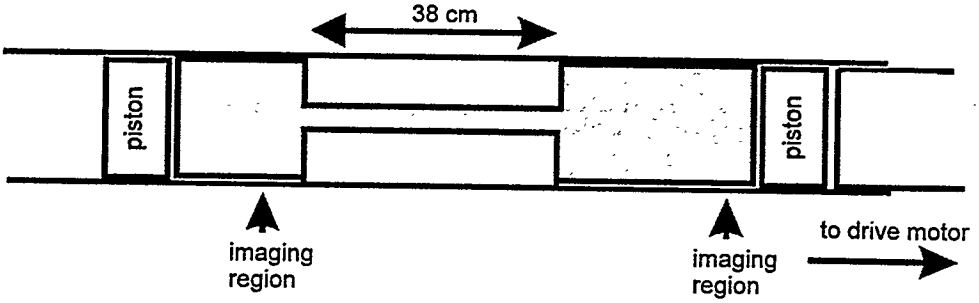


**Figure 1**

## Suspensions

The suspensions tested are made of 50% PMMA spherical particles suspended in a viscous liquid with the same density as the particles (1.89 g/cm$^3$.) Two sets of particles were used, both with broad, unimodal distributions of diameters. The larger, Diakon MG102 from ICI-United Kingdom, has a mean diameter of 675 μm. The second, Lucite 4F from DuPont, Chemical Co., has a mean diameter of 100 μm.

The suspending liquid is a solution of 14 % tetrabromoethane, 36% UCON oil, and 50% Triton-X100. It exhibits Newtonian rheology with a viscosity of 5 Pa s at 23 ° C. (See Abbott, *et al*, **J Rheol 35**(5) 773, 1991.)

## Results

Some representative images are shown in Figure 2. On the left, six images are arranged in two sets of three showing fluid fraction, axial velocity, and 'radial' velocity from the top down. The left set is form 100 μm particle suspension measurements and the right set is from the larger particle suspension. On the right, two images of the fluid enriched region that develops at the driven piston face are shown.

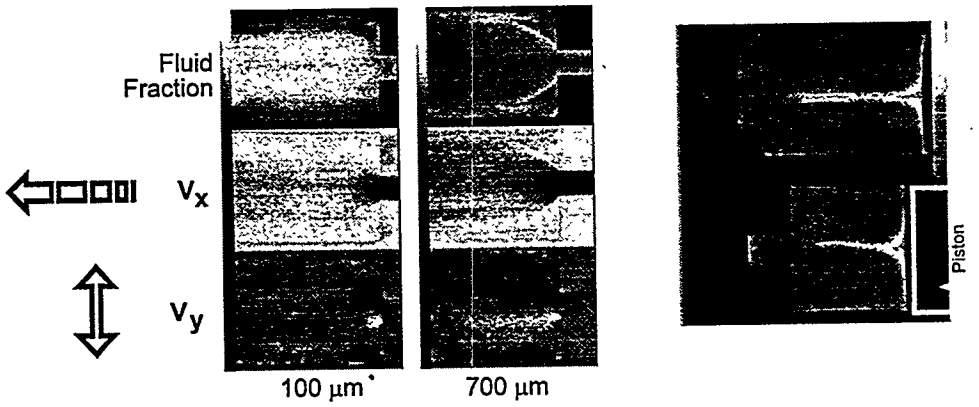


Figure 2. Several NMR images of fluid fraction and velocity components obtained. See text for description.

## Conclusions

- NMRI studies of simple suspensions in pipe flows with sudden expansions and contractions show that complex spatial variations in particle concentration were induced. The patterns observed in the expansion region may be qualitatively explained by shear-induced migration.
- The solid-depleted regions were observed near the driven piston face. This inhomgeneity could be imaged after the piston had travelled 2 (large) tube diameters.
- Particle diameter effects are strong in these flows.

# Nuclear Magnetic Resonance Imaging Measurements of Average and Fluctuating Velocity Distributions in Sphere Suspension Flow

Robert L. Powell
Joseph D. Seymour
Chemical Engineering &
Materials Science

Michael J. McCarthy
Kathryn L. McCarthy
Food Science &
Technology

University of California
Davis, CA 95616

We present NMR measurements of the average and fluctuating fluid velocity distributions for laminar tube flow of a suspension of spheres for volume fractions from $\phi$=0.0, the suspending fluid case, to $\phi$=0.362. The multiple length and time scales present in multi-phase systems require care in interpreting experimental data for comparison with theory due to the interaction between the scales of the system and the scales of the experimental probe.

The suspending medium was a Newtonian fluid composed of deionized water, 57 wt%, 75-H-90,000 polyalkylene glycol oil (Union Carbide), 28 wt%, and sodium chloride, 15 wt% which was added to increase the fluid density near to that of the suspended spheres. The density and viscosity of the fluid are $\rho$=1,120 kg/m$^3$ and $\mu$=0.13 Pa s. The suspended phase consisted of polymethylmethacrylate (pmma) spheres of density $\rho$=1,190 kg/m$^3$. Sphere volume fractions of $\phi$=0.0, 0.085, 0.29 and 0.36 were used. The sphere sizes for each of these volume fractions varied somewhat due to the large quantity of spheres required, over 10 kg for the maximum concentration. For $\phi$=0.085 the mean sphere radius is 265 $\mu$m. For $\phi$=0.29 the radial distribution is bimodal with 23% spheres of mean radius 265 $\mu$m and 77% spheres of mean radius 118 $\mu$m. For $\phi$=0.36 the radial distribution is bimodal with 16% spheres of mean radius 265 $\mu$m and 84% spheres of mean radius 118 $\mu$m. The ratio of sphere sizes in the bimodal suspensions, i.e. $\phi$=0.29 and 0.36, is 2.2. The ratios of the particle radii to the tube diameter are 0.01 for the large spheres and 0.0045 for the small spheres.

The NMR system consists of a 2T Oxford magnet connected to a General Electric CSI-II spectrometer. The imaging is done on the $^1$H protons of the fluid phase of the material at 85.5 MHz. The flow loop is 26.2 mm internal diameter plexiglass tubing with a positive displacement pump. The imaged region is 175 diameters downstream from the entrance. The axial direction of the flow in the tube is aligned with the z-axis of the stationary applied magnetic field.

The flow regimes studied were in the low particle Reynolds number range and large particle Péclet number range. We obtain joint spatial-velocity spin density distribution images for each sphere concentration studied which can be interpreted as average axial velocity profiles for the fluid phase. The velocity profile for the suspending fluid is in agreement with a parabolic Newtonian profile. The average velocity data for $\phi$=0.085 also show no variation from a parabolic profile. The average velocity profiles for the concentrated suspensions exhibit shear thinning behavior with blunted average velocity profiles.

Finally, we have shown that there is a the relation between velocity fluctuations and the intensity ratio for the flow to no flow images. Normalization of the flow image by the no flow image at each position eliminates intensity effects due to fluid density, $T_2$ relaxation and diffusion. The distributions of the intensity ratios for the flow to no flow images at each concentration to the intensity ratio for the flow to no flow images at $\phi$=0.0 is a direct measure of the change in signal intensity distribution due fluid velocity fluctuations. The distributions indicate increase in the minus log of the ratio of intensity ratios due to fluctuations in velocity, with increase in particle concentration in qualitative agreement with the trend in the suspension temperature as a function of concentration in the simulation of Nott and Brady (1994)+ for a sphere radius to channel height ratio of 0.027. The relatively insignificant effect on intensity in the dilute suspension, $\phi$=0.085, is consistent with the average nature of the NMR velocity measurement. The probability for finding a sphere in a volume located at any point in the fluid, x, for a dilute suspension of uniformly, independently distributed spheres is equal to the number density of the spheres, $P(x)=\phi/V_{sphere}$, where $V_{sphere}$ is the volume of a single sphere. For the experimental resolution used to obtain a typical image the voxel dimension is 0.075 $mm^3$ and the probability of a sphere being in a voxel is calculated to be 0.082 spheres per voxel. Since each observation in the NMR experiment is independent the total probability that a sphere is in a voxel in the final image is a multiple of the single probability for each signal average. This yields low probability for a sphere to be in a voxel and the velocity in a voxel is relatively unperturbed.

**Acknowledgments**

Funding for this research was provided by Nestle Westreco Inc. and The TAPPI Foundation. The authors thank Dr. R.J. Kauten of UC Davis and Dr. T.Q. Li of KTH Stockholm for many fruitful discussions regarding NMR.

+ Nott, P.R. & Brady, J.F. 1994 . *J. Fluid Mech.* **275** 157.

# The viscosity and sedimentation of aggregating colloidal dispersions in a Couette flow.

W. Wolthers, D. van den Ende, M.H.G. Duits and J. Mellema
*Rheology Group, Faculty of Applied Physics,*
*University of Twente,*
*P.O. box 217, 7500 AE Enschede, The Netherlands*

May 23, 1995

## Abstract

In order to interpret the time dependence of the measured torque in a steady shear experiment on an aggregating dispersion in a Couette geometry, a microrheological model has been used in which two existing models are integrated. In this microrheological model, the theory of Potanin *et al.* (1995) for fractal aggregation in shear flow is combined with the theory of Acrivos *et al.* (1994) for the sedimentation and resuspension of non-colloidal hard spheres. The former theory describes the viscosity as a function of shear rate, while the latter predicts the stress increase in a Couette device due to sedimentation. The connection between the two theories is made by identifying the aggregate parameters of the former with the hard sphere parameters (size and volume fraction) of the latter.

The experimentally studied aggregated system, consists of silica spheres sterically stabilized by stearyl alcohol chains. When such spheres are dispersed in cyclohexane they behave like hard spheres, but after the addition of a certain amount of polystyrene molecules they can become aggregated due to the phenomenon of depletion flocculation. The rheological experiments were carried out with primary particles having a radius $a$ of 38 [nm] at one volume fraction $\phi = 8\%$. For the measurements a Contraves Low Shear 40 with a concentric cylinder geometry was used. The apparatus is a controlled shear rheometer with a gap height of 8.0 [mm].

The parameters of the aggregates as a function of the shear stress are obtained by measuring a flow curve before sedimentation effects become significant and fitting this curve with the theory of Potanin *et al.* (1995). In this theory the aggregates are described as spheres. Their radius and volume fraction are decreasing functions of shear rate. The theory contains two coefficients which can be adjusted to obtain the best fit to the experimental data. The experimental results together with the best model fit are shown in Fig. 1. In table I the from the fit resulting values of $\phi_a$ (volume fraction of aggregates) and $R_h/a$ (radius of the aggregates) are listed.

**Table I.** The aggregate parameters as a function of shear rate $\dot{\gamma}$.

| $\dot{\gamma}$ [$s^{-1}$] | 0.096 | 0.37 | 1.45 | 5.30 | 21.0 | 81.3 |
|---|---|---|---|---|---|---|
| $R_h/a$ [-] | 202 | 177 | 144 | 112 | 80.7 | 56.5 |
| $\phi_a$ [-] | 0.53 | 0.49 | 0.43 | 0.37 | 0.30 | 0.24 |

During the sedimentation of the primary particles, the aggregate size and volume fraction become a function of both time and position in the rheometer. The primary particle fluxes are calculated using the viscous resuspension theory of Acrivos *et al.* (1994). The connection between their model and our aggregated colloidal dispersion is made by identifying $R_h$ and $\phi_a$ of the aggregates with respectively their hard sphere radius and volume fraction. In the Figs. 2 and 3 the results of the long term sedimentation experiments are plotted. The stress-time results are shown from the moment at which the viscosity reached its steady state value. One can see that the application of the combined theory results in a good prediction of the global behavior of the experimental curves. This result corroborates both the existing theories and the combined theory provides a method for estimating the sedimentation rate of aggregates in a shear flow.

## References


Acrivos, A., X. Fan and R. Mauri, "On the measurement of the relative viscosity of suspensions," J. Rheol. **38**, 1285 - 1296 (1994).

Potanin, A.A., R. de Rooij, D. van den Ende and J. Mellema, "Microrheological modeling of weakly aggregated dispersions," J. Chem. Phys. **102**, 5845 - 5853 (1995).


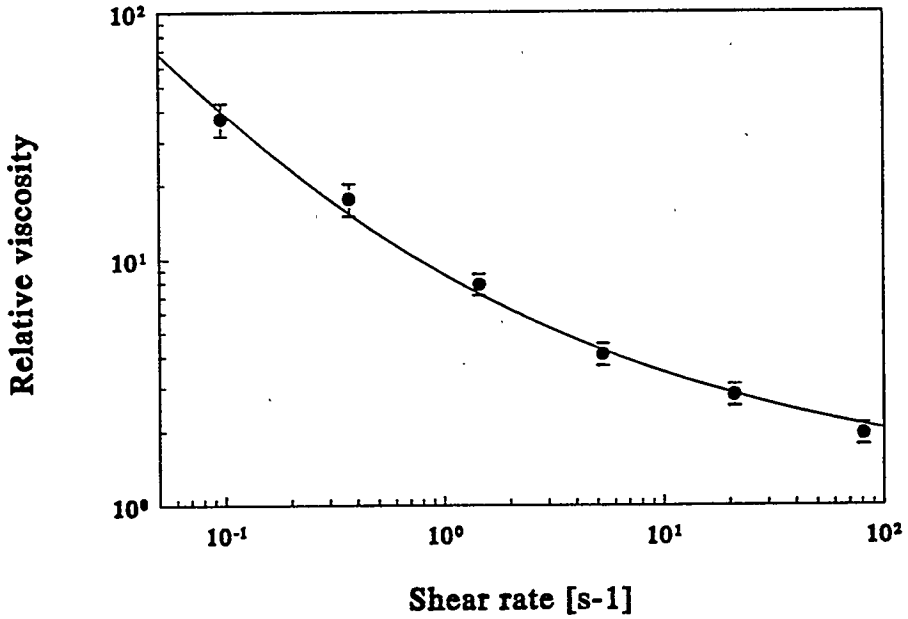


**Fig. 1.** The steady state relative viscosity as a function of shear rate: —, the aggregation model fit; •, experimental results $\phi = 8.0$ %.

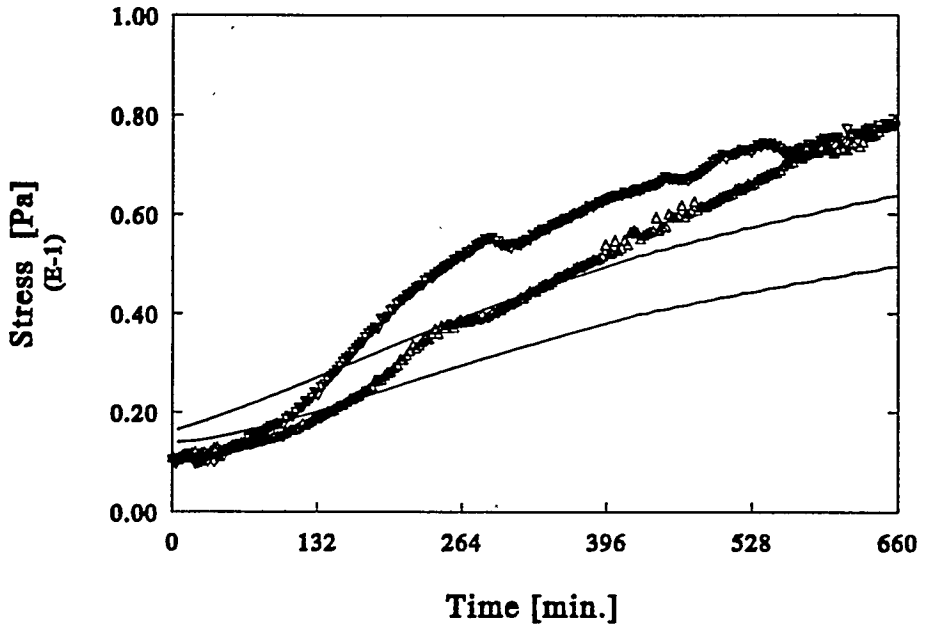


**Fig. 2.** The stress response as a function of time for $\dot{\gamma} = 0.37$ [$s^{-1}$]: —, theoretical predictions; $\triangle$ and $\triangledown$, experimental results.

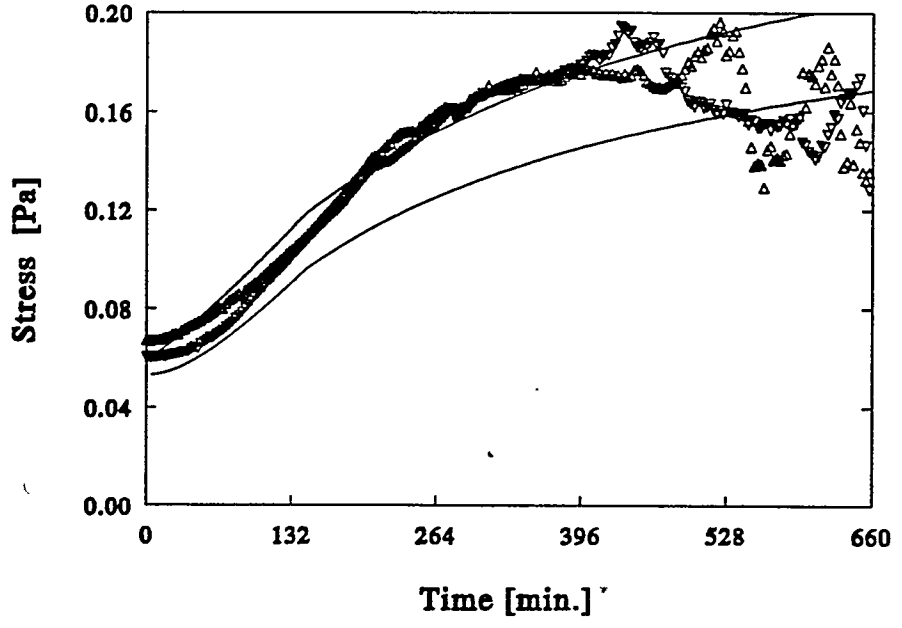


**Fig. 3.** The stress response as a function of time for $\dot{\gamma} = 5.30$ [$s^{-1}$]: —, theoretical predictions; $\triangle$ and $\triangledown$, experimental results.

# Microstructure in a strongly-sheared suspension and its impact on rheology and self-diffusivity

John F. Brady & Jeffrey F. Morris*

*Division of Chemistry and Chemical Engineering*
*California Institute of Technology*
*Pasadena, CA 91125*

The combined effects of Brownian motion and an interparticle force of hard-sphere type upon the particle configuration in a strongly sheared suspension have been analyzed. Under the influence of hydrodynamic interactions alone the pair-distribution function has symmetry properties that yield a Newtonian constitutive behavior and a zero self-diffusivity in the limit $Pe^{-1} \equiv 0$, where $Pe = \dot{\gamma}a^2/2D$, with $\dot{\gamma}$ the shear rate, $a$ the particle size and $D = kT/6\pi\eta a$ the diffusivity of an isolated particle. Fore-aft symmetry, in which a second sphere is equally likely to lie on an approaching (fore) or receding (aft) trajectory relative to the reference sphere, holds under these conditions. However, if particles are maintained at a minimum separation of $b > 2a$, as $Pe \to \infty$ there is a boundary layer of thickness $aPe^{-1}$ in which the affects of Brownian diffusion and advection balance, leading to an asymmetry of the pair-distribution function of $O(Pe)$, with an excess of particles along the compressional axes. The product of the magnitude of the asymmetry and the thin boundary layer leads to an $O(1)$ contribution (dependent on $b/a$) as $Pe \to \infty$ yielding a nonNewtonian (normal stresses) rheology. This broken symmetry and boundary-layer structure produce shear-induced self-diffusivities that are $O(\dot{\gamma}a^2)$ as $Pe \to \infty$. For dilute suspensions in the absence of hydrodynamic interactions the self-diffusivity is predicted to be $\boldsymbol{D}^s = -a^2/27\eta\ \partial\boldsymbol{\Sigma}'/\partial\phi$, where $\boldsymbol{\Sigma}'$ is the bulk stress (less the solvent and Einstein viscosity contributions) and $\phi$ is the volume fraction of spheres.

*Present address: Koninklijke/Shell-Laboratorium, Amsterdam (Shell Research BV); Postbus 38000, 1030 BN Amsterdam, The Netherlands.

# Hydrodynamic Diffusion in Sheared, Sedimenting Suspensions at Finite Reynolds Numbers

Heng-Kwong Tsao and Donald L. Koch
School of Chemical Engineering,
Cornell University
Ithaca, NY 14853

The hydrodynamic particle diffusivity is studied in a dilute, monodisperse, sheared suspension of sedimenting spheres. The particle Reynolds numbers are assumed small, i.e., $Re_\gamma^{1/2} \ll Re \ll 1$ where $Re \equiv U_t a/\nu$ and $Re_\gamma \equiv \gamma a^2/\nu$, $U_t$ is the terminal velocity of the particles, a is the particle radius, and $\nu$ is the kinematic viscosity of the fluid.

In the absence of fluid inertia, the variance of the velocity and the particle diffusivity in a suspension of randomly positioned particles depends on the macroscopic dimension of the suspension. These quantities will only take on values that are independent of the size of the suspension if particle interactions lead to a screening of the conditionally averaged fluid velocity disturbance caused by each particle. In an unsheared, sedimenting suspension at finite particle Reynolds numbers, inertial effects lead to weaker divergence of the velocity variance and hydrodynamic diffusivity, than are predicted in the absence of inertia. However, these quantities still depend on either the system size or a particle-interaction-induced hydrodynamic screening mechanism (D. L. Koch, Phys. Fluids A 5, 1141 (1993)).

The divergence of the velocity variance and hydrodynamic diffusivity in a sedimenting suspension at finite Reynolds number results from the slow decay of the fluid velocity disturbance in a particle's wake. A linear shear flow alters the structure of the wake produced by a sedimenting particle and this effect can lead to a finite velocity variance and hydrodynamic diffusivity in a suspension of randomly distributed particles.

We consider the three geometries in which the gravitational acceleration is parallel to the flow (x-), gradient (y-), and vorticity (z-) directions of the simple shear. When $P \equiv Re/Re_\gamma^{1/2} \gg 1$, the shear is sufficiently weak so that it does not affect the fluid velocity disturbance at the $O(aRe^{-1})$ separation from a particle where the wake first forms. In case

(z), the shear flow leads to a more rapid spread of the wake at an $O(aRe_\gamma^{-1/2}P)$ distance above the particle. The faster spreading of the wake causes the fluid velocity to decay like $1/z^2$ in the sheared wake, resulting in a finite $O((\phi U_t^2/Re)\ln(P))$ velocity variance. The mean-squared displacement of a particle grows in proportional to $t\ \ln^2 t$. In case (y), the wake begins to spread faster due to shear flow at an $O(aRe_\gamma^{-1/2}P^{1/3})$ distance above the particle and this leads to a finite velocity variance and hydrodynamic diffusivity. In case (x), the shear flow drives the particles into a region of closed interparticle trajectories. This effect will lead to a clustering of particles and an instability of the homogeneous suspension.

# UNSTEADY FLOWS OF TWO - PHASE MEDIA IN TUBES DUE TO LOCAL SUPPLY OF MASS AND ENERGY

V.P.Korobeinikov.
Institute for Computer Aided Design, Russian Academy of Sciences and Russian National Committee on Theoretical and Applied Mechanics, Moscow, Russia.

Let we have a tube (or a canal) filled by gas or fluid with suspended solid particles. At time t=to an inflow of analogous mixture begins into this tube across an opening. As a result we have interaction and nonstationary motion of both media. The problem may be of interest for theory of unsteady flows in nozzles, in combustion chambers of internal engines, in diffusion of pollution of air space, in shock tube flows and corresponding flows in canals, lakes, river mouth near a see bay. It can be formulated for coupled heat conductivity - diffusion equations system, for fluid dynamics equations, shallow water motion equations. The simple variant of the problem is: at time t=0 finite amount of "ink" is suddenly released in a section of straight canal where water velocity is constant. The distribution of the ink matter along the canal for t>0 have to be found. The solution can be obtained by using the fundamental solution of linear diffusion equation. For the case of two phase or two-component gas media with velocities, pressure and densities are variable in space and time. We have to study solutions of two-phase fluid dynamics equations. In the paper the self-similar problem on local supply of mass and energy in dusty gas is studied. The following results were obtained:1) The parameters of inlet flow and initial state for medium in conical, wedge type and plane tubes( for which two contact surfaces and two shock waves are formed in the flow) are found; 2)the arising in dusty gas of zones with high concentration of solid particles (ro-layers) was proved. For two-dimensional plane case the problem of lifting of particles of a layer near the canal bottom was solved numerically. The particles diffusion in viscous boundary layer with including of Saffman force influence is also briefly discused. The comparison of the results with experiments are made. The extensions of the results to shallow water flows with suspended particles is considered. The author obtained these results working together with colleagues and students mentioned in the References.

References: 1.N.S.Zakharov, V.P.Korobeinikov, Mekhanika Zhidkosti i Gaza #4, 1979,pp.70-77; 2.V.P.Korobeinikov, Archivum Combustions, v.9, #1/4, 1989, pp.149-152; 3.V.P.Korobeinikov, V.V.Markov, I.S.Menshov, Dokl. Acad. Nauk SSSR, v.290, 1986, pp.818-820; 4.V.P.Korobeinikov, G.G.Tivanov, Dokl. Acad. Nauk SSSR, v.310, 1990, pp.1320-1323; 5.A.N.Gavrilov, Dokl.Acad. Nauk SSSR, v.312, 1991, pp.1417-1420; 6.V.P.Korobeinikov, Proc. 5th Intern. Symp. on CFD, v.2, Sendai 1993, pp.76-83; 7.A.N.Osiptsov et Al., Appl. Math. Mech., v.12 #6, 1991, pp.531-538.

IUTAM Symposium on Hydrodynamic Diffusion of Suspended Particles

Estes Park, Colorado, 22-25 July 1995

# EXPERIMENTAL TECHNIQUES for SUSPENSIONS and DISPERSIONS

**Jérôme MARTIN and Dominique SALIN**

and Laboratoire Fluides, Automatique et Systèmes Thermiques
Bâtiment n°502 - Campus Universitaire - 91405 Orsay Cedex France

Addressing the many different issues of experimental techniques suitable for analyzing suspensions and dispersions is quite a challenge and we will focus on some particular aspects, allowing to compare them in terms of physical basis, resolution, accuracy, safety hazard and cost. The very first question to ask is what piece of information we want and what about the constraints on the system. For instance, looking for direct observation of particules velocity in a suspension, you can design an experiment with video techniques etc.... But if the given dispersion is concentrated and opaque you have to adapt different techniques to get insight into that particular system.

Instead of listing, we will try to classify techniques in terms of general methods such as transparency, scattering, tracer or specific methods related to the physical property of the dispersion itself. In this symposium we are mainly dealing with liquid/solid systems. The granular material (solid/gaz) is observed mainly with video imaging but also with NMR which will be described in a following lecture by Fukushima et al.

Tracking single particule paths can be achieved by different visualization methods : the position of a single tagged particule is followed in 3D space and time : the "video" could be CCD, or X Ray cameras [1, 2]. The fluid and the other particles have to be transparent to the corresponding rays and also a large viscosity is often required to have time enough to perform measurements (1000 frames/s could be obtained with high speed cameras) In the same class of methods fluorescent photochemical and radioactive tracer method have been used [3]. Speckle velocimetry provide the same type of information.

Concentration measurements are usually derived from transparency to either optical beam, γgraphy, Xrays or even NMR [4, 7]. The accuracy is typically 1 % in concentration and the spatial resolution that of the beam size (a few mm for optics and γ, down to 100 μm for X). Measurements are fast for optics but the other two are counting methods which accuracy involves the square root of time. Large concentrations lead to opacity and multiple scattering, limiting these techniques to low concentrations.

Dynamic quasi-elastic light scattering is well suited to measure the collective diffusive behaviour of the dispersion. Routinely used in colloïdal dispersions, i.e. submicron particles, non-colloïdal dispersion requires a good choice of the wave vector and an adaptation of the method [8].

A special class of technique, not only because of its use by the speaker [9], is acoustics which is linked to the hydrodynamics properties of the dispersion itself. Basically the two acoustic measurements are the sound velocity V and the sound wave attenuation.V is linked to

the density and the compressibility of the dispersion and therefore is concentration dependent ; note that generally the larger the concentration, the larger the velocity variations, qualifying this technique for large concentrations up to the packing. The attenuation in the suspension is related to the suspension viscous loss which is nothing but its concentration dependent settling velocity. At higher frequency Rayleigh scattering allows to discriminate between large and small particles. The typical accuracy in concentration is better than 0.05 % and the spatial resolution that of the transducers (1 or 2 mm). Note also that most dispersion systems are transparent to acoustics but a dispersion system involving, even a tiny, amount of gaz bubble is avoided.

Most of the techniques overviewed in this talk do not require years of pratice on that topic and a good experimentalist can adapt them to the system he wants to study. This is definitely not the case of NMR technique which requires years of training and a continuous interference between the technique and systems (so is it for X, CT scanner [10]). But when microscopic information is needed we have to go to such techniques. Note that a promising technique is the NMR impulsion gradient which can give the velocity field of the fluid.

## REFERENCES


[1] H. Nicolai, B. Herzhaft, E.J. Hinch, L. Oger and E. Guazzelli, Phys. Fluids 7, 12 (1995).

[2] L.A. Mondy, A.L. Graham and J.L. Jensen, J. Rheol. 30, 1031 (1986).

[3] R.E. Falco and C.C. Chu . Proc. SPIE 814, 706 (1987).

[4] R.H. Davis and M.A. Hassen, J. Fluid. Mech. 196, 107 (1988).

[5] A. Dunand and A. Soucemarianadin, Soc. Petr. Eng. of AIME 14, 259 (1985).

[6] D. Bruneau, R. Anthore, F. Feuillebois, X. Auvray and C. Petitpas, J. Fluid Mech. 221, 577 (1990).

[7] S. Lee, Y. Jang, C. Choi and T. Lee, Phys. Fluids A4, 2601 (1992.

[8] J.Z. Xue, E. Herbolzheimer, M.A. Rutgers, W.B. Russel and P.M. Chaikin, Phys. Rev. Lett. 69, 1715 (1992).

[9] D. Salin and W. Schön, J. Phys. Lett. 42, L-477 (1981).
J. Martin, N. Rakotomalala and D. Salin, Phys. Rev. Lett. 74, 1347 (1995).
J-C. Bacri, M. Hoyos, N. Rakotomalala, D. Salin, M. Bourlion, G. Daccord, R. Lenormand and A. Soucemarianadin, J. Phys. (France) III 1, 1455 (1991

[10] F.M. Auzerais, R. Jackson, W.B. Russel and W.F. Murphy, J. Fluid. Mech. 221, 613 (1990).

# NMR Imaging of Particle Migration in Concentrated Suspensions

Alan L. Graham[1], James R. Abbott[1], Eiichi Fukushima[2], Stephen A. Altobelli[2], Nhan Phan-Thien[3], Lisa A. Mondy[4], and Tom Stephens[5]

[1]Los Alamos National Laboratory, Los Alamos, New Mexico 87545 (USA)
[2]Lovelace Medical Foundation, 2425 Ridgecrest Dr., S.E, Albuquerque, New Mexico 87108 (USA)
[3]Mech. Eng. Dept., University of Sydney, Sydney, New South Wales 2006 (Australia)
[4]Sandia National Laboratories, Albuquerque, New Mexico 87185 (USA)
[5]Naval Air Warfare Center, China Lake, California 93555 (USA)

Nuclear magnetic resonance (NMR) imaging has been used to observe the evolution of concentration and velocity profiles of initially well mixed suspensions undergoing flow in a wide gap between rotating concentric or eccentric cylinders. More detailed descriptions of the experiments in concentric cylinders and of the NMR imaging techniques used can be found in earlier papers [Abbott, et. al (1991); Mondy, et. al (1994)]. The suspensions consist of large, noncolloidal spherical or rodlike particles suspended in a viscous Newtonian liquid with the same density as the particles. Particles migrate away from the high shear-rate region near the rotating inner cylinder even under conditions in which inertial forces are usually considered negligible. Large concentration gradients can be established after only a short time.

In the concentric cylinder device, the particle migration rate increases with the mean particle volume raised to $\sim$0.7 power (for spheres, the radius raised to somewhat higher than 2). The migration rate and the final steady-state concentration profiles depend only weakly on the particle size polydispersivity or the particle aspect ratio. In a Newtonian suspending fluid, the particle migration does not depend on the strain rate or on the suspending liquid viscosity.

In Phillips' et al. model (1991), a steady state will occur when the migration due to spatial variations in the particle interaction frequency (caused by gradients in shear rate or solids volume fraction) is balanced by that due to spatial variations in viscosity (caused by gradients in solids concentration). The relative effect of these two mechanisms are set by two empirically derived constants $K_\eta$ and $K_c$. With constants obtained from these experiments on suspensions with average solids volume fraction $\phi$=0.55, the model ade-

quately predicts migration in suspensions with average $\phi$ down to 0.45. At lower concentrations, comparison of the model to data suggests that the "constants" need to be modeled as functions of concentration.

Experimental measurements have also been taken to study shear-induced migration of spherical particles in a concentrated suspension ($\phi$=0.50) subjected to flow in the wide gap between a rotating inner cylinder placed eccentrically within a fixed outer cylinder (a cylindrical bearing), so that the eccentricity ratio is 1/2. A flow reversal is predicted for a Newtonian liquid in this geometry (Wannier 1950); however, the magnitude of the reversed velocity seen in a Newtonian liquid is about 1% of the velocity of the inner shaft and much smaller than can be distinguished with the NMR technique. Figure 1 shows the NMR image of the cylindrical bearing. The presence of a high concentration region, not at the outer wall, but in a region within the gap seems to indicate that a flow reversal occurs in the suspension. Visual observations of a tracer particle in the suspension confirmed that, indeed, a region of very slow (of order 1 mm/minute) reverse flow occurs.

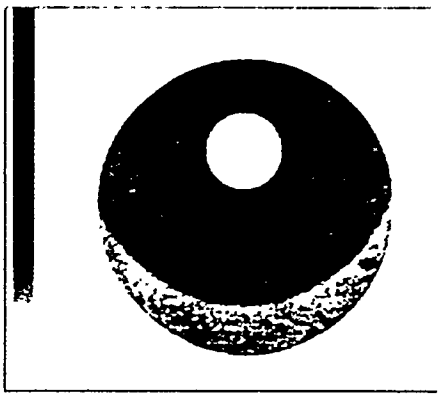

Figure 1. NMR image of a cylindrical bearing with an eccentricity ratio equal to 1/2. Darker regions represent higher liquid fraction (lower $\phi$).

We have modeled the flow between eccentric rotating cylinders following the equations presented in Phillips et al. (1991). The values for the parameters $K_\eta$ and $K_c$ are the same as those used by Phillips et al. We employ a psuedo-transient finite volume scheme, which is based on the method of artificial compressibility due to Chorin (1967). The computational domains are discretized using unstructured triangular cells (Jin and Wiberg, 1990), and the field variables are assumed piece-wise constant.

The experimentally measured and the numerically predicted concentra-

tion and velocity profiles along the narrow and the wide gaps are given in Fig. 2. Although the overall agreement with the data is fair, we find no recirculation, in contrast to the experimental observation of a tracer particle, mentioned above. However, the concentration profile is reasonably well-predicted (as seen from Fig. 2a) considering the uncertainty in the experimental data and the simplicity of the model theory.

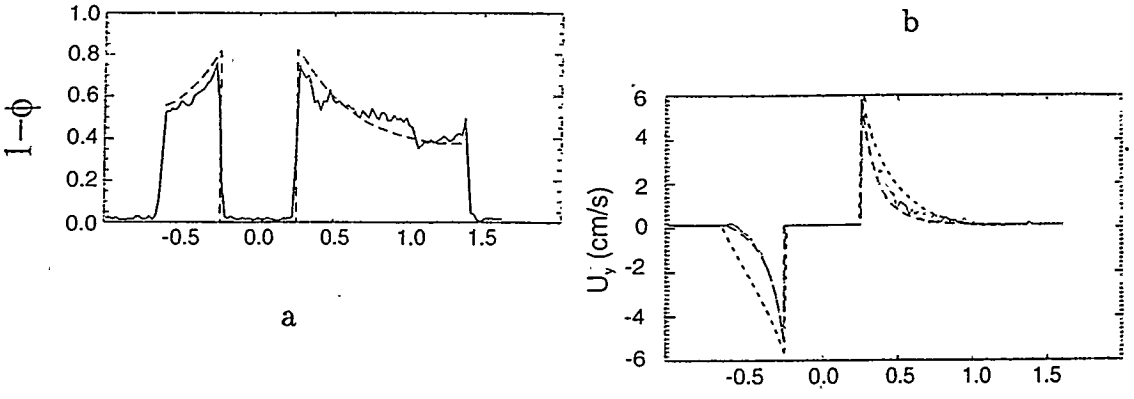


Figure 2. Steady-state velocity and concentration profiles along the x-axis of a cylindrical bearing with an eccentricity ratio equal to 1/2. Numerical (– – –), experimental (solid line), Newtonian (Wannier 1950, - - -).

ACKNOWLEDGMENTS

This work was sponsored by the U.S. Department of Energy at Los Alamos National Laboratory under Contract W-7405-ENG-36 with the University of California, and at Sandia National Laboratories under Contract DE-AC04-94-AL85000. Partial support was provided by the U.S. Department of Energy, Division of Engineering and Geosciences, Office of Basic Energy Sciences and through Dr. R. S. Miller's section of the Mechanics Division, Office of Naval Research.

REFERENCES

Abbott, J. R.; Tetlow, N.; Graham, A. L.; Altobelli, S. A.; Fukushima, E.; Mondy, L. A. and Stephens, T. S. *J. Rheo.*, **1991**, *35*, 773.

Chorin, A. J. *J. Comp. Phys.*, **1967**, *2*, 12.

Jin, H. and Wiberg, N.-E. *Int. I. Num. Methods Eng.* , **1990**, *29*, 1501.

Phillips, R.J.; Armstrong, R.C.; Brown, R.A.; Graham, A. L. and Abbott, J.R., *Phys. Fluids A*, **1992**, *4*, 30.

Wannier, G. H. *Quart. Appl. Math.*, **1950**, *8*, 1.

# Experimental Studies of the Motion of Concentrated Suspensions in Two-Dimensional Channel Flow

by

M. K. Lyon and L. G. Leal

Department of Chemical and Nuclear Engineering
University of California
Santa Barbara, CA 93106

## Abstract

Over the past few years our laboratory has been concerned with the development of a method to accurately measure velocity and concentration profiles for the pressure driven flow of a concentrated suspension through a narrow gap rectangular channel. Results from two recent models developed by Phillips et al. [1] and Nott and Brady [2] suggest that under steady flow conditions, the shape of these two coupled profiles depends on the bulk particle concentration, and in the case of the latter, the ratio of particle diameter to channel gap-width. Although many experimental studies have been undertaken to measure these profiles, the results to this point have only provided qualitative concentration information, i.e. a nonuniform concentration distribution [3], or were inconsistent in that a modified velocity profile was reported (relative to that for a Newtonian fluid under equivalent flow conditions), but with a uniform concentration profile [4,5]. Our objective, therefore, is to ascertain experimental velocity and concentration profile data to test the applicability of these current models, as well as aid in the development of any relevant future models.

The experimental method utilized in our lab is a modified Laser Doppler Velocimetry (LDV) technique. The term "modified" refers to the use of a model system in which the index of refraction of the suspending and particulate phases are closely matched. This is necessary in order to overcome turbidity effects inherent in the application of optical methods to concentrated systems, and has enabled us to obtain scattered light signals from individual particles as they pass through the probe volume. Because the scattered light signals result from local regions of refractive index mismatch within individual particles, they are rather weak. Therefore, we have implemented an optical geometry which maximizes the scattered light intensity and yields a geometric probe volume that is smaller in size than the suspended particles. Data acquisition includes an absolute measure of the local particulate phase velocity, and an absolute local particle concentration, which is attained by measuring the time between consecutive particles through the probe volume and normalizing based upon our knowledge of the total particle flux through the channel. A total of twelve experiments were performed corresponding to particle volume fractions of 0.30, 0.40, and 0.50 and particle diameter to channel gap-width ratios of 0.042, 0.059, 0.072, and 0.100, respectively.

Comparing the area under the measured velocity profiles with that corresponding to a Newtonian fluid under identical flow conditions suggests the absence of a relative slip velocity between the particulate and suspending phases. Such a finding is consistent with the aforementioned models, which either do not account for this phenomena [1], or neglect it, arguing that it scales like the square of the particle diameter to gap-width ratio [2]. Although earlier data from our lab [6] reported particle velocities that lagged as

much as 50% behind those of the suspending liquid, we now believe that these results were anomalous and may have been a consequence of poor spatial resolution and inadequate degassing of the flow system.

Qualitative results for increasing bulk concentration of particles within the suspension reveal a larger particle concentration in the vinicity of the channel centerline and increased blunting of the velocity profile consistent with model predictions [1,2]. Similarly, decreasing the ratio of particle diameter to channel gap-width yields a greater blunting of the velocity profile, but this effect is extremely weak over the range considered.

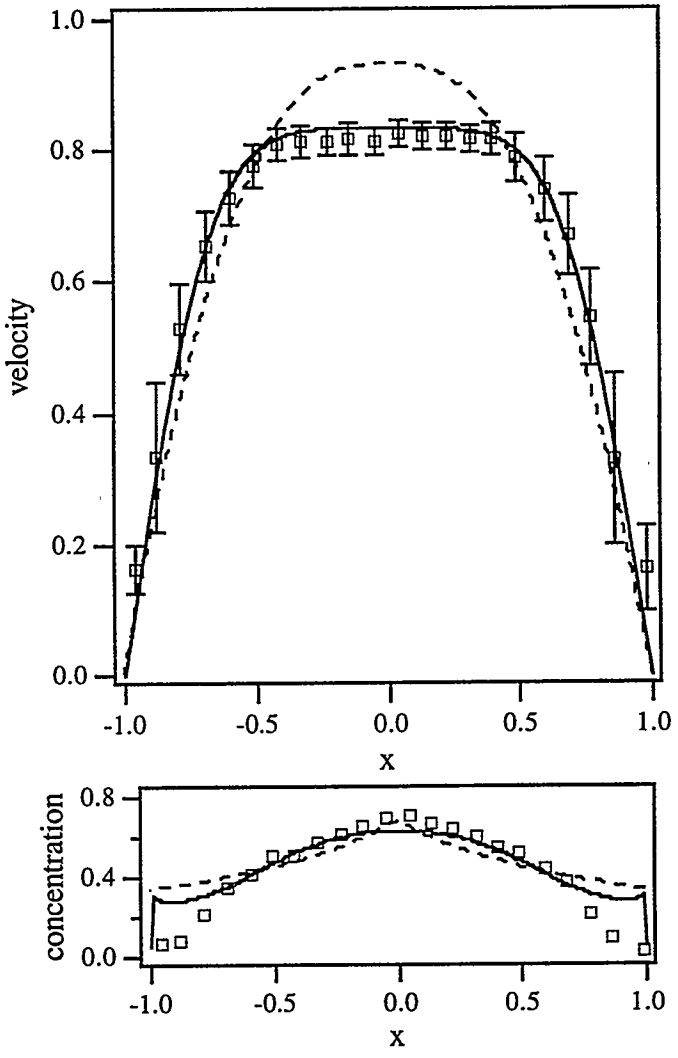


Figure 1. Velocity and concentration profiles for $\phi_{bulk} = 0.50$ and $a/H = 0.059$: ❑, data points; ---, theory of Phillips et al.; —, theory of Nott and Brady.

Recently, we have completed velocity and concentration profile calculations utilizing the diffusion [1] and statistical mechanical [2] models mentioned above for comparison with our experimental data. A typical result, shown in figure 1, is for a bulk particle concentration of 0.50, and ratio of particle diameter to channel gap of 0.059. As can be seen, the latter theory provides better agreement with our data, particularly in regards to

the velocity profile, where, except for the two points adjacent ot the channel walls, the theoretical solid curve lies within the standard deviation of all the data points.

We are currently expanding our experimental method to obtain data from particles incorporating a fluorescent dye. This will allow discrimination of particle size for measurements on suspensions with a bimodal size distribution, as well as independent suspending fluid velocity measurements that utilize small tracer particles.

References


1. R.J. Phillips, R. C. Armstrong, R. A. Brown, A. Graham, J. R. Abbot, 1992, Phys. Fluids A **4**, 30.
2. P.R. Nott, J.F. Brady, 1994, J. Fluid Mech. **275**, 157-199.
3. S.A. Altobelli, R.C. Givler, E. Fukushima, 1991, J. Rheol. **35**, 721.
4. A. Karnis, S.G. Mason, 1967, J. Colloid Sci. **22**, 531.
5. S.W. Sinton, A.W. Chow, 1991, J. Rheol. **35**, 1991, 735.
6. C.J. Koh, P. Hookham, L. G. Leal, 1994, J. Fluid Mech. **226**, 1-32.

# SHEAR-INDUCED MIGRATION OF PARTICLES IN A FLOWING VISCOUS CONCENTRATED SUSPENSION

By

**A. Shauly, A. Averbakh, R. Semiat and A. Nir ***

Department of Chemical Engineering, Technion, Haifa 32000, Israel.

The shear-induced migration of non-Brownian particles in flowing viscous suspensions was studied using laser-Doppler anemometry (LDA) and numerical simulations. Measurement systems and techniques were developed to apply LDA to velocity detection in the bulk of highly concentrated suspensions flowing in a rectangular duct with a slender aspect ratio. The penetration of the laser beams into the bulk of the suspension, with minimal light scattering, was facilitated by rendering the suspension transparent. Matching of the refractive indices of the solid and fluid phases was maintained by a careful control of the suspension temperature during each run, and was monitored on-line. Measurements were carried out in suspensions with particle concentration between 0.1 and 0.5. Numerical simulations of similar flows in circular pipes and rectangular ducts, including phenomenological models for particle shear-induced diffusion, were solved and qualitatively compared to the measured results.

Velocity profiles in the direction of the flow and in the direction perpendicular to the primary streamlines were obtained for various particle concentrations, $\phi_S$. These profiles were measured at a distance of 30 cm from the flow entrance (about 75 times the duct cross sectional narrow dimension). At relatively low particles concentration, $\phi_S < 0.3$, the suspension velocity profiles were identical with those expected for profiles in a homogeneous Newtonian fluid. Measurements in the direction perpendicular to the main flow recorded signals which did not indicate a significant net motion in the lateral direction. For the higher particles concentration, $\phi_S > 0.3$, the suspension velocity profiles deviated significantly from those expected for a homogeneous Newtonian fluid. This deviation increased with the increase of $\phi_S$. The detected lateral velocity increased as well and showed motion directed from the side walls toward the duct center. Since, under the conditions of the experiment, the flow is practically always fully developed everywhere, the net lateral velocity in the duct cross

section is due to particles drift caused by shear-induced migration. It was found that the migration intensity does not increase monotonically with the increase of particle concentration and that it has a maximum at an intermediate value near $\phi_S \sim 0.4$. This reflects the combined opposing actions of the driving forces for particles migration, the shear rate gradients and the effective viscosity and concentration gradients (Leighton and Acrivos, 1987), as well as the fact that the migrating particles move in an extremely viscous environment when particle concentration is very high. It is interesting to note that at all particles concentrations the magnitude of the net averaged lateral velocity is much lower than the standard deviation (STD) of the corresponding measurements. The instantaneous measurement detects also periodic motions resulting from particle rotation. With $\gamma$ and $a$ being the shear strength and particle radius, respectively, the periodic motions are typically of $O(\gamma a)$ while the shear induced diffusion coefficient is of $O(\gamma a^2)$. This difference is further enhanced due to particles aggregation into bigger clusters.

The measurements are corroborated by numerical solutions of dynamic mass and momentum balances based on the phenomenological model of Phillips et al. (1992). Steady and transient states were solved for suspension flow in circular and rectangular geometries. Following Seifu et al. (1994), the problem was formulated in terms of a shear-induced 'migration potential', $P$, the evolution of which was followed. The major results of the calculations agree qualitatively well with the LDA measurements. At steay states, in which $P$ is uniform in a cross section of the flow, the suspension velocity profiles along the larger axis of the rectangular duct are flat at lower $\phi_S$ and more rounded at relatively high $\phi_S$. Rather unexpectedly the calculations predict that, although the location of the LDA measurements point is far from where a steady state is achieved, there is a significant pressure gradient drop for the high concentration suspensions even at such a short distance. Furthermore, lateral fluxes are predicted at this measurement location having profiles similar to those measured in the experiments. The intensity of these fluxes (or lateral velocities) does not grow monotonically with the increase in suspension particle concentration but, rather, exhibits a maximum at about $\phi_S \sim 0.4$, qualitatively agreeing with the experimental observations. These characteristics were found for both circular cross section pipe and

rectangular duct. The measured particle migration velocities are higher considerably than those predicted by the simulation. The difference can not be attributed to the choice of the phenomenological model and can not be bridged by a change in it's coefficients. It might be, however, due to migration and rotation of large clusters of particles, rather than individual particles, which tend to aggregate due to traces of interparticle surface forces or due to a size distribution as was recently suggested by a study of self diffusion of bimodal suspensions using Stokesian Dynamics (Chang and Powell, 1994).

**References**

Chang, C. and Powell, R. L., 1994, *Self-diffusion of bimodal suspension of hydrodynamically interacting spherical particles in shearing flow,* J. Fluid Mech. **281**, 51 - 80.

Leighton, D. and Acrivos, A., 1987, *The shear-induced migration of particles in concentrated suspensions,* J. Fluid Mech. **181**, 415 - 439.

Phillips, R. J., Armstrong, R. C., Brown, R. A., Graham, A. L. and Abbott, J. R., 1992, *A constitutive equation for concentrated suspensions that accounts for shear-induced particle migration,* Phys. Fluids A **4**, 30 - 40.

Seifu, B., Nir, A. and Semiat, R., *Viscous dissipation rate in concentrated suspensions,* Phys. Fluids **6**, 3189 - 3191.

* To whom correspondence should be addressed.

# NMRI Studies of Granular Flows in a Rotating Horizontal Cylinder

E. Fukushima, S.A.Altobelli, A. Caprihan, M. Nakagawa and L. Z. Wang
The Lovelace Institutes, 2425 Ridgecrest, SE, Albuquerque, NM 87108

## Introduction

We have developed nuclear magnetic resonance imaging (NMRI) techniques to measure parameters of granular flows. In particular, we have measured velocity components, concentration (density), and particulate diffusion for flows in a horizontal cylinder partially filled with mustard, sesame or sunflower seeds [1]. The cylinder was rotated about its axis inside the bore of a horizontal superconducting magnet. The NMRI measurements were obtained from central slices, 0.3 - 1.0 cm thick, where the flow was not influenced by the end walls of the cylinder. Liquid state NMR techniques may be used because of the strong signal obtained from the seeds' internal oils. We have also studied these flows with a discrete numerical simulation [2].

## NMRI Techniques

We have used two methods for measuring velocity and concentration. One is to non-invasively tag the particles with a rectangular grid and measure the evolution of the pattern as a function of time. The average velocity of each rectangular cell is obtained from the displacement of the center of the cell, and other parameters such as shear and vorticity can be obtained from the deformation and rotation of the cell. The evolution of the tags for different delays can be linked in a movie loop to enhance the visualization. This is a simple and robust method because the tagging can simply be appended to a standard imaging operation and the results do not depend on the signal intensity but only on displacements that can be measured in the image [3]. The trade-off is that spatial resolution is limited.

The second method uses the fact that NMRI can measure both the phase and amplitude of the magnetization that evolves due to motion during the imaging operation [4]. We design time varying magnetic field gradient pulses in such a way that the gain in magnetization phase at the end of an echo sequence is proportional to the average velocity of the image voxel. In this way, a complete velocity field can be mapped in 2- or 3-D.

Images of velocity component fluctuations are obtained by adapting NMR methods for measuring molecular diffusion. The relation between the measured

fluctuation images and the granular temperature is not completely established in part because density fluctuations are not included in the standard descriptions of the NMR signal.

The spatial resolution of methods of the second type is the same as the spatial resolution of the image. In the present experiments this is a fraction of a mm. Routine images are $128^2$ or $256^2$ and require many minutes to create.

## Results

An example of the first type of NMRI experiment is shown in Figure 1. The flow is composed of a large lower region moving in rigid body rotation with a thin shear layer above it. The "free-surface" is slightly curved with a point of inflection. Most of the flows studied were in this regime.

Figure 1. Grid-tag experiment of flowing mustard seeds at 18 rpm. The delays between tagging and imaging are 1, 10, 20, 50, and 100 ms, from left to right. The tagged cells translate and deform as a function of time.

Figure 2 shows an image of the horizontal component of velocity obtained from an NMRI experiment compared to one calculated by direct numerical simulation [2]. The shading of the image in the rigid body region shows that the velocity is proportional to the vertical coordinate, as expected. Note that the velocity is higher in the flowing layer than at the cylinder wall. This is due to the difference in thickness of the two counterflowing layers and also to the lower density in the flowing layer. The numerical simulation produces a qualitatively similar picture, and correctly captures some trends. For instance, both experiments and simulation show that the dynamic angle of repose is proportional to rotation speed $\Omega$, and that flowing layer thickness increases roughly as $\Omega^{1/2}$.

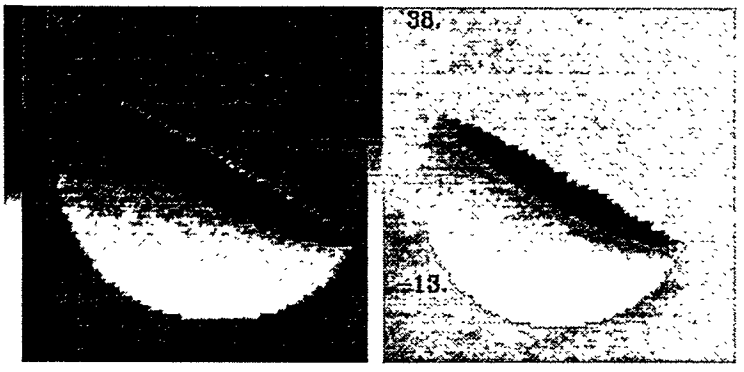


Figure 2. X-velocity component images obtained from NMRI (left) and direct numerical simulation (right). Light color indicates motion to the left, and dark color indicates motion to the right.

## Conclusions

Excellent results for velocity and concentration of flowing and colliding particles have been obtained non-invasively. We studied flows in geometries that are otherwise impossible to study because of the optical opacity of the materials. In addition, we obtained data for diffusion and collisional losses which must be related to granular temperature. New fast imaging methods, demonstrated in a small flow system [5], will reduce the time required to produce NMRI data to tens of milliseconds. We expect that with continued development NMRI will prove increasingly valuable in studies of granular mechanics.

## References

1. M. Nakagawa, S. A. Altobelli, A. Caprihan, E. Fukushima, and E. K. Jeong, *Experiments in Fluids* **16**, 54-60 (1993).
2. O. R. Walton and R. L. Braun, "Simulation of rotary-drum and repose tests for frictional spheres and rigid sphere clusters," *in Proceedings, Joint DOE/NSF Workshop on Flow of Particulates and Fluids*, September 29 - October 1, 1993, Ithaca, NY; pp. 131-148.
3. M. V. Icenogle, A. Caprihan, and E. Fukushima, *J. Magn. Reson.* **100**, 376-381 (1992).
4. A. Caprihan and E. Fukushima, *Physics Reports* **198**, 195-235 (1990).
5. K. Kose, *J. Magn. Reson.* **92**, 631-635 (1991).